IGNITION TIME MEASUREMENTS ON FABRIC ASSEMBLIES UNDER VARIOUS GEOMETRIC CONFIGURATIONS

A THESIS

Presented to

The Faculty of the Division of Graduate

Studies and Research

By

Robert Leighton Acree

In Partial Fulfillment

of the Requirements for the Degree

Master of Science in Mechanical Engineering

Georgia Institute of Technology

October, 1974

IGNITION TIME MEASUREMENTS ON FABRIC ASSEMBLIES

UNDER VARIOUS GEOMETRIC CONFIGURATIONS

Approved:

P. Durbetaki, Chairman

W. C. Boteler

C. K. Lee

Date Approved by Chairman: 12/17/1974

ACKNOWLEDGMENTS

I would like to thank the members of the reading committee for their advise and helpful criticisms. Appreciation is extended to Dr. Pandeli Durbetaki for his valuable guidance, concern, and interest during the progress of this study. Thanks are also due Dr. Calvin Lee for his advise and contributions to the radiative ignition tests, and to Professor Winston Boteler for his comments on this thesis. The problems dealt with in this thesis were originally suggested by Dr. Wolfgang Wulff.

The technical staff of the School of Mechanical Engineering deserve thanks for their help during this work. The support of the National Science Foundation under Grant GI 31882 is acknowledged with appreciation.

Special permission was obtained from the Division of Graduate Studies to vary the numbering system used for the tables and figures in this thesis.

I wish to thank Greg Wedel for his invaluable advise and friendship during this research. And finally, I express my appreciation to my parents for their constant encouragement during the progress of this work.

TABLE OF CONTENTS

LIST OF TABLES

Table | Page

LIST OF ILLUSTRATIONS

Figure Page

NOMENCLATURE

a	distance from leading edge	mm
A_1-A_7	coefficients, equation (B7)	
B	coefficient, equation (37)	
c	specific heat	Ws/kg-°K
C_1-C_4	integration constants, equations (15-16)	
d	fabric thread diameter	mm
D	diameter of fabric sample	cm
D_e	burner exit diameter	cm
e	radiative emissivity	
E	activation energy	Ws/g mole
F	configuration factor	
Fo	Fourier number, equation (18)	
g	gravitational acceleration	m/s^2
G	inter-fabric air gap	cm
Gr	Grashof number, equation (6)	
h	free convection film coefficient	W/cm^2-°K
$2h_c$	flame convective film coefficient	W/cm^2-°K
Δi	reaction enthalpy	Ws/g
j	exponent, equation (37)	
k	thermal conductivity	W/cm-°K
k/δ	thermal conductance	W/cm^2-°K
K	preexponential factor	1/s
L	height above burner exit	cm

m	mass per unit length	mg/cm
$\dot{m}$	mass flow rate	g/h
n	order of reaction	
Nu	Nusselt number, equation (6)	
p	pressure	N/m^2
Pr	Prandtl number, equation (6)	
P(B/I)	probability of burn given ignition	
P(I/E)	probability of ignition given exposure	
P(E/U)	probability of exposure given use	
q	heat flux per unit area	W/cm^2
q^*	nondimensional heating intensity	
R	universal gas constant	Ws/g mole-°K
Re	Reynolds number, equation (36)	
$\bar{s}$	sample variance	s
T	absolute temperature	°K
T^*	normalized temperature, equations (B5) and (B6)	
t	time	s
V	velocity	m/s
W_o	incident radiant heat flux	W/cm^2
x	relevant scaling length	cm

Greek Symbols

α	radiative absorbtivity	
$\bar{\alpha}$	inclination angle	
α^*	proportionality constant, equations (9,10)	
β	coefficient of thermal expansion	1/°K

δ	fabric thickness	mm
ε	decomposable mass fraction	
η	normalized time, equation (20)	
θ	normalized temperature, equation (21)	
λ	reacted mass fraction	
μ	dynamic viscosity	kg/m-s
ν	kinematic viscosity	m^2/s
π_{10}-π_{114}	front fabric parameters, Table 1	
π_{20}-π_{214}	back fabric parameters, Table 2	
$\tilde{\rho}$	radiative reflectivity	
$\rho\delta$	specific mass	mg/cm^2
σ	Stefan-Boltzmann constant	$W/m^2\text{-}°K^4$
τ	radiative transmissivity	
ϕ	stoichiometric equivalence ratio	

Subscripts

b	back fabric
c	convective
d	thread diameter
e	burner exit
en	endothermic reaction
ex	exothermic reaction
f	front fabric
g	gas flame
G	interlayer air gap
i	ignition
m	melting

md	moisture desorption
mix	mixture
o	initial
p	constant pressure
r	radiative
ref	reference value
s	stainless steel screen
w	surface temperature
1-4	surfaces of the fabric assembly, Figure 1
∞	ambient conditions

Superscripts

-	averaged value
*	normalized
a	measured film coefficient
b	film coefficient, equation (37), $x = \delta$
c	film coefficient, equation (35), $x = \delta$
d	film coefficient, equation (37), $x = d$

SUMMARY

This thesis is concerned with the determination of fabric ignition time under radiative and convective heating. Ignition time was measured and analyzed for the geometries of multilayer assemblies exposed to a radiative ignition source and edge exposure to a flame.

The Fire Hazard and Combustion Research Laboratories of the School of Mechanical Engineering at the Georgia Institute of Technology have been engaged in a research program studying the ignition phenomena of fabrics. The objective of this research has been to obtain the understanding required to set rational and reasonable flammability standards and criteria. The flammability of fabrics has been shown to be a function of fabric material properties, relevant geometry, and the ignition time for a given heating intensity.

This work is an extension of fabric ignition time measurements to relevant geometric configurations. In all flammability studies the central problem is to relate test methods of the laboratory to actual conditions encountered in the ignition of fabrics. Relevant fabric configurations must be assessed in the evaluation of fabric flammability hazards. Relevant configurations include the multilayer fabric assemblies and the edge exposure to a flaming

ignition source.

Ignition time measurements were conducted on commonly encountered pairs of fabrics under radiative heating and on the edges of single fabrics exposed to a flame. Analytical models were formulated to predict the ignition time of both systems under specified heating conditions and geometry.

Ignition tests were conducted on fabric pairs consisting of two identical cotton fabrics and of a polyester fabric with a cotton fabric behind it. Ignition times ranged from 3.7 to 24.5 seconds. For edge exposure to a flaming heat source tests were conducted on cotton and synthetic blends. Ignition times varied from 0.07 to 2.6 seconds. Results from the ignition tests were correlated with results from previous ignition tests.

This work was supported by the National Science Foundation under the Research Applied to National Needs Program, Grant Number GI-31882A#1.

CHAPTER I

INTRODUCTION

Relevance of Fabric Flammability Research

Accidental fires claim the lives of 12,000 Americans each year and inflict property damage and related losses that costs the United States an estimated $11.4 billion per year. Tragically, an additional 300,000 persons are injured in fires, with one in six requiring more than six weeks of hospitalization [1].* Garments which ignite and injure the consumer contribute greatly to this tremendous loss. Each year 3,000 to 5,000 deaths are due to flaming fabrics, and more than half of the total burn injuries result from this source. Recent studies show that clothing burn victims are burned more severely than burn victims spared clothing fire, and are four times more likely to die [2].

In response to this problem, Congress enacted the Flammable Fabrics Act of 1953 (and further amended it in 1967) directing the Secretary of Commerce to establish reasonable fabric flammability safety criteria so as to protect the public from excessive hazards of fabric-related burn injuries. These standards are currently being sought through basic research into the flammability of fabrics,

*Numbers in brackets designate references in the Bibliography.

and their establishment will ultimately result in a reduction of the overall fire hazard.

Previous Accomplishments

In order to establish the technical and scientific foundation for the required legislation, the United States textile industry and the United States Government have initiated a cooperative effort in sponsoring research designed to lay down this scientific foundation. To formulate and administer such programs the Government-Industry Research Committee on Fabric Flammability (GIRCFF) was formed, whose members represented the National Science Foundation, the National Bureau of Standards, the American Textile Manufacturers Association, the Cotton Council of America, and the Man-Made Fiber Producers Association.

The principal connection between burn injury hazard and the deterministic processes leading to burn injury were established in Reference [3]. The relationship is based on the quantitative assessment of hazard in terms of accident probability, and the dependence of accident probability on the subsidiary probabilities associated with all conceivable events occurring between the production of the fabric and the accidental burn injury. The probability of fabric ignition for a given exposure P(I/E) was related in Reference [4] to the ratio of the time it takes a fabric to ignite under given exposure conditions, called the ignition

time, over the time the fabric is exposed to a given ignition source, that is, the exposure time. The overall hazard may be expressed by

$$P(B/U) = P(E/U) \cdot P(I/E) \cdot P(B/I) \qquad (1)$$

that is, the probability of burn injury given the intended usage is specified by the subsidiary probabilities of exposure given usage, ignition given exposure, and burn injury given ignition.

Research on fabric flammability has been directed towards the assessment of the overall garment fire hazard. Four separate research groups were selected by the GIRCFF to study the phenomena of ignition, preignition heat transfer, propagation of flame, and the assessment of burn injury. These are the Georgia Institute of Technology, the Gillette Research Institute, the Massachusetts Institute of Technology, and Factory Mutual Research Corporation. The accomplishments of these groups are reported in References [4-10].

The ignition of fabrics was studied at the Fire Hazard and Combustion Research Laboratories of the School of Mechanical Engineering at the Georgia Institute of Technology. Fabric ignition times were determined for fabric samples exposed to a specified heat flux for both convective and radiative heating. Comparison between analyses and experimentally determined ignition times indicate the significance

of pyrolysis in delaying predicted ignition times by a factor of two to three. An extensive collection of thermal and physical property data on fabric materials was made [4,5].

The ignition phenomenon of fabrics was also studied at Factory Mutual Research Corporation. Minimum ignition times were determined for fabrics exposed to convective heating, and were related to fabric density. The ignition of single yarns was also studied [8].

Further Advances Required

The determination of the relationship between fabric behavior in a laboratory test and the hazard it represents in actual use is the central problem in the development of rational safety standards [11]. In previous ignition studies single fabrics were tested under normal impingement to an ignition source [4,5,6]. It is necessary to expand these test methods, as actual ignition situations encounter less simplified geometries and heating conditions. Two such geometries are the heating of multi-layer assemblies and the edge impingement of a gas flame.

Multi-layer fabric systems are predominant in clothing and furnishings. The possible interaction of fabric layers must be quantitatively determined before the general behavior of a fabric can be established with the confidence that is required to propose rational fabric flammability standards. Only single fabrics have been investigated in

previous and current ignition time studies.

The problem of heat transfer through multi-layer fabric systems has been studied analytically [12,13]. Morse, et al. [12], analyzed a two layer model undergoing intense radiative heating. Results of a preliminary parametric analysis showed that at air gaps greater than 0.1 inches, the heat transfer is predominantly by radiation while at gaps of less than 0.1 inches convection is predominant. It was concluded that gaps between fabric layers are of primary importance in determining the heat transfer through the fabric system.

Morris [13] studied the thermal insulation properties of multiple fabric layers. It was shown that the conductive resistance of the overall fabric system could be approximated by the sum of the conductive resistances of the individual layers if the surfaces were smooth, and the fabrics were in contact. The insulating properties of both single and multiple layered fabric systems were largely attributed to the volume of air contained within the fabric system.

It has been suggested by Miller [14] that various polymer combinations in a fabric system will chemically interact during thermal decomposition and/or burning. In a current research program he proposes to demonstrate chemical mechanisms of interaction through classical analytical techniques. Preliminary results show that early decomposition products of synthetic fibers effect a chemical

modification of cellulosic materials producing a material with somewhat different flammability properties. Miller has shown previously that the effects of chemical fire retardants may be transferred between composite layers of fabric [15].

Experimental evidence of the effect of the angle of flame impingement upon fabric ignition time has been reported by Champion [16] and by Heskestad, et al. [9]. Champion measured ignition times for circular fabric samples at 0° and 45° inclination angle, and found little variation in ignition time with inclination angle. The ignition times appeared to vary directly with the measured film coefficients. Heskestad, et al. varied the angle of impingement from 0° to 62° from the horizontal. For a diffusion flame only a 20% variation in ignition time was obtained. Earlier tests [9] at Factory Mutual indicated a variation in ignition tests with inclination angle of up to four times, a discrepancy which was not later explained.

The effects of edge ignition are predominant in many garment fires which originate from loose free-hanging fabrics. These include the ignition of hanging fabrics such as draperies, as well as shirt sleeves and hems where the ignition of the fabric edge spreads rapidly up the fabric. This phenomenon of edge ignition has not been studied previously by the GIRCFF research groups.

Research Objectives

The first objective of this thesis is to assess the effect of fabric interaction on the ignition time of a multiple layer fabric assembly. Relevant parameters will be determined to describe the heating and ignition of multi-layer fabric assemblies undergoing radiative heating. Ignition time results are to be correlated with results from previous ignition time studies.

The second objective of this thesis is to assess the effect of fabric orientation on the ignition time of single fabrics exposed to a convective ignition source. Parameters to be studied include the effect of the proximity of the edge to a flame and the effect of the angle of flame impingement. Ignition time results are to be correlated with results from previous ignition time studies.

CHAPTER II

MULTI-LAYER FABRIC INTERACTION

Two problems associated with the overall fire hazard of fabric systems are the ignition of multi-layer assemblies and the ignition of fabrics exposed to a flame. The purpose of this chapter is to assess the effect of the interaction of parallel fabric layers upon fabric ignition time under radiative heating. The problem of edge exposure to a flame will be considered in Chapter III.

Analytical models are developed to simulate the thermal response and predict the ignition time of a fabric assembly of fabric layers separated by a specified air gap. Ignition times were experimentally determined for fabric pairs consisting of similar and dissimilar fabric compositions. Parameters investigated include the effects of inter-layer spacing, heating intensity, and fabric composition. Evidence of possible synergism of fabric layers of differing composition was examined through comparison of results on similar and dissimilar fabrics. Test data and analysis are correlated with previous radiative ignition time data [4,5].

Modeling Analysis

The purpose of the analysis is the derivation of the relations which govern the ignition, or melting, of fabric

assemblies under radiative heating. First, destruction criteria must be defined. Destruction of igniting fabrics is defined by the occurrence of thermal excursion of the fabric surface, which is associated with the heat release of combustion. Synthetic fabrics, however, do not ignite but rather melt and shrink away from the heat source. Thus destruction of melting fabrics is defined by the breakdown of fabric structure with melt-through of the fabric. Melting is assumed to occur at the unique melting temperatures reported in References [4,5]. The fabric system is considered destroyed by the ignition, or melting, of either front or rear fabrics. Destruction times are determined from the thermal response of the fabric with time, and were taken to be the time required for the thermal excursion for the igniting fabrics, or the time required for the attainment of melting temperature in the case of melting fabrics.

Problem Formulation

A two layer fabric assembly separated by a specified air gap is shown in Figure 1. It is assumed that the overall dimensions are large with respect to the air gap, and that the heat transfer through the layers of fabric may be considered one dimensional. The fabrics are approximated by thermally thin semi-transparent slabs for which the fine structure of the fabric is neglected, i.e., the yarn structure, fabric weave, porosity, etc. [4]. Subsurface temperature gradients are neglected due to the thinness of

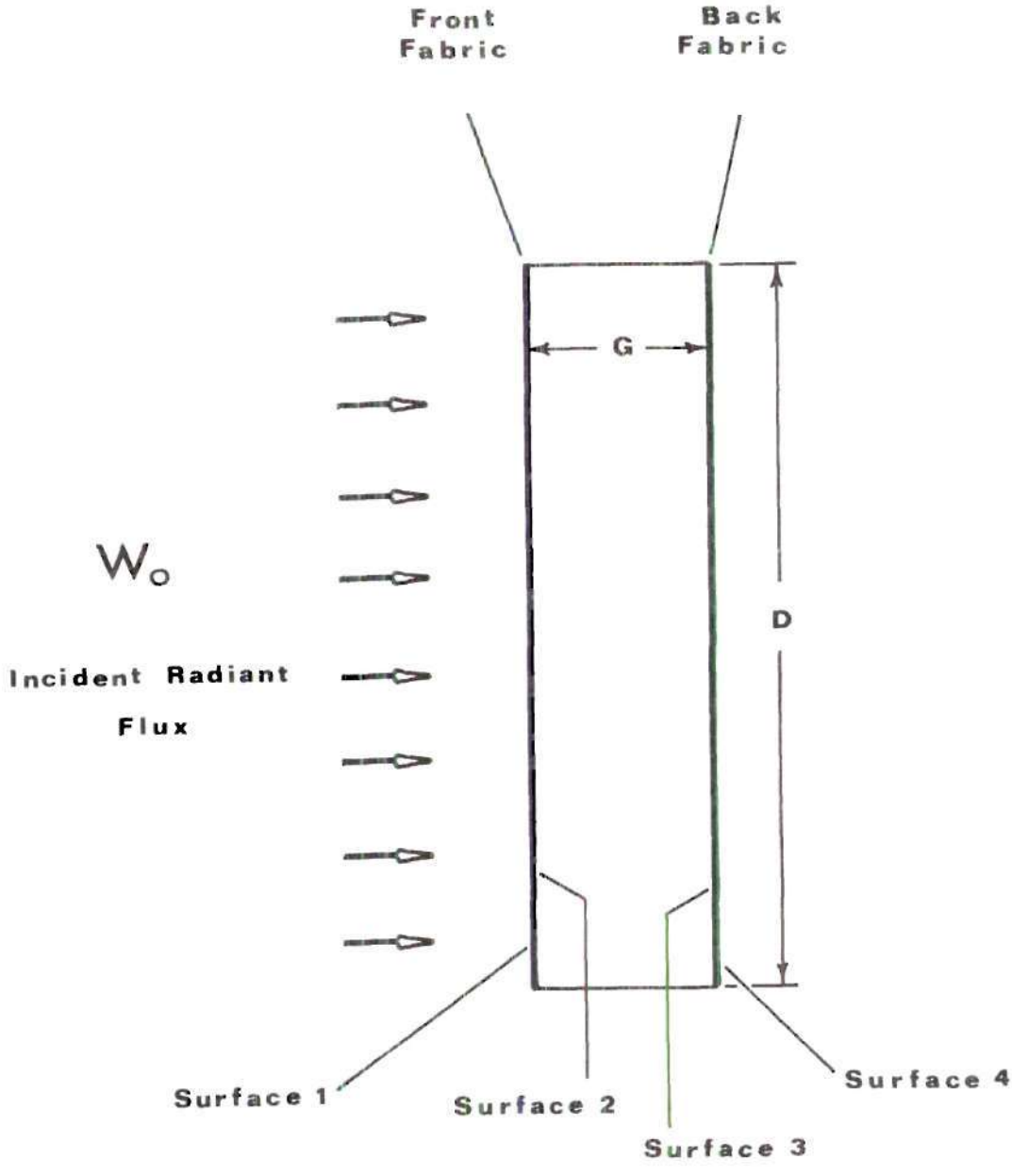

Figure 1. Geometry of the Fabric Assembly

the fabric material. The system is exposed to radiant heating and is assumed to undergo radiative and convective cooling, as well as experience moisture desorption, endothermic pyrolysis, and exothermic combustion (in the case of igniting fabrics). Conservation of energy for the front fabric may be written as

$$(\rho\delta)_f \, c_f \frac{dT_f}{dt} = \alpha_f\left[1 + \frac{\tau_f \tilde{\rho}_b}{1-\tilde{\rho}_f\tilde{\rho}_b}\right]W_o - h_1(T_f - T_\infty)$$

$$- h_2(T_f - T_b) - \sigma e_f F_{1\infty}(T_f^4 - T_\infty^4)$$

$$- \sigma F_{23}(T_f^4 - T_b^4)/[1/e_f + 1/e_b - 1]$$

$$- (\Delta i)_{f,md} \, \varepsilon_{f,md} \, (\rho\delta)_{f,o} \frac{d\lambda_{f,md}}{dt}$$

$$- (\Delta i)_{f,en} \, \varepsilon_{f,en} \, (\rho\delta)_{f,o} \frac{d\lambda_{f,en}}{dt}$$

$$+ (\Delta i)_{f,ex} \, \varepsilon_{f,ex} \, (\rho\delta)_{f,o} \frac{d\lambda_{f,ex}}{dt} \qquad (2)$$

where $\rho\delta$ is the specific mass, c is the specific heat, T is the absolute temperature, t is time, α, $\tilde{\rho}$, and τ are the radiative absorbtivity, transmissivity, and reflectivity, respectively. W_o is the incident heat flux, h is the convective film coefficient, σ is the Stephan-Boltzmann

constant, e is the emissivity, ε is the decomposable mass fraction participating in the particular reaction, F is the radiative exchange factor, Δi is the reaction enthalpy, and λ is the reacted mass fraction for the specific reaction. Subscripts f and b refer to the front and back fabrics respectively, and numerals 1, 2, 3, and 4 refer to the fabric assembly surfaces as defined in Figure 1. Subscripts o, ∞, md, en, and ex refer to initial conditions, ambient conditions, moisture desorption, endothermic gasification, and exothermic reaction, respectively.

The term on the left side of equation (2) is interpreted as the net energy storage of the front fabric. The eight terms of the right side are the total absorbed radiant heat flux, the convection at surface 1, the convection at surface 2, the radiative cooling of surface 1, the radiative cooling of surface 2, the heat absorbed by moisture desorption in the front fabric, the heat absorbed by endothermic pyrolysis of the front fabric, and the heat liberated by exothermic reaction of the front fabric. The expression for the absorbed incident radiation includes the effect of the rereflectivity between parallel fabric layers [17].

The reaction rates of moisture desorption, pyrolysis, and exothermic reaction are described in terms of nth-order Arhenius type relations. The decomposition rates are given by equations of the form

$$\frac{d\lambda}{dt} = K(1-\lambda)^n \exp(-E/RT) \tag{3}$$

where the reaction kinetic parameters are K, the preexponential factor, n, the order of the reaction, and E, the activation energy. R is the universal gas constant. Three such equations describe the mass decomposition rates of moisture desorption, endothermic pyrolysis, and exothermic reaction.

The equation for conservation of energy for the back fabric may be written as

$$\begin{aligned}(\rho\delta)_b\, c_b \frac{dT_b}{dt} = {} & \frac{\alpha_b \tau_f}{1-\tilde{\rho}_f\tilde{\rho}_b} W_o - h_4(T_b-T_\infty) \\ & - h_3(T_b-T_f) - \sigma F_{4\infty} e_b (T_b^4-T_\infty^4) \\ & - \sigma F_{23}(T_b^4-T_f^4)/[1/e_f + 1/e_b - 1] \\ & - (\Delta i)_{b,md}\, \varepsilon_{b,md}\, (\rho\delta)_{b,o} \frac{d\lambda_{b,md}}{dt} \\ & - (\Delta i)_{b,en}\, \varepsilon_{b,en} (\rho\delta)_{b,o} \frac{d\lambda_{b,en}}{dt} \\ & + (\Delta i)_{b,ex}\, \varepsilon_{b,ex}\, (\rho\delta)_{b,o} \frac{d\lambda_{b,ex}}{dt}\end{aligned} \tag{4}$$

Three equations of the form of equation (3) are used to describe the decomposition rates of the back fabric by moisture desorption, endothermic gasification, and exothermic

reaction.

Expressions for the free convection at surfaces 1 and 4 are available from standard heat transfer texts. For the free convection from a flat vertical plate, the heat transfer rate may be expressed by

$$Nu_x = 0.59\ (Gr_x\ Pr)^{1/4} \tag{5}$$

where x is the relevant scaling length, and the Nusselt, Prandtl, and Grashof numbers are defined by

$$\left.\begin{aligned} Nu_x &= \frac{hx}{k} \\ Pr &= \frac{c_p \mu}{k} \\ Gr_x &= \frac{g\beta(T_w - T_\infty)x^3}{\nu^2} \end{aligned}\right\} \tag{6}$$

The parameters not yet defined are k, the thermal conductivity, μ, the dynamic viscosity, g, the acceleration due to gravity, β, the coefficient of thermal expansion, and ν, the kinematic viscosity. Properties are those of air and are evaluated at the mean temperature between the surface and ambient temperatures [18].

The problem of the combined effects of conduction and convection in an enclosed air gap (as is the case between surfaces 2 and 3) has been studied for a wide range

of parameters by Eckert and Carlson [19]. The following expression is suggested for the average conductive and convective heat transfer through an air medium

$$Nu_G = 1 + 0.00166 \frac{G}{D} (Gr_G)^{0.9} \qquad (7)$$

where G is the spacing between layers and D is the height of the air layer. The above relation is valid when $Gr_G < 1000$ and $D/G > 1$. For small air gaps and moderate temperature differences between the two surfaces, the Nusselt number is close to unity and heat transfer is primarily by conduction.

The correlations of Eckert and Carlson were obtained for the steady state heating of an enclosed air layer. Use of the steady state heat transfer relations for the problem of the transient heating of a fabric assembly involves the assumption that the heating of the fabric assembly is quasistatic.

The four equations describing the heating of the front fabric are the equation of conservation of energy, and the three rate equations for the mass decomposition by moisture desorption, endothermic gasification, and exothermic reaction. The heating of the back fabric is described by a set of four similar equations. The two energy equations are coupled by the radiative and convective exchange between surfaces 2 and 3. The total response of the fabric

system is given by the simultaneous solution of these eight equations.

Solution of the system of equations described above requires numerical integration due to the non-linearity of the equations. Before attempting to integrate these eight equations, partial modeling will be used to obtain approximate solutions for the heating of the fabric assembly. Models for inert heating with and without convective cooling will be developed in the following sections, after which the numerical solution to the complete formulation will be presented.

Partial Modeling Analysis

For inert heating of a fabric assembly, in the absence of radiative and convective cooling, the incident heating is balanced by the sensible heat storage of the fabric layer. Temperatures of the fabric layers are governed by

$$(\rho\delta)_c \frac{dT}{dt} = \alpha^* W_o \tag{8}$$

where the proportionality constants for the absorbance of the front and back fabrics include the rereflectivity between fabric layers. These are defined by

$$\alpha_f^* = \alpha_f\left(1 + \frac{\tau_f \tilde{\rho}_b}{1-\tilde{\rho}_f\tilde{\rho}_b}\right) \tag{9}$$

$$\alpha_b^* = \frac{\tau_f \alpha_b}{1-\tilde{\rho}_f \tilde{\rho}_b} \tag{10}$$

Integration of equation (8) between initial time and ignition time yields the following expression for the destruction time

$$t_{i,m} = \frac{(\rho\delta)_c (T_{i,m}-T_\infty)}{\alpha^* W_o} \tag{11}$$

Two ignition times are predicted for the fabric assembly, however, destruction of the assembly occurs when the shorter of the two is reached.

For the case of radiant heating combined with convective cooling, the energy balances for the front and back fabrics are coupled by the convection between them. For the fabric assembly shown in Figure 1 these equations may be written as

$$(\rho\delta)_f c_f \frac{dT_f}{dt} = \alpha_f^* W_o - h_2(T_f-T_b) - h_1(T_f-T_\infty) \tag{12}$$

$$(\rho\delta)_b c_b \frac{dT_b}{dt} = \alpha_b^* W_o - h_3(T_b-T_f) - h_4(T_b-T_\infty) \tag{13}$$

Film coefficients h_2 and h_3 for the heat transfer between the surfaces of the air gap are equivalent for

negligible thermal capacity of the air gap. These film coefficients are approximated by the conductive resistance of the air medium, for Nusselt number close to unity. The convective film coefficient is given by

$$h_2 = h_3 = \frac{k_{air}}{G} \tag{14}$$

Film coefficients h_1 and h_4 are determined for the free convection from a vertical surface by

$$\frac{h\,x}{k} = 0.59\ (Gr_x\ Pr)^{1/4} \tag{5}$$

Film coefficient h_4 is approximated by h_1, with an associated error in the value of h_4 of -10%.*

The coupled energy balances (12) and (13) may be separated and integrated to yield expressions for T_f and T_b, given as

$$T_f = T_\infty \frac{(h_2+h_1)(\alpha_f^* W_o+h_1 T_\infty) + (h_1)(\alpha_b^* W_o+h_1 T_\infty)}{(h_2+h_1)^2 - (h_2)^2}$$

$$+ T_\infty C_1\ \exp(\lambda_1 t) + T_\infty C_2\ \exp(\lambda_2 t) \tag{15}$$

---

*Verified through numerical solution of the complete formulation.

$$T_b = T_\infty \frac{(h_2+h_1)(\alpha_b^* W_o+h_1 T_\infty) + (h_1)(\alpha_b^* W_o+h_1 T_\infty)}{(h_2+h_1)^2 - (h_2)^2}$$

$$+ T_\infty C_3 \exp(\lambda_3 t) + T_\infty C_4 \exp(\lambda_4 t) \qquad (16)$$

where the equations have been simplified using the approximations $h_1 = h_4$ and $h_2 = h_3$. Initial conditions are

at $t = 0$ $\qquad T_f = T_\infty$

$$T_b = T_\infty \qquad (17)$$

Eigenvalues are determined from the solution of the separated differential equations for T_f and T_b. The constants C_1 through C_4 are determined from initial conditions and the requirements for satisfying the governing differential equations (12) and (13). Derivation of equations (15) and (16) and evaluation of the constants are presented in Appendix B.

Ignition time predictions for a given heating intensity may be expressed by a normalized ignition time and a normalized heating intensity. These cannot be obtained by normalizing the lumped parameter governing differential equations (2) and (4) or (12) and (13) for the heating of the fabric assembly, but are useful parameters for plotting fabric ignition time data and analyses. Normalized ignition

time is presented by the Fourier number, defined as the ratio of destruction time to thermal diffusivity, given by

$$Fo_{i,m} = \frac{(k/\delta)t_{i,m}}{c(\rho\delta)} \tag{18}$$

Normalized heating intensity is given by the ratio of the total absorbed radiant heat to the conducted heat flux, as

$$q_r^* = \frac{\alpha^* W_o}{(k/\delta)(T_{i,m}-T_\infty)} \tag{19}$$

The effect of air gap upon destruction time is shown in Figure 2, in which ignition time of the front fabric in the two fabric assembly is plotted versus inter-layer gap. The heating intensity is held constant at 9.25 W/cm^2 for the assembly of GIRCFF fabric number 5 front and back (100% cotton fiber, see Table A3 in Appendix A). Destruction time predictions by the inert models with and without convective losses are plotted in Figure 3 to compare the results of the two partial models developed in this section. The fabric assembly used in Figure 3 is that of fabric number 5 front and back, with G = .318 cm.

From the partial modeling analysis it is concluded that rereflectivity between fabric layers results in an increase in total incident heating proportional to $\alpha^* - \alpha$. Also, it is concluded that convection between

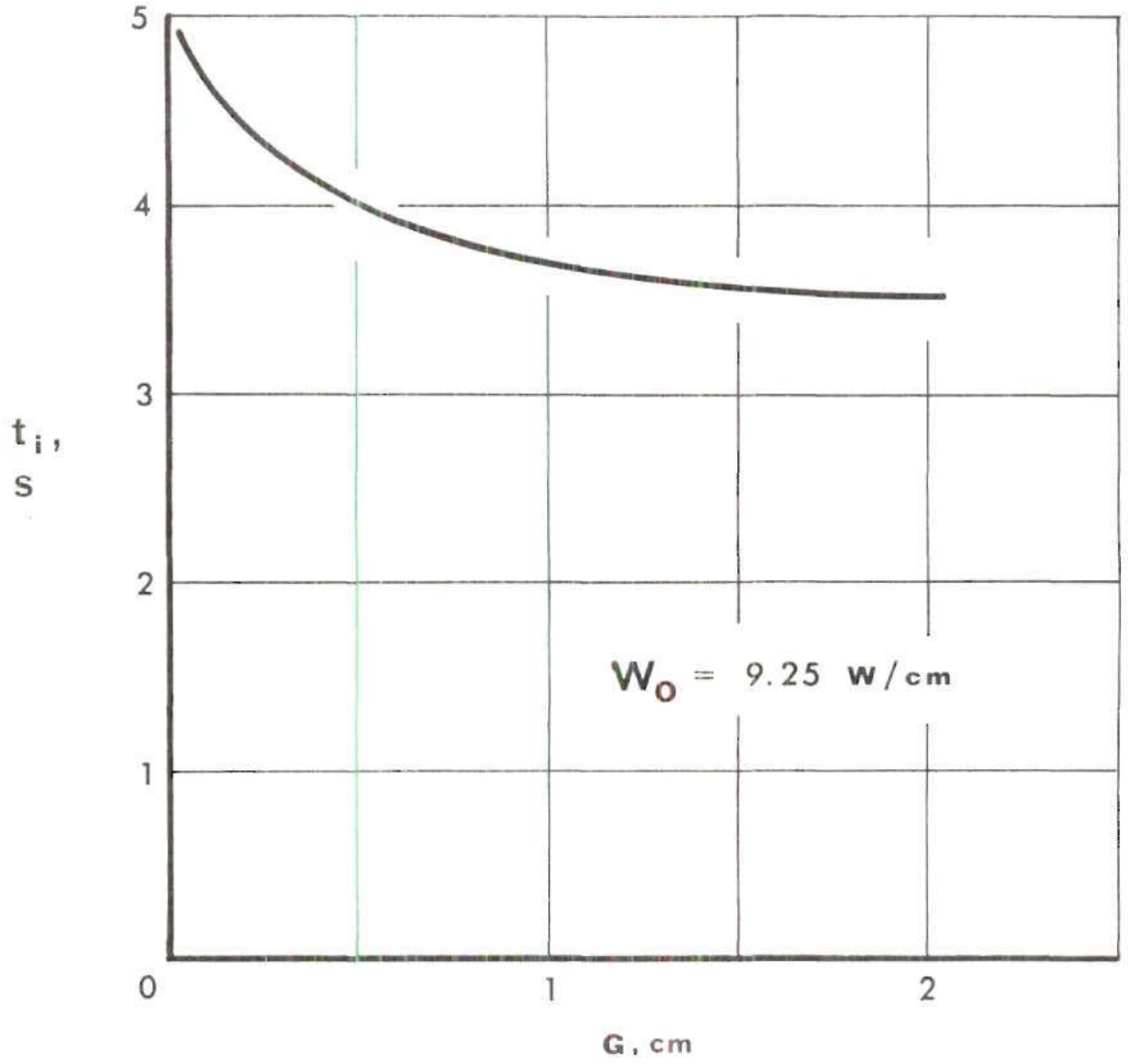

Figure 2. Effect of Air Gap on Ignition Time of the Front Fabric (Ignition time predicted from inert heating with convective heat losses for GIRCFF fabric number 5 front with fabric number 5 back)

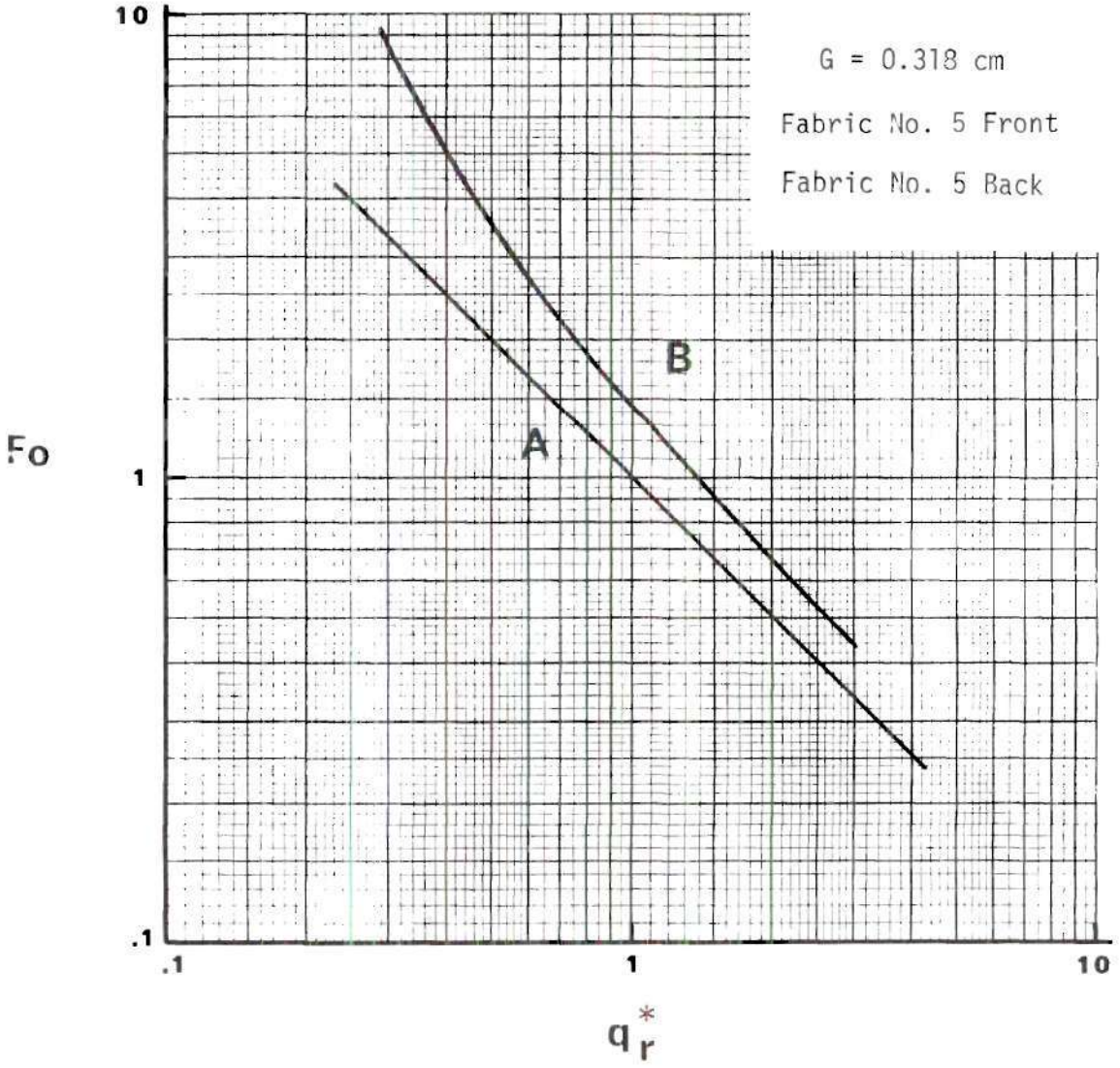

Figure 3. Comparison of Predicted Ignition Times of Front Fabric (Curve A represents inert heating without convective or radiative losses and curve B represents inert heating with convective losses but without radiative losses)

fabric layers decreases with increasing inter-layer spacing.

The solution of the complete radiative ignition model requires the numerical integration of the system of eight equations derived in the problem formulation of the previous section. The solution of the complete model is presented in the next section.

Numerical Solution for Radiative Heating

The governing equations (2) and (4) which describe the total heating of the fabric assembly include the effects of radiative and convective heat losses, as well as gas phase reactions. Inclusion of these terms make the governing equations highly non-linear. Consequently, the solution to the set of equations developed in the problem formulation requires simultaneous numerical integration. This was accomplished using a fourth-order Runge-Kutta algorithm, employing a Univac 1108 digital computer, and using temperature dependent property data obtained from References [4,5].

The governing equations were made more tractable by the introduction of relevant scaling parameters for time and temperature. The independent variable time is scaled by the ratio of radiant power flux to the sensible energy storage of the fabric. Nondimensionalized time η is given by

$$\eta = \frac{t}{t_{ref}} \tag{20a}$$

where

$$t_{ref} = \frac{c_f(\rho\delta)_{f,o}(T_{f,i,m}-T_\infty)}{\alpha_f[1+\tau_f\tilde{\rho}_b/(1-\tilde{\rho}_f\tilde{\rho}_b)]\ W_o} \tag{20b}$$

and where properties are evaluated at initial conditions. The dependent variable temperature is scaled by the ratio of the amount of temperature rise from initial temperature to the amount of temperature rise required for ignition. Nondimensionalized temperature θ is defined for each fabric by

$$\theta = \frac{T-T_\infty}{T_{i,m}-T_\infty} \tag{21}$$

For the case of idealized heating for which the radiant heat flux is balanced by the sensible energy storage, t_{ref} represents the ignition time and $\theta = 1$ the ignition temperature.

Substitution of the above variables into equation (2), which describes the overall heating of the front fabric, yields the following normalized differential equation

$$\frac{d\theta_f}{d\eta} = \pi_{11} - \pi_{12}\theta_f - \pi_{13}(\theta_f-\pi_{20}\theta_b) - \pi_{14}[(\pi_{10}\theta_f+1)^4-1]$$

$$- \pi_{15}[(\pi_{10}\theta_f+1)^4 - (\pi_{20}\theta_b+1)^4] - \pi_{16}\frac{d\lambda_{f,md}}{d\eta}$$

$$- \pi_{17}\frac{d\lambda_{f,en}}{d\eta} + \pi_{18}\frac{d\lambda_{f,ex}}{d\eta} \tag{22}$$

The decomposition rates for the solid are given in terms of nth-order Arhenius type relations, written as

$$\frac{d\lambda_{f,md}}{d\eta} = \pi_{19}(1-\lambda_{f,md})^{n_{f,md}} \exp[-\pi_{110}/(\pi_{10}\theta_f+1)] \quad (23)$$

$$\frac{d\lambda_{f,en}}{d\eta} = \pi_{111}(1-\lambda_{f,en})^{n_{f,en}} \exp[-\pi_{112}/(\pi_{10}\theta_f+1)] \quad (24)$$

$$\frac{d\lambda_{f,ex}}{d\eta} = \pi_{113}(1-\lambda_{f,ex})^{n_{f,ex}} \exp[-\pi_{114}/(\pi_{10}\theta_f+1)] \quad (25)$$

The governing differential equation for the heating of the back fabric is given by

$$\frac{d\theta_b}{d\eta} = \pi_{21} - \pi_{22}\theta_b + \pi_{23}(\pi_{10}\theta_f-\theta_b) - \pi_{24}[(\pi_{20}\theta_b+1)^4-1]$$

$$+ \pi_{25}[(\pi_{10}\theta_f+1)^4 - (\pi_{20}\theta_b+1)^4] - \pi_{26}\frac{d\lambda_{b,md}}{d\eta}$$

$$- \pi_{27}\frac{d\lambda_{b,en}}{d\eta} + \pi_{28}\frac{d\lambda_{b,ex}}{d\eta} \quad (26)$$

where the mass decomposition rates for the back fabric are given by

$$\frac{d\lambda_{b,md}}{d\eta} = \pi_{29}(1-\lambda_{b,md})^{n_{b,md}} \exp[-\pi_{210}/(\pi_{20}\theta_b+1)] \quad (27)$$

$$\frac{d\lambda_{b,en}}{d\eta} = \pi_{211}(1-\lambda_{b,en})^{n_{b,en}} \exp[-\pi_{212}/(\pi_{20}\theta_b+1)] \qquad (28)$$

$$\frac{d\lambda_{b,ex}}{d\eta} = \pi_{213}(1-\lambda_{b,ex})^{n_{b,ex}} \exp[-\pi_{214}/(\pi_{20}\theta_b+1)] \qquad (29)$$

Radiative ignition parameters for the set of eight equations (22) through (29) are defined in Tables 1 and 2.

The above system of equations consists of 36 parameters for the thermal response of the fabric assembly. The eight dependent variables θ_f, $\lambda_{f,md}$, $\lambda_{f,en}$, $\lambda_{f,ex}$, θ_b, $\lambda_{b,md}$, $\lambda_{b,en}$, and $\lambda_{b,ex}$ were determined by the simultaneous integration of equations (22) through (29). Temperature response and energy components using McCarter's pyrolysis data for a typical assembly are shown in Figures 4 and 5. Temperature response and energy components using modified pyrolysis kinetics are shown in Figures 6 and 7. Reaction kinetic parameters used for these integrations are listed in Table 3.

Destruction time predictions for the front fabric were obtained for an igniting and a melting fabric assembly. Both heating intensity and inter-layer spacing were varied, and the predicted destruction times are plotted in Figure 8. Curves A represent ignition time results for an assembly of two 100% cotton fabrics (GIRCFF fabric number 5 front and back) using McCarter's pyrolysis data. Curves B represent

Table 1. Definition of Radiative Ignition Parameters, Front Fabric.

$$t_{ref} = (\rho\delta)_{f,o}\, c_{f,o}\, (T_{f,i,m} - T_\infty) \,/\, [\alpha_{f,o}\{1 + \tau_{f,o}\tilde{\rho}_{b,o}/(1-\tilde{\rho}_{f,o}\tilde{\rho}_{b,o})\}W_o]$$

$$\Pi_{10} = (T_{f,i,m} - T_\infty) \,/\, T_\infty$$

$$\Pi_{11} = \alpha_f\, [1+\tau_f\tilde{\rho}_b/(1-\tilde{\rho}_f\tilde{\rho}_b)]\, W_o\, t_{ref} \,/\, [(\rho\delta)_f\, c_f\, (T_{f,i,m} - T_\infty)]$$

$$\Pi_{12} = h_1\, t_{ref} \,/\, [(\rho\delta)_f\, c_f]$$

$$\Pi_{13} = h_2\, t_{ref} \,/\, [(\rho\delta)_f\, c_f]$$

$$\Pi_{14} = \sigma\, e_f\, F_{1\infty}\, T_\infty^4\, t_{ref} \,/\, [(\rho\delta)_f c_f\, (T_{f,i,m} - T_\infty)]$$

$$\Pi_{15} = \sigma\, F_{23}\, T_\infty^4\, t_{ref}\, [1/e_f + 1/e_b - 1] \,/\, [(\rho\delta)_f\, c_f\, (T_{f,i,m} - T_\infty)]$$

$$\Pi_{16} = \Delta i_{f,md}\, (\rho\delta)_{f,o}\, \varepsilon_{f,md} \,/\, [(\rho\delta)_f\, c_f\, (T_{f,i,m} - T_\infty)]$$

$$\Pi_{17} = \Delta i_{f,en}\, (\rho\delta)_{f,o}\, \varepsilon_{f,en} \,/\, [(\rho\delta)_f\, c_f\, (T_{f,i,m} - T_\infty)]$$

$$\Pi_{18} = \Delta i_{f,ex}\, (\rho\delta)_{f,o}\, \varepsilon_{f,ex} \,/\, [(\rho\delta)_f\, c_f\, (T_{f,i,m} - T_\infty)]$$

$$\Pi_{19} = t_{ref}\, K_{f,md}$$

$$\Pi_{110} = E_{f,md} \,/\, R\, T_\infty$$

$$\Pi_{111} = t_{ref}\, K_{f,en}$$

$$\Pi_{112} = E_{f,en} \,/\, R\, T_\infty$$

$$\Pi_{113} = t_{ref}\, K_{f,ex}$$

$$\Pi_{114} = E_{f,ex} \,/\, R\, T_\infty$$

Table 2. Definition of Radiative Ignition Parameters, Back Fabric.

$$\Pi_{20} = (T_{b,i,m} - T_\infty) / T_\infty$$

$$\Pi_{21} = \alpha_b \left[\tau_f/(1-\tilde{\rho}_f\tilde{\rho}_b)\right] W_o \, t_{ref} / \left[(\rho\delta)_b \, c_b \, (T_{b,i,m} - T_\infty)\right]$$

$$\Pi_{22} = h_4 \, t_{ref} \, (T_{f,i,m} - T_\infty) / \left[(\rho\delta)_b \, c_b \, (T_{b,i,m} - T_\infty)\right]$$

$$\Pi_{23} = h_3 \, t_{ref} \, (T_{f,i,m} - T_\infty) / \left[(\rho\delta)_b \, c_b \, (T_{b,i,m} - T_\infty)\right]$$

$$\Pi_{24} = \sigma \, e_b \, F_{4\infty} \, T_\infty^4 \, t_{ref} / \left[(\rho\delta)_b \, c_b \, (T_{b,i,m} - T_\infty)\right]$$

$$\Pi_{25} = \sigma \, F_{23} \, T_\infty^4 \, t_{ref} \, (1/e_f + 1/e_b - 1) / \left[(\rho\delta)_b \, c_b \, (T_{b,i,m} - T_\infty)\right]$$

$$\Pi_{26} = \Delta i_{b,md} \, (\rho\delta)_{b,o} \, \varepsilon_{b,md} / \left[(\rho\delta)_b \, c_b \, (T_{b,i,m} - T_\infty)\right]$$

$$\Pi_{27} = \Delta i_{b,en} \, (\rho\delta)_{b,o} \, \varepsilon_{b,en} / \left[(\rho\delta)_b \, c_b \, (T_{b,i,m} - T_\infty)\right]$$

$$\Pi_{28} = \Delta i_{b,ex} \, (\rho\delta)_{b,o} \, \varepsilon_{b,ex} / \left[(\rho\delta)_b \, c_b \, (T_{b,i,m} - T_\infty)\right]$$

$$\Pi_{29} = t_{ref} \, K_{b,md}$$

$$\Pi_{210} = E_{b,md} / R \, T_\infty$$

$$\Pi_{211} = t_{ref} \, K_{b,en}$$

$$\Pi_{212} = E_{b,en} / R \, T_\infty$$

$$\Pi_{213} = t_{ref} \, K_{b,ex}$$

$$\Pi_{214} = E_{b,ex} / R \, T_\infty$$

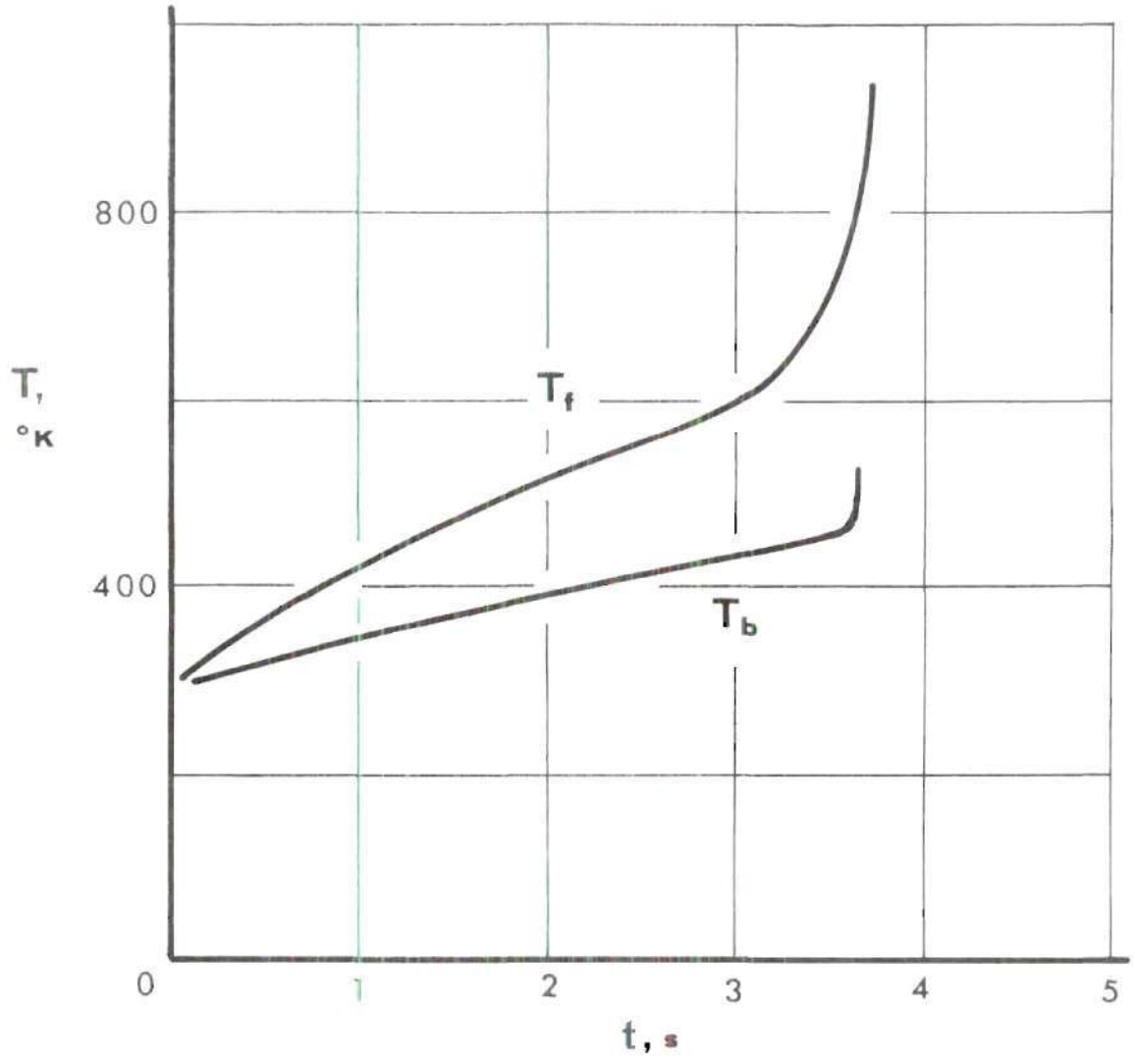

Figure 4. Temperature Response Using McCarter's Pyrolysis Data (Table 3, GIRCFF fabric number 5 front with fabric number 5 back)

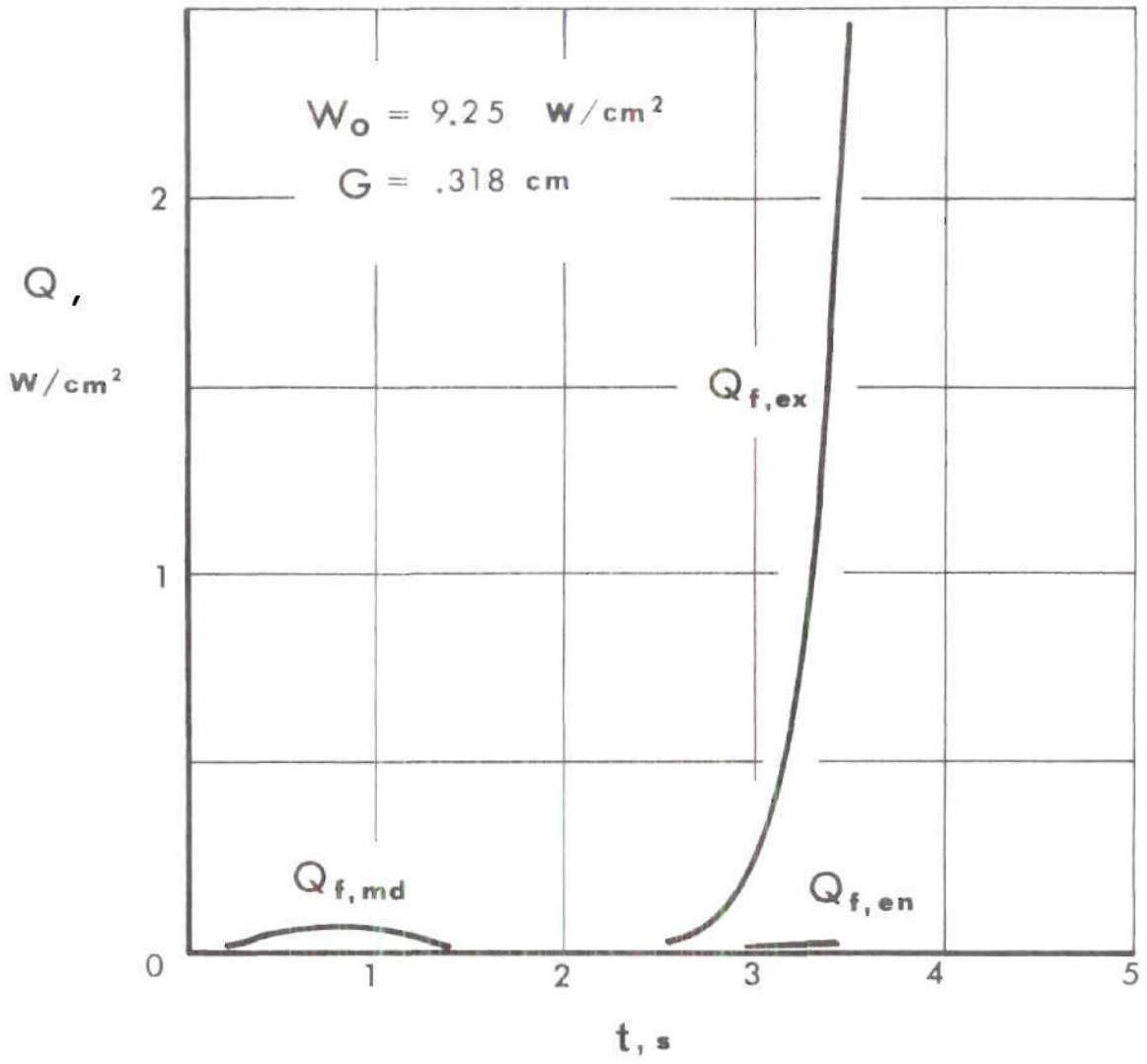

Figure 5. Energy Components of Moisture Desorption, Pyrolysis, and Exothermic Reaction (Using McCarter's pyrolysis data in Table 3 for GIRCFF fabric number 5 front with fabric number 5 rear)

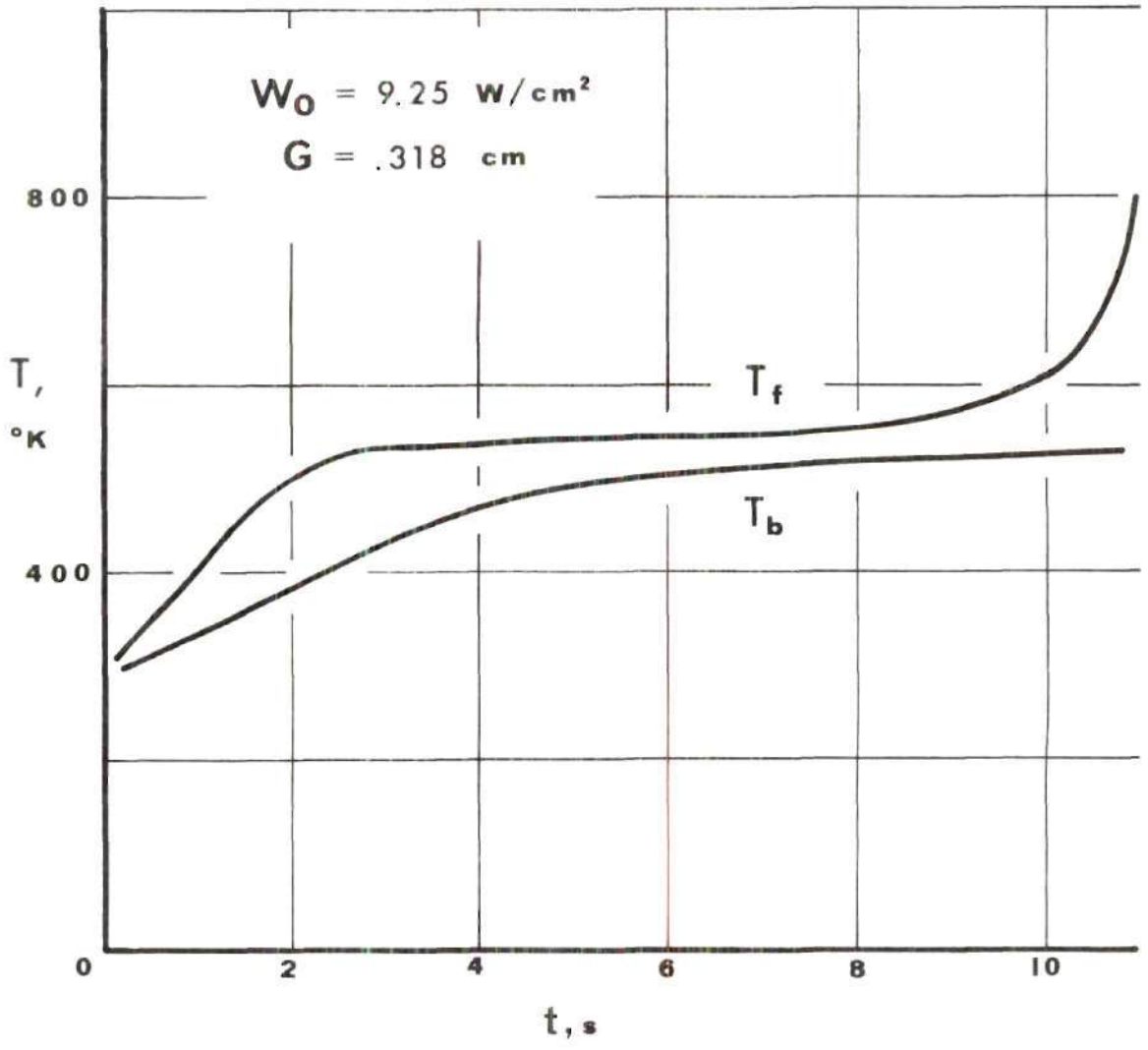

Figure 6. Temperature Response Using Modified Pyrolysis Data (Table 3, GIRCFF fabric number 5 front with fabric number 5 back)

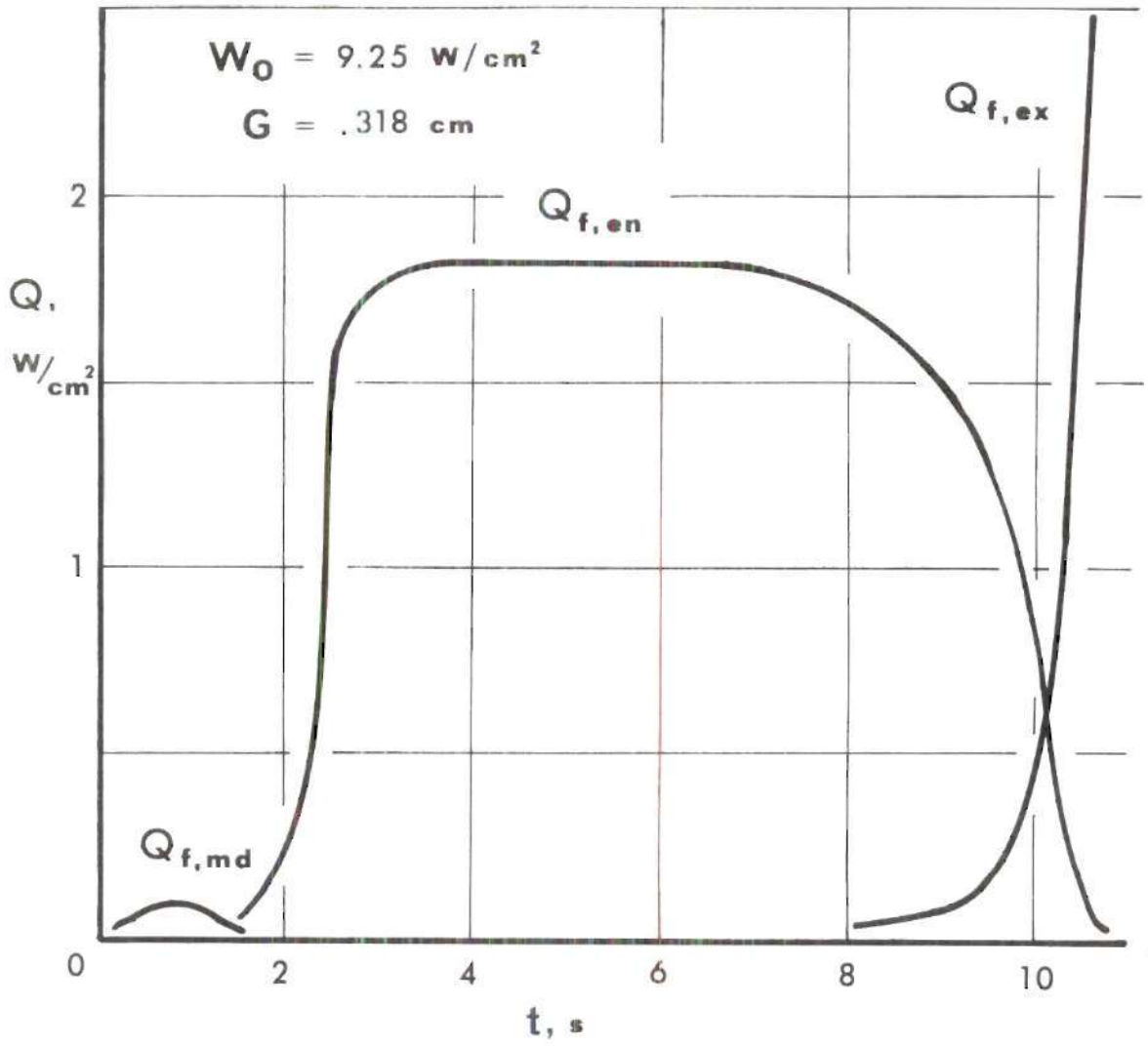

Figure 7. Energy Components of Gas Phase Reactions Using Modified Pyrolysis Data (Table 3, GIRCFF fabric number 5 front with fabric number 5 rear)

Table 3. Reaction Kinetics Parameters Used in the Numerical Solution (GIRCFF fabric number 5 after Reference [5]).

Moisture Desorption:

(Δi)	= 101.6 Ws/g	Π_{16}	= 0.2254
ε	= 4.28 %	Π_{19}	= 1.03×10^{14}
K	= 4.88×10^{13} 1/s	Π_{110}	= 39.75
n	= 2.6		
E	= 97.4 kWs/g mole		

Endothermic Pyrolysis, McCarter's Data: *

(Δi)	= 83.74 Ws/g	Π_{17}	= 0.0444
ε	= 50.0 %	Π_{111}	= 2.02×10^{14}
K	= 9.54×10^{12} 1/s	Π_{112}	= 89.49
n	= 1.1		
E	= 219.5 kWs/g mole		

Endothermic Pyrolysis, Modified Kinetics: **

(Δi)	= 2.00 kWs/g	Π_{17}	= 2.161
ε	= 50.0 %	Π_{111}	= 2.02×10^{14}
K	= 9.54×10^{12} 1/s	Π_{112}	= 57.07
n	= 1.1		
E	= 140.0 kWs/g mole		

Exothermic Reaction:

(Δi)	= 14.78 kWs/g	Π_{18}	= 32.79
ε	= 45.7 %	Π_{113}	= 1.94×10^{10}
K	= 9.20×10^{9} 1/s	Π_{114}	= 58.13
n	= 1.6		
E	= 142.6 kWs/g mole		

* Reduced by Reference [4] from the data of Dr. McCarter of NBS.
** Discussed in Numerical Solution for Radiative Heating.

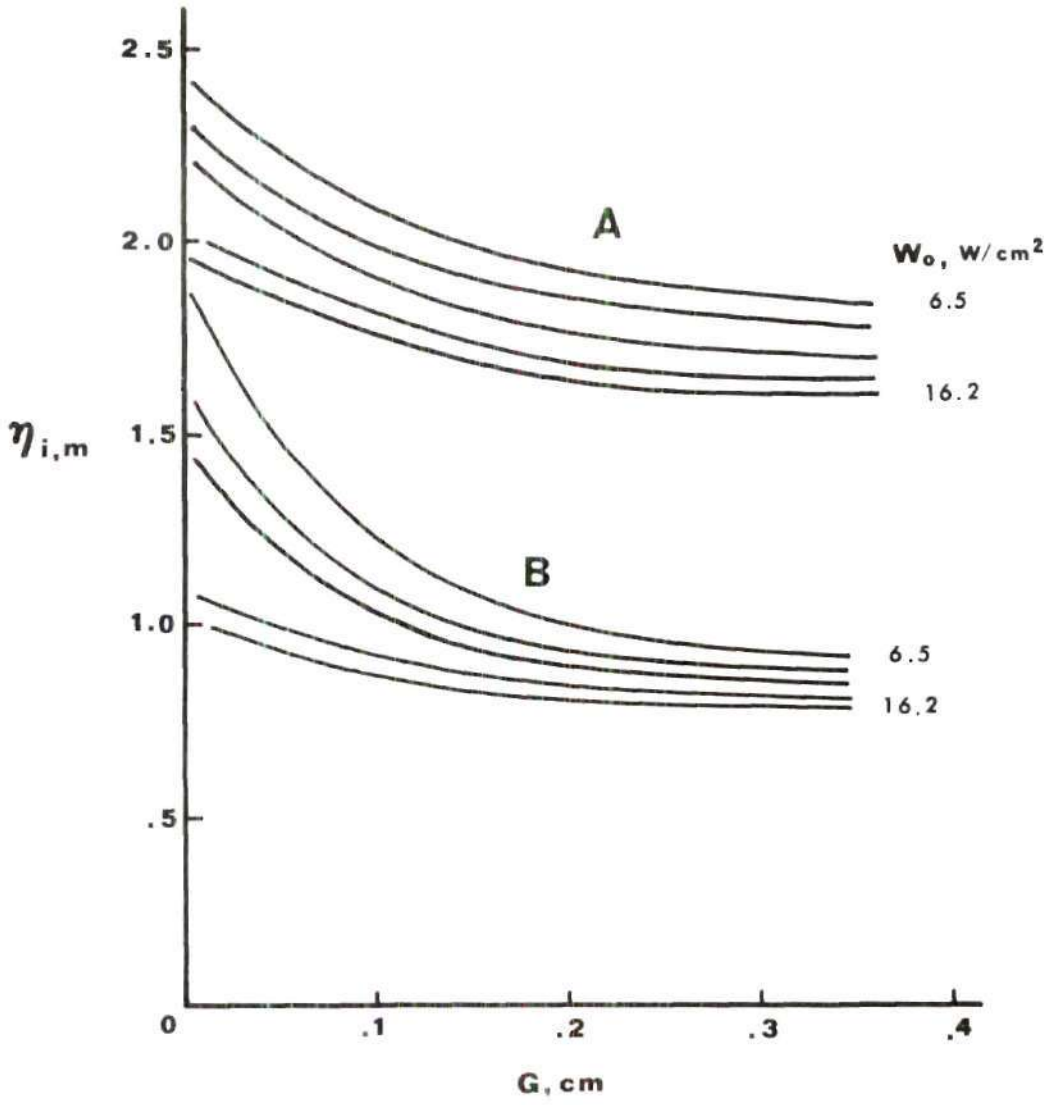

Figure 8. Predicted Destruction Times for the Front Fabric from the Numerical Solution for Radiative Heating (Curves A represent GIRCFF fabric number 5 front with fabric number 5 back, curves B represent fabric number 2 front with fabric number 5 back)

melting time results for an assembly of a 100% polyester as the front fabric (GIRCFF fabric number 2) with fabric number 5 as the back fabric.

Several observations are made from the numerical solution for radiative heating. First, the ignition temperatures predicted from the numerical solution for the cotton fabric indicates an ignition temperature somewhat higher than that obtained using the Setchkin furnace [4,5]. By taking ignition to occur at the intercepts of the inert heating region and the thermal excursion, an ignition temperature of 355°C is obtained for GIRCFF fabric number 5. This is 41°C higher than the reported ignition temperature.

A second observation is the significance of air gap on destruction time. From Figure 8 it is seen that fabric destruction time is longest at the smallest gaps. This is attributed to the increase in convection film coefficients h_2 and h_3, and convected flux, at decreasing air gap.

A third observation is the significance of endothermic gasification upon the fabric ignition time, as shown in the temperature responses of Figures 4 and 6. Figure 4 was obtained using McCarter's pyrolysis data, for which the pyrolysis mass fraction reached a value of only 0.0001 by the time of ignition. The insignificance of pyrolysis in Figure 4 is attributed to the fact that the reported activation energy is 50% higher than that for the exothermic reaction and that the reaction enthalpy for pyrolysis is

only 0.5% of that for exothermic reaction. Physical observations indicate that endothermic reactions are significant prior to combustion. Thus it is reasonable to assume that the activation energy for pyrolysis is actually lower than that of the exothermic reaction. Also, reaction kinetics data for other pyrolysing solids indicate that the reaction enthalpy of gasification is of the order of 0.05 to 0.08 of the reaction enthalpy of exothermic reaction. Thus the reported reaction enthalpy is thought to be unrealistic, and a higher value is approximated from the exothermic reaction data of Reference [5]. The inherent difficulties in measurement of reaction kinetics have been discussed by Tesner [20]. The modified pyrolysis data are presented in Table 3.

This completes the radiative ignition time analysis. Equipment and procedures used to measure the assembly destruction times are presented in the next sections.

Experimental Measurements

The purpose of the ignition time tests is to relate the exposure time to a known heat flux, to the probability of fabric ignition. An apparatus was required to expose a fabric assembly to a constant intensity heat flux with instrumentation capable of detecting ignition and measuring the ignition time.

Apparatus and Instrumentation

The Radiative Ignition Time Apparatus (RITA) was used to expose 2.54 cm diameter fabric samples to a variable intensity heat flux of between 0.25 and 20.0 W/cm^2, with transient response in exposure on the order of 0.02 seconds. This apparatus has been used in previous ignition studies to obtain radiative ignition times on single fabrics, and complete details of this equipment are available in References [4,5].

The apparatus consists of a radiant quartz lamp heater, Model Number 5208-5 from Research, Inc., and a mechanical shutter system for the rapid exposure of the sample to the heater. Humidity and temperature of the environment were controlled by a thermostatically and psychrometrically regulated chamber built by Environair Systems, Inc., which houses the RITA, and is shown in Figure 9. Ambient temperature and relative humidity were regulated automatically to within ± 0.2°C and ± 2%, respectively. The apparatus assembly inside the environmental chamber is shown in Figure 10.

Existing fabric holders were used for the fabric assembly ignition tests. Aluminum spacing rings were fabricated to separate the fabric layers and were 0.159 and 0.318 cm thickness (±0.002 cm). A spacing ring and fabric holder are shown in Figure 11.

Basic operating principles were to bring the radiant

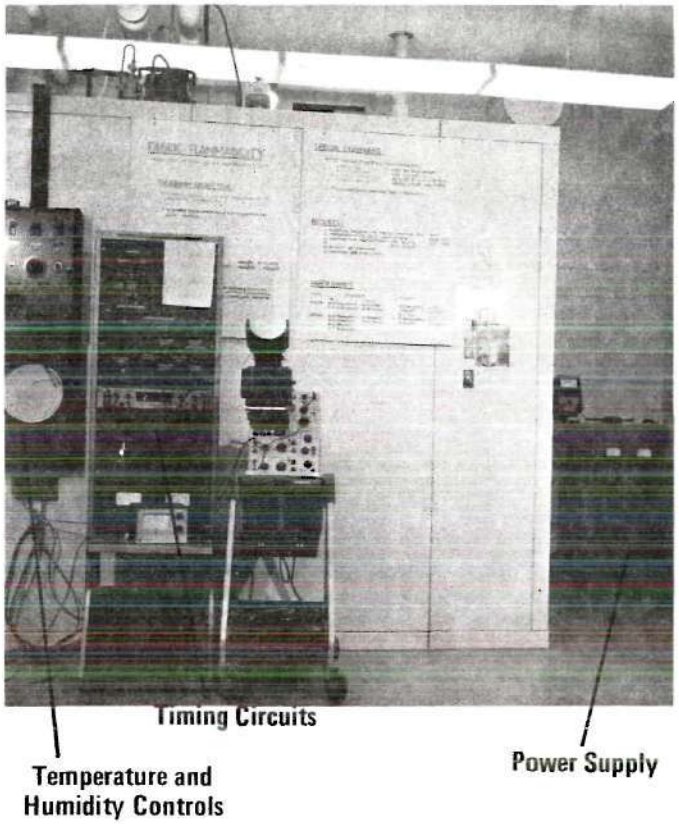

Figure 9. Environmental Chamber and Ancillary Equipment.

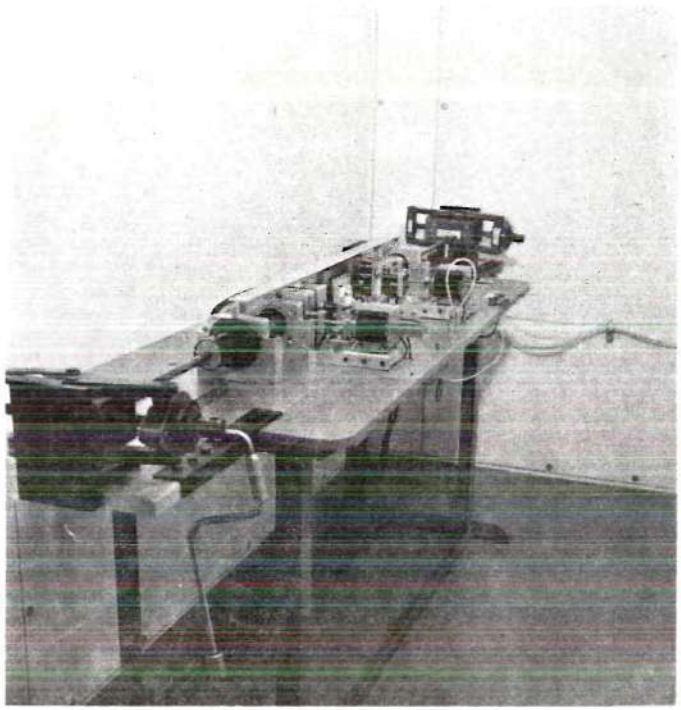

Figure 10. Radiative Ignition Time Apparatus Inside of Environmental Chamber.

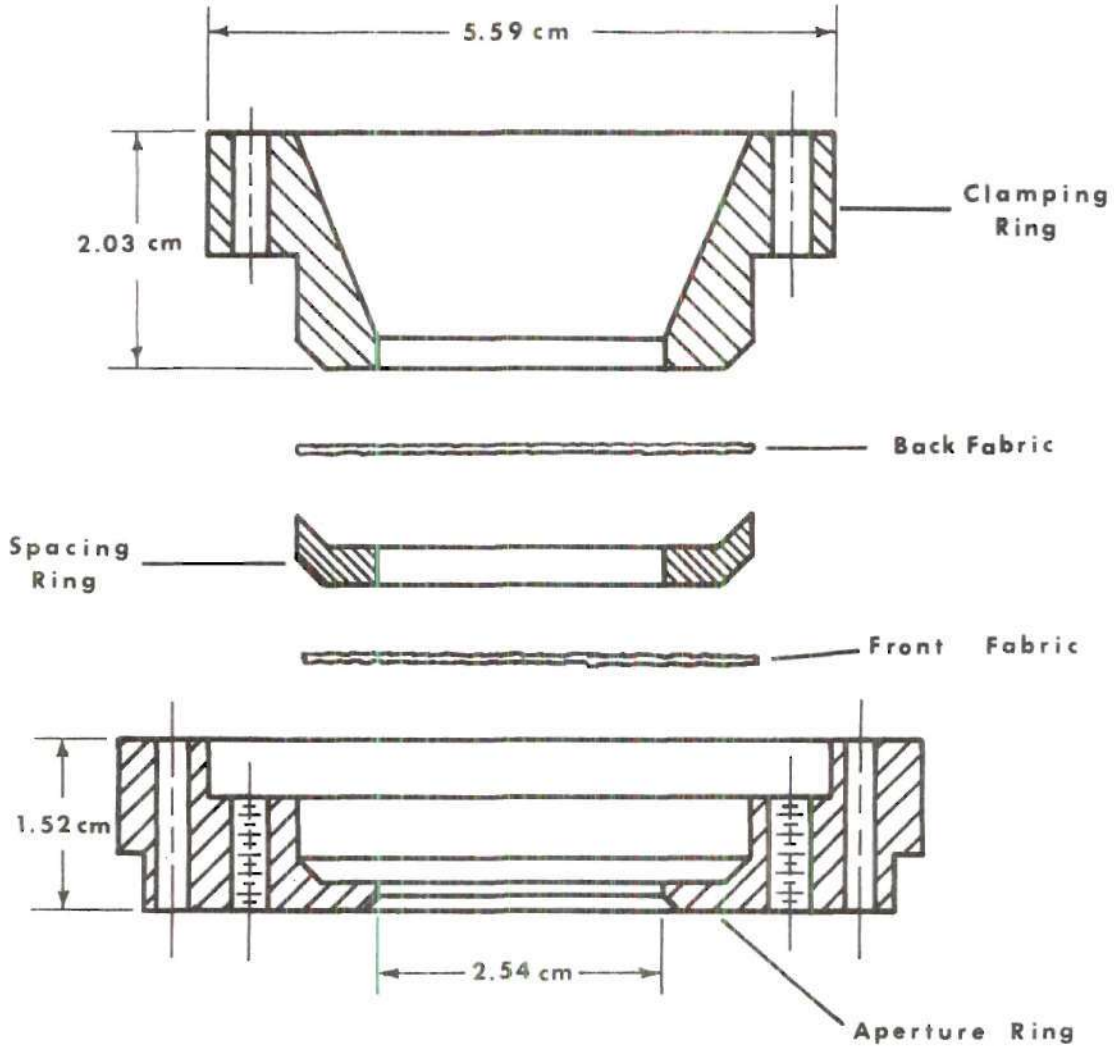

Figure 11. Cross-Sectional View of the Fabric Assembly Holder

heater to equilibrium temperature just prior to exposure, while keeping the fabric isolated, and then opening the shutters to suddenly and completely expose the fabric to the radiant heater. The thermal response of the fabric system was then monitored for the occurrence of ignition or melting.

The time-temperature history was recorded using a Textronic dual beam oscilloscope, Model Number 502A, on Polaroid film. For igniting fabrics, the front fabric was monitored by an infrared detector, Model Mark 1 Infrascope by Barnes Engineering. The back fabric was monitored using a Temptron Infrascope, Model IT-7310. For melting fabrics the response of the total system was monitored by using simply the Barnes Infrascope. For ignition detection of the front fabric a mirror was employed, Kerr Dental Supply Type 5C, and was supported near the front surface. The mirror and infrascope orientation are shown in Figures 12 and 13.

Preheat time for the heater was controlled by a mechanical timing mechanism. A Hewlett-Packard VTVM, Model Number 500-H, was used to measure idle heater voltage. Calibration of incident heat flux and preheat time for given voltage were obtained from Reference [4]. A schematic of the instrumentation is shown in Figure D3 in Appendix D.

Testing procedures used in the measurement of ignition and melting times are discussed in the next section.

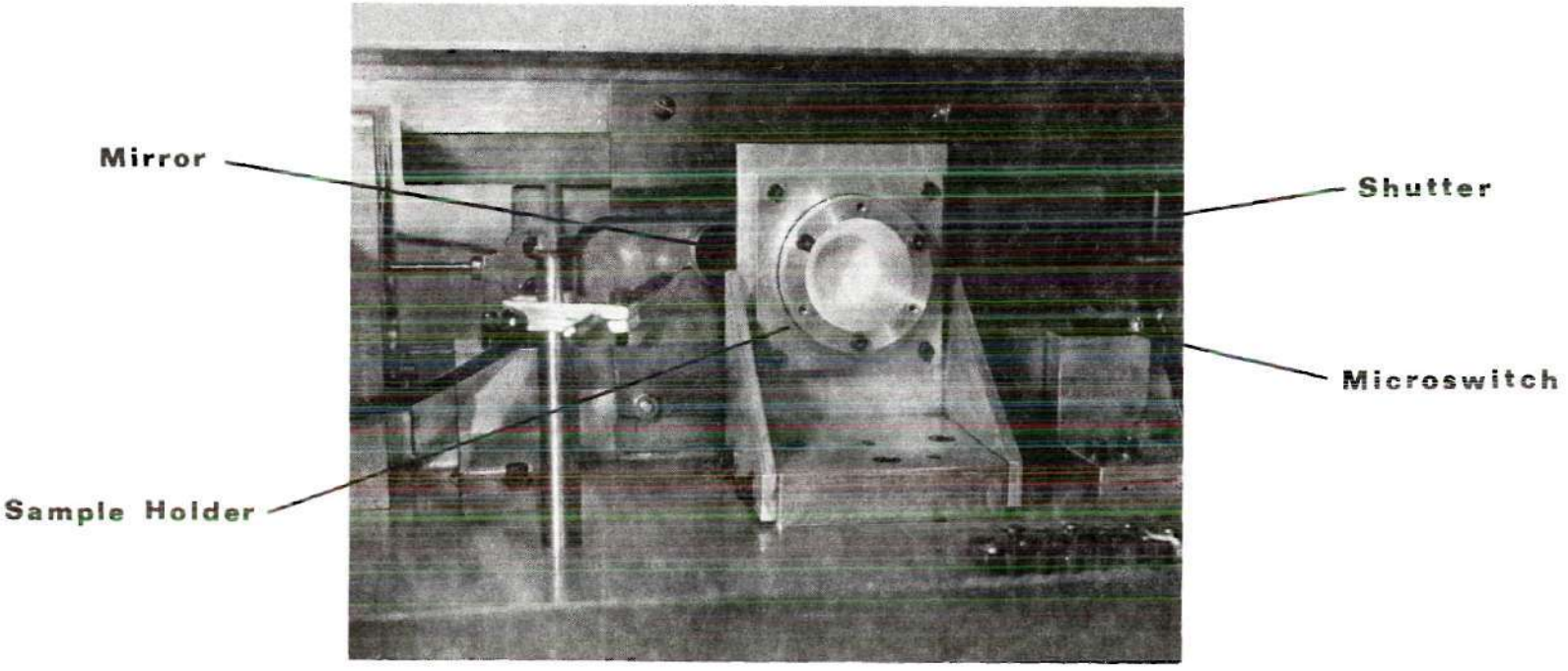

Figure 12. Experimental Arrangement for Fabric Assembly Ignition Tests.

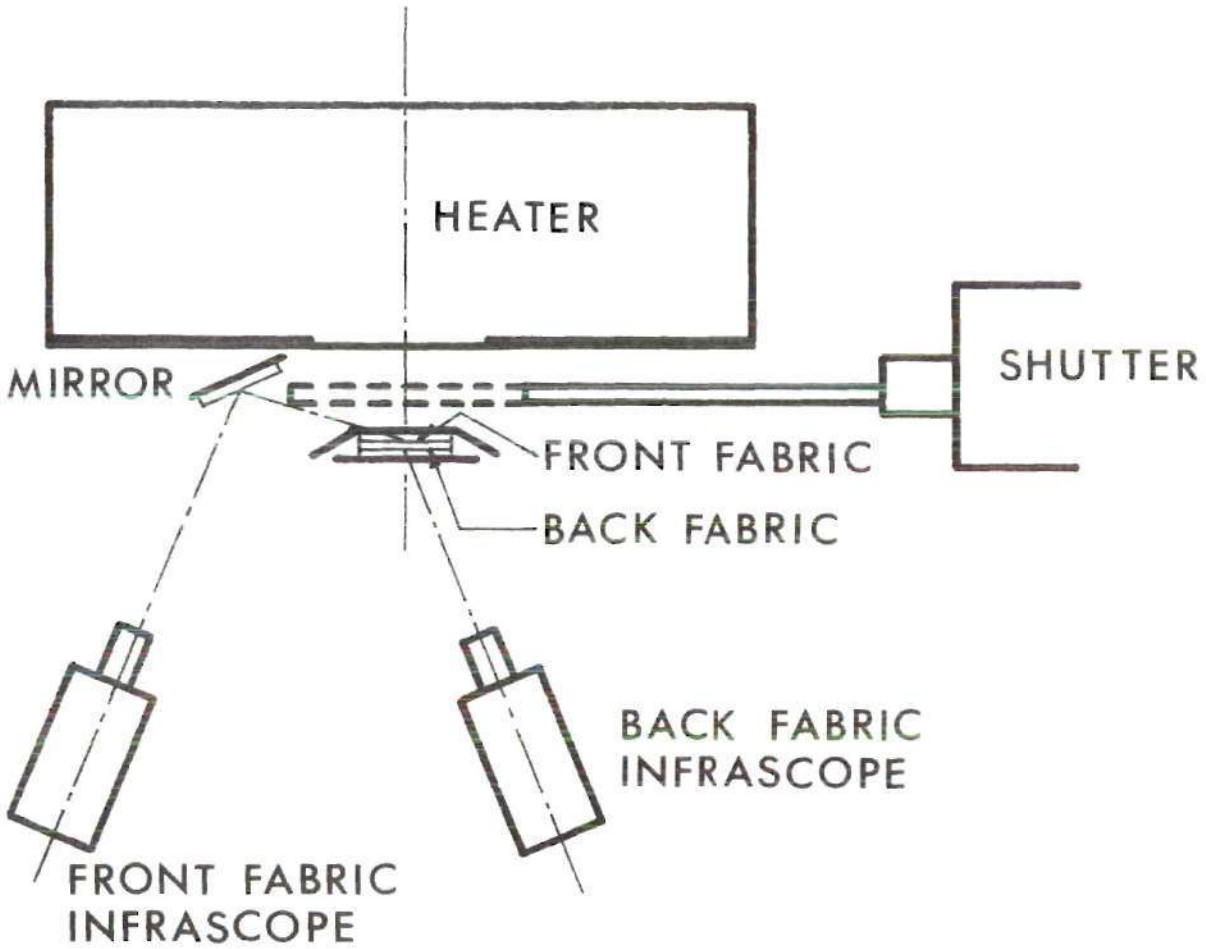

Figure 13. Schematic of Experimental Arrangement for Ignition Test on Fabric Assemblies

Experimental Procedures

The procedures followed in the determination of fabric destruction time consisted of the preparation and preconditioning of the fabric, and the exposure of the fabric sample to the radiant heater until the occurrence of ignition or melting. The heating and destruction processes were also observed visually. Destruction time of the igniting fabrics was determined by the occurrence of a luminous flame, whereas the melting fabrics were considered destroyed when the fabric structure decomposed and melt-through occurred.

Ambient test conditions were controlled by conducting the radiative tests inside the environmental control chamber. The desired test conditions of 22°C and 30% relative humidity were set on the Honeywell control unit (shown in Figure 9) and maintained automatically. Chamber temperature and relative humidity were measured using wet and dry bulb thermometers.

Fabric specimens were prepared from material selected and furnished by the GIRCFF. One and one half inch (3.81 cm) diameter pieces were cut from large sheets by means of a circular die which yielded cleanly cut samples of appropriate size for the fabric holder. The samples were stored in the environmental chamber at the desired ambient testing conditions for a minimum period of 24 hours prior to testing to insure properly preconditioned moisture content and temperature.

The basic operating principles of the RITA were discussed in the previous section. The proper idle heater voltage for the desired heat flux, and the proper preheat time (for the heater to reach equilibrium before shutter opening) were set. For igniting front fabric tests, the Barnes infrascope was positioned and focused on the front fabric through the mirror, as shown in Figure 13. The Temptron infrascope was positioned to the rear of the environmental chamber and focused on the back fabric. For a melting front fabric, no significant response was obtained from the front infrascope. Thus destruction and melt through were determined by the use of a single infrascope (the Barnes) located directly behind the back fabric and in line with the heater. The shutter mechanism was cocked and held in place by the release solenoid.

The preconditioned fabric pair was placed in a clean fabric holder, separated by the appropriate spacing ring, or in the case of zero gap tests, after the two fabrics had been gently pressed to insure initial contact. The fabric holder was then mounted on the holder support behind the shutter. After allowing proper warmup time for the infrascope amplifiers and the oscilloscope, the firing sequence was initialized. The heater was turned on and the shutter released automatically by the timing device once heater equilibrium was reached. Opening of the shutter contacted with the microswitch which in turn triggered the oscilloscope.

The emf output of the infrared detector as a function of time was then recorded on Polaroid film.

Visual observation of fabric heating and destruction was made from inside the control chamber. Relevant events in the heating process such as the start of pyrolysis and the occurrence of ignition or melt-through were timed with stopwatches for later correlation with the oscilloscope trace. Ignition and flame occurrence, as well as the decomposition of the fabric, were observed from the plane of the fabric. Observation of melt-through was made through the mirror.

Test data and its reduction are presented in the next section.

Data Reduction and Results

Destruction times were obtained from the oscilloscope traces of infrascope emf. Ignition tests recorded the heating history of the front and rear fabrics. Melting time tests recorded the transmitted flux of the heater through the assembly. Ignition times were determined from the intercept of the tangents of the inert heating region and the exponential rise due to the onset of combustion. Melting times were determined from the intercepts of the tangents of the inert heating period and the sudden rise in transmitted flux due to the melt through of the fabric. Destruction time was determined as the ignition or melt through of either front or rear fabrics, and for the

combinations tested, was that of the front fabric. Sample oscilloscope traces for ignition and melting tests are shown in Figures D1 and D2 of the Appendix, respectively.

The reduced data obtained from the destruction time tests were the destruction time, $t_{i,m}$, the total incident heating intensity, W_o, and the air gap, G. Ignition time and heating intensity were normalized by equations (18) and (19) to permit correlation with previous radiative ignition time studies.

A total of 143 tests were conducted on the RITA to determine the interaction of two parallel fabric layers. Tests were designed to examine the effects of variable heating intensity and variable inter-fabric spacing upon the fabric assembly destruction time. The five heating intensities were 6.5, 7.6, 9.25, 13.8, and 16.2 W/cm^2. Fabric spacing was set at 0.00, 0.159, and 0.318 cm.

The combination of fabric number 5 front with fabric number 5 back was used for the majority of the tests to determine the effects of gap and heating intensity upon ignition time. A sample test data sheet is presented in Figure D1 of the Appendix. A statistical summary of these tests is presented in Table 4, in which $\bar{t}_{i,m}$ is the mean destruction time of the front fabric and $\bar{s}$ is the sample variance. Results for this combination are presented in Figure 14.

Tests were conducted on the combination of fabric

Table 4. Summary of Fabric Assembly Ignition Tests (Fabric number 5 front with fabric number 5 back).

W_o	Gap	Number of Tests	$\bar{t}_{i,m}$	$\bar{s}$
W/cm^2	cm		s	s
6.50	0.000	5	28.45	0.609
	0.159	9	22.34	0.945
	0.318	4	22.94	0.740
7.60	0.000	1	22.50	---
	0.159	1	17.50	---
	0.318	7	17.65	0.747
9.25	0.000	10	15.08	0.225
	0.159	5	13.00	0.526
	0.318	8	12.54	0.713
13.80	0.000	1	11.10	---
	0.159	9	8.21	0.406
	0.318	5	7.50	0.207
16.20	0.000	1	8.80	---
	0.159	1	6.16	---
	0.318	4	6.48	0.171

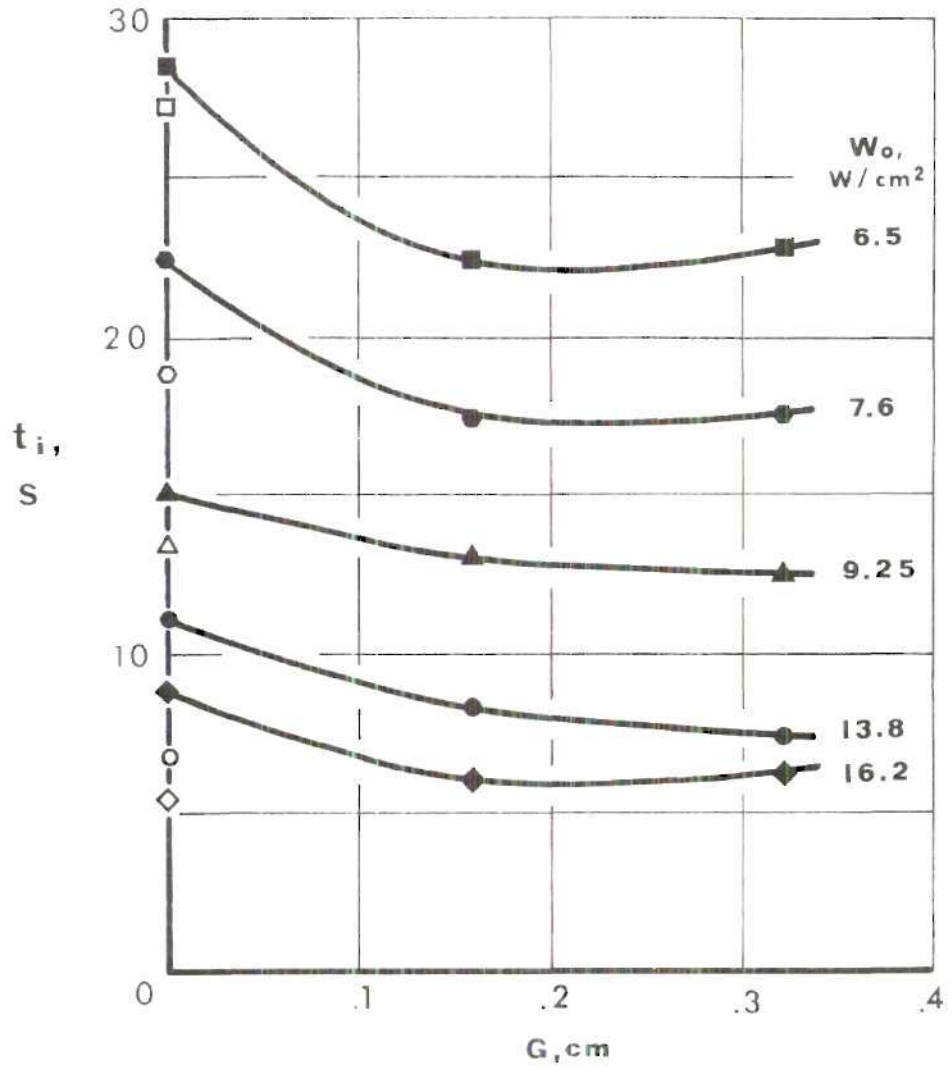

Figure 14. Ignition Time of the Front Fabric as a Function of Spacing (GIRCFF fabric number 5 front with fabric number 5 back, open points designate previous single fabric ignition times [5])

number 2 front with fabric number 5 back to determine the interaction of a synthetic and a natural fiber material under radiative heating. A sample test data sheet is presented in Figure D2 of the Appendix. Melting times of the front fabric for this combination are shown in Figure 15.

Normalized destruction time measurements for the front fabric are presented in Figure 16. Curve A represents an inert heating model (without convective or radiative losses) for a composite assembly. Curve B represents the numerical solution for the heating of two fabric number 5's at G = .318 cm, using McCarter's pyrolysis data. Curve C represents the numerical solution for the heating of two fabric number 5's at G = .318 cm, using the modified pyrolysis kinetics. Numerical values of the reaction kinetics used to obtain curves B and C are listed in Table 3.

Discussion of the ignition and melting time results is presented in the next section.

Discussion of Results

Destruction time data for the front fabric is shown plotted in Figures 14 through 16. From Figure 14 it is seen that at heating intensities greater than about 8 W/cm^2 the ignition time of the fabric assembly is longer than that for a single fabric, by as much as 100% at the highest heating intensity. At low heating intensities, the opposite trend is seen, with ignition time occuring sooner by as much as

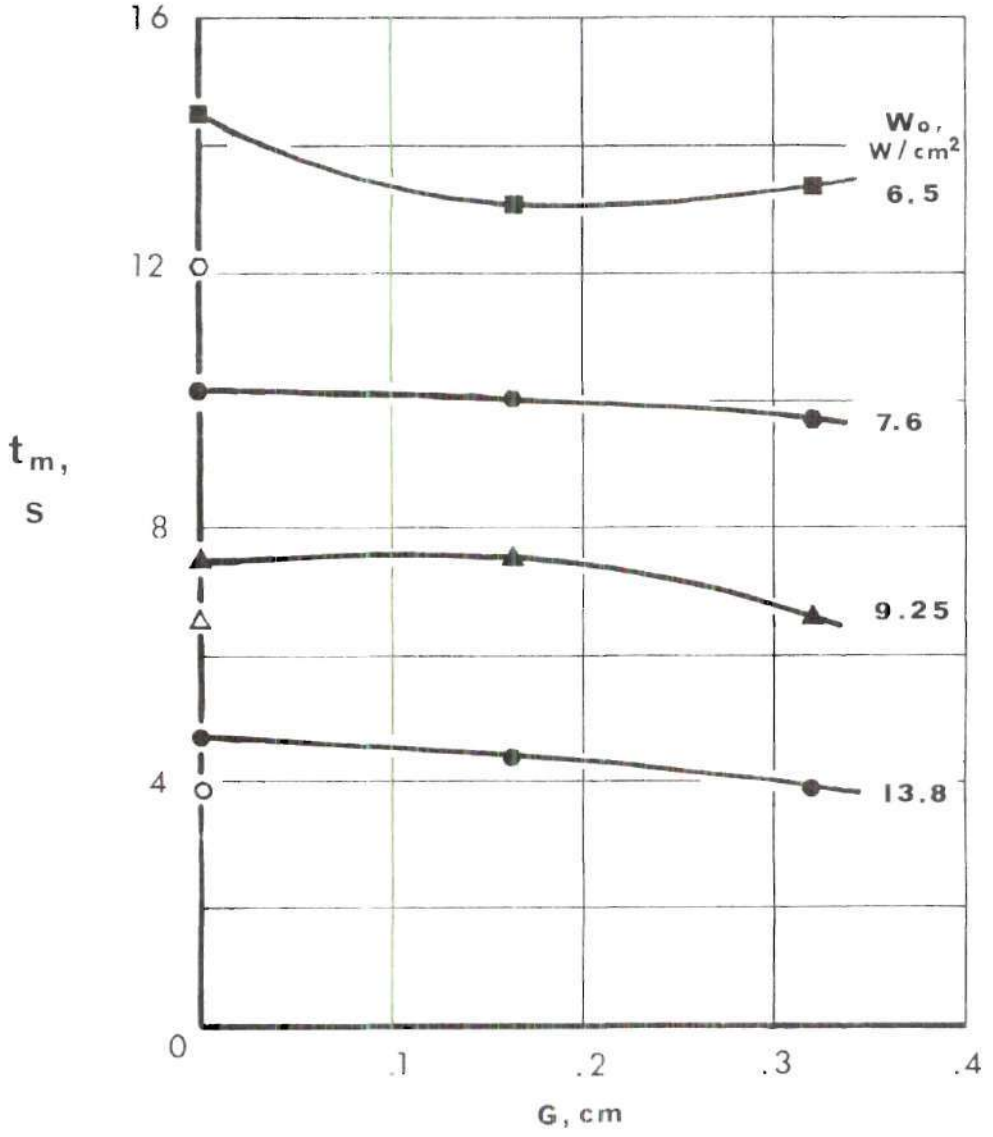

Figure 15. Melting Time of the Front Fabric as a Function of Spacing (GIRCFF fabric number 2 front with fabric number 5 back; open points designate previous single fabric destruction times [5])

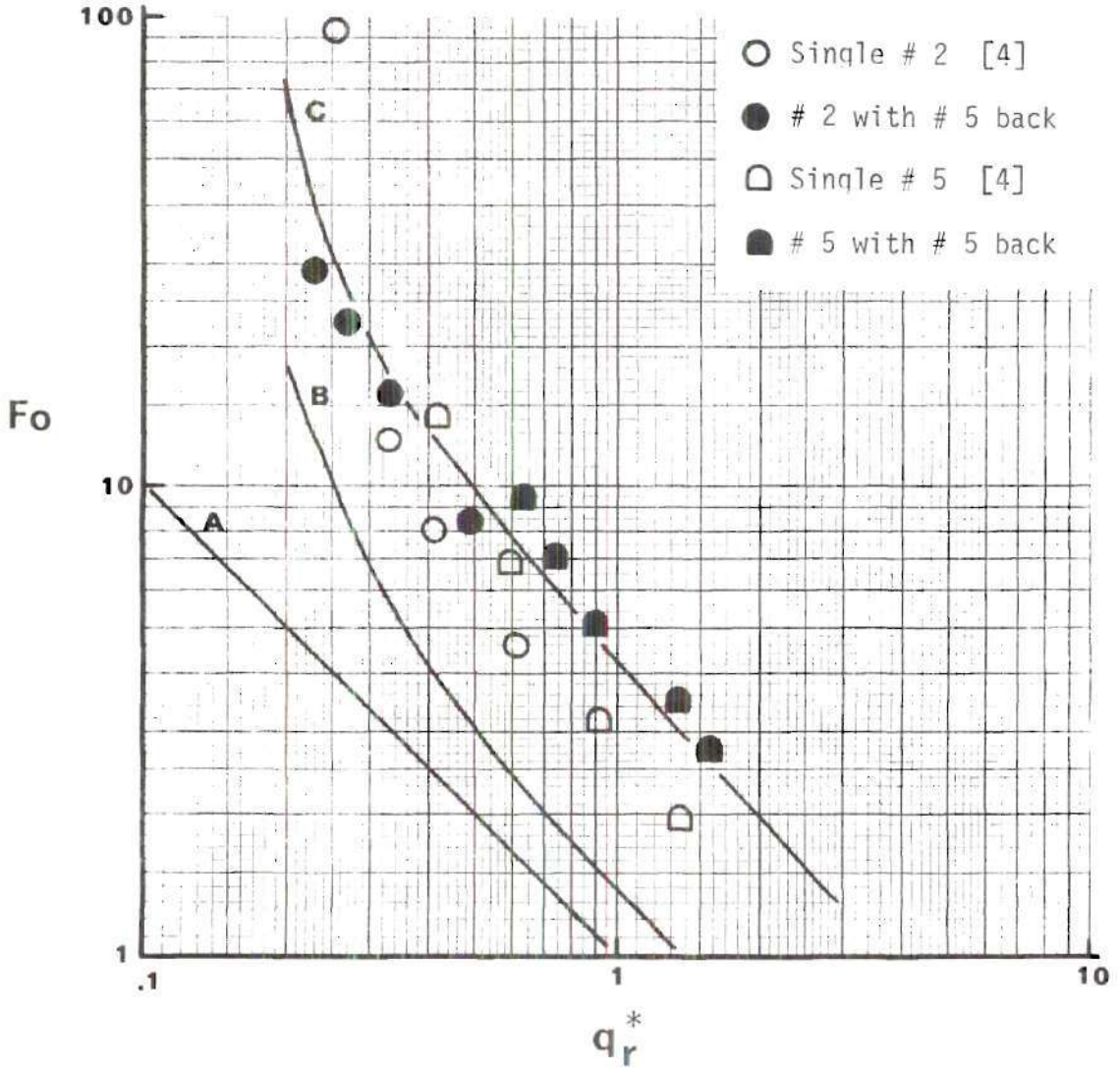

Figure 16. Front Fabric Destruction Time Data in a Two Fabric Assembly Correlated with Various Analyses (Curve A is inert heating without convection, curve B is the numerical solution using McCarter's pyrolysis data, and curve C is the numerical solution using the modified pyrolysis kinetics, all computed for fabric number 5 front with fabric number 5 back at G = 0.318 cm)

50% at the lowest heating intensity.

For the fabric combination of the polyester fabric with the cotton fabric behind it, destruction of the polyester fabric is now possible at a heating intensity of 6.5 W/cm^2, whereas for a single layer of the polyester it was not. The general experimental trends appear very similar for both assemblies of two cotton fabrics (GIRCFF fabric number 5 front and back) and of polyester (fabric number 2) front with fabric number 5 back.

In comparing destruction time data for both combinations it is noted that at heating intensities greater than 13 W/cm^2 the destruction times are longer than the destruction times obtained for single fabrics. As the gap increases at these high fluxes the destruction time decreases slightly, showing the decreased convective interchange between front and back fabrics.

At moderate fluxes of 9.25 W/cm^2 the ignition time increases at the very small gap and then decreases to a time close to the ignition time of the single fabric. This is best explained by the decrease in convective fluxes with distance, as at small distances convective interchange is greatest, and front fabric destruction time longest. As gap increases however, convection decreases but the effect of rereflectivity and radiation do not. Consequently, destruction time decreases. At moderate heating fluxes and small gaps, rereflectivity is very nearly balanced by the

increased convective losses.

At low heating intensities destruction time for the front fabric is reduced by 30% for the case of two fabrics number 5. Destruction is now made possible in the case of the pair of 2 and 5 when it would not be possible for single fabric number 2. Both fabric combinations show that minimum ignition time occurs for a gap of approximately .159 cm, with an increase in ignition time as gap increases from .159 to .318 cm. This conclusion is consistent with both fabric pairs tested, but is in variance with predicted trends. Assuming that the differences in ignition time are statistically significant, this discrepancy is attributed to mass convection of pyrolysate gases which was neglected in the problem formulation. It is anticipated that the mechanics of gas flow are most significant at lower heating intensities.

Statistical analysis of ignition data indicates that the uncertainty associated with multilayer test are no greater than those associated with single layer fabric ignition tests. A statistical summary is presented in Table 3. Typical variance for single fabric ignition tests is reported to be approximately 5% [5]. For composite assembly tests it varies from 0.9% for high intensity to 3.6% for the low intensity.

It is noted that for the fabric pair of numbers 2 and 5 that destruction is possible at a lower incident heat flux than is possible for the single fabric number 2. This can

be directly attributed to the increase in total absorbed heat due to the rereflection of the rear fabric, which for combination of 2 and 5 amounts to a 17% increase. For air gaps greater than .159 cm convective losses from the front fabric are also reduced by 25% due to the insulating effect of the rear fabric.

Comparison of experimental and analytical results indicates that ignition occurs later by a factor of three to four. This result is similar to previous attempts to use a surface ignition criterion for fabric ignition. Experimentally, ignition was observed to occur in the gas phase, sometimes at the solid surface and sometimes completely in the gas phase (depending upon heating intensity). Mass transfer of decomposition products has been shown to be a significant heat transfer mechanism for intense radiative heating [21]. However, predicted trends have been experimentally obtained although the ignition simulation is not completely valid.

Normalized destruction time data is compared with previous single fabric destruction times in Figure 16. It is seen that the fabric assembly tests fall in the same general range as the single fabric tests. It can also be seen that for the range of heating intensities used, the lower limits of minimum heating intensity required for an ignition were not obtained. This is due to the fact that fabric assemblies ignite at lower heating intensities than

do single fabrics. It is also noted that in general melting fabrics have shorter destruction time than igniting fabrics.

From a comparison of melting time data for single layers of polyester, and assemblies of polyester with a cotton fabric behind it, no significant differences are noted. There is apparent thermal interaction between fabric layers of the assembly as predicted in the analyses, but there is no evidence of chemical interaction between fabric layers. At present there is no published data with which to correlate these results.

CHAPTER III

FABRIC ORIENTATION

The two problems associated with the overall fabric fire hazard studied in this investigation are the ignition of multi-layer systems and the ignition of fabrics exposed to a flame. The purpose of this chapter is to measure and assess the effects of fabric orientation with respect to the flame on the ignition time of single fabrics exposed to a flaming heat source.

The geometry of interest is the edge exposure to a premixed combusting gas jet. Parameters to be assessed include angle of impingement and variation of heating intensity. Edge impingement to a gas flame is anticipated to yield higher heating rates than previously studied. Results will be correlated with previous flame ignition time studies.

Modeling Analysis

The purpose of the modeling analysis is to determine the governing relations and parameters which describe the edge ignition of fabrics. The response of the fabric under convective heating is required for the prediction of the fabric ignition time. For the general model shown in Figure 17 the equation for lumped parameter conservation of

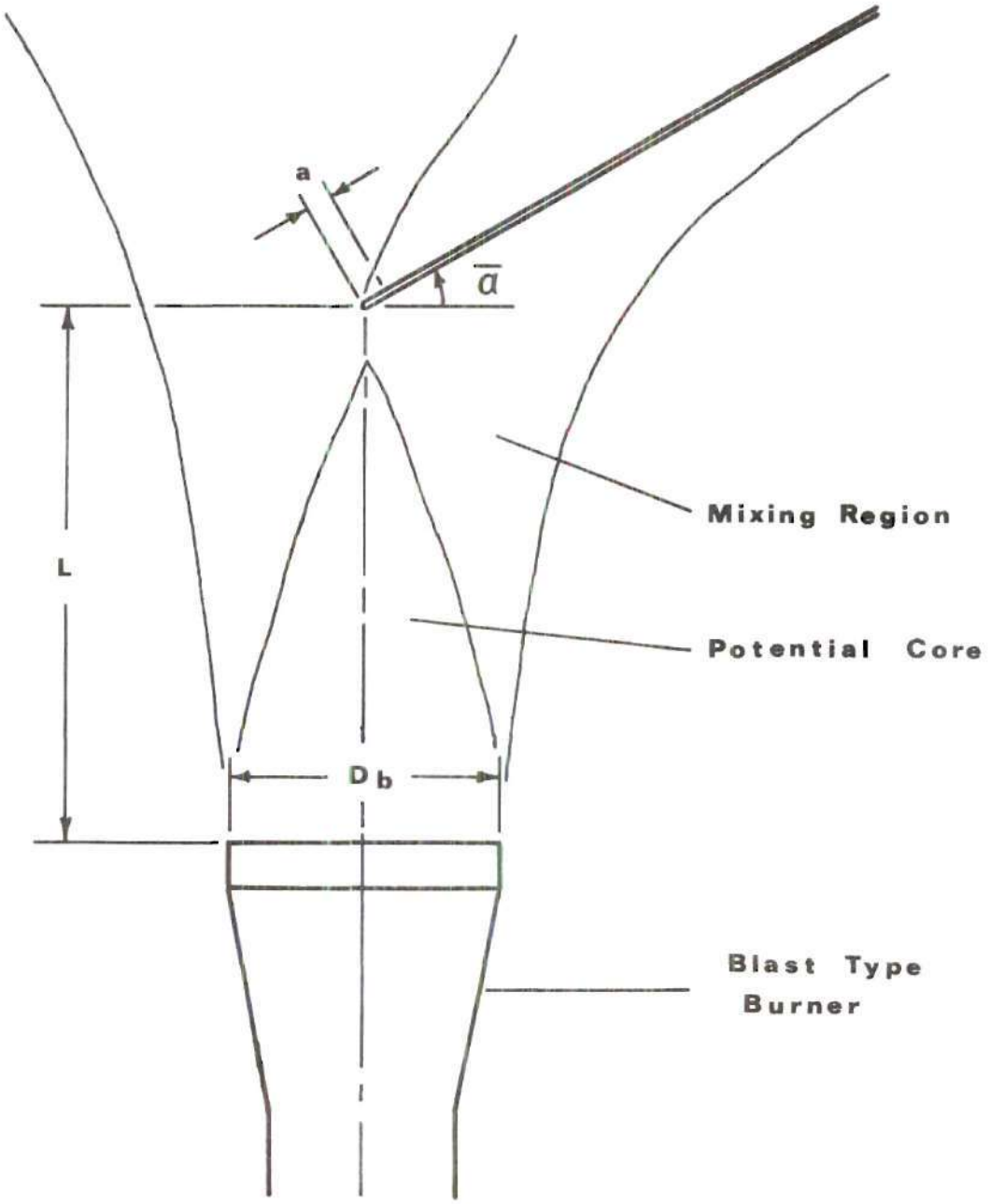

Figure 17. The Geometry of Fabric-Flame Interaction

energy under gas flame heating may be written as

$$(\rho\delta)_c \frac{dT}{dt} = 2\bar{h}_c (T_g - T) - 2 \sigma e F (T^4 - T_\infty^4)$$

$$- \Delta i_{md} \frac{d\lambda}{dt}md - \Delta i_{en} \frac{d\lambda}{dt}en + \Delta i_{ex} \frac{d\lambda}{dt}ex \quad (30)$$

where $2\bar{h}_c$ is the mean front and back convective film coefficient, T_g is the flame temperature, and the energy components have been described previously in the radiative ignition analysis of Chapter II. Reaction rates for moisture desorption, pyrolysis, and exothermal combustion are described in terms of nth-order Arhenius type relations, as given by equation

$$\frac{d\lambda}{dt} = K(1-\lambda)^n \exp(-E/RT) \quad (3)$$

Equation (30) may be simplfied through physical considerations. The exothermic reaction, together with its ensuing thermal feedback to the fabric, are neglected because of the energy evolved during oxidation is overwhelmed by the heat supplied to the fabric by the gas flame. Also, for the case of low humidity, it is reasonable to neglect moisture desorption. It has been shown that for high heating rates that radiative cooling may be neglected with an associated error of approximately 5% [5]. Thus for the case of high convective heating the conservation of energy

equation may be written as

$$(\rho\delta)_c \frac{dT}{dt} = 2h_c (T_g - T) \tag{31}$$

where the convective heating coefficient $2h_c$ is as yet unspecified.

An ignition criterion for this inert model is the attainment of the measured ignition temperatures [4]. These temperatures were obtained by heating of fabric specimens in a Setchkin furnace. Ambient gas temperature at the time of ignition was defined as the ignition temperature.

The above governing equation may be integrated to give the temperature response of the fabric, and its ignition time. Direct integration of equation (31) yields

$$\theta = \theta_o \exp(-2h_c t/(\rho\delta)c) \tag{32}$$

where θ_o is the nondimensionalized initial temperature. The ignition time, obtained from equation (32), is expressed by

$$t_{i,m} = \rho\delta\ \bar{c}/2\bar{h}_c\ \ln[\frac{T_g - T_o}{T_g - T_i}] \tag{33}$$

The fabric specific mass is assumed to remain constant during the preignition heating. The specific heat is approximated by a temperature averaged value, $\bar{c}$, defined by

$$\bar{c} = \frac{1}{T_i - T_o} \int_{T_o}^{T_{i,m}} c(T)dT \qquad (34)$$

The key problem associated with the use of this ignition model is the determination of the appropriate film coefficient to describe the heating rate of the flame. This requires modeling of the fabric and the choice of appropriate scaling dimensions for the fabric-flame interaction.

Inspection of photomicrographs of the GIRCFF fabrics reveals the randomness of the substructure of the fabrics, a fact that makes modeling of the fabric geometry difficult. However, the fabrics are characterized by the lengths d, the fabric thread diameter, and δ, the fabric thickness. The intersticial spacing of the fabric weave is also a possible parameter, but is very random. The photographs do reveal that the fabrics can be generally classified according to weave structure and geometry.

A first class of fabrics are those for which the thread diameter is of the same general dimensions as the fabric thickness. These fabrics are not densely woven and present the appearance of a fine mesh screen. Fabrics of this type are GIRCFF fabrics number 2, 10, 12, 16, and 17.

A second class of fabrics are those of the same general weave as the first group but with a more densely packed substructure. These fabrics appear to have flat surfaces, and consist of GIRCFF fabrics number 4, 6, 13, and 14.

A third classification of the fabrics consists of those with small thread diameter with respect to the fabric thickness. For these fabrics the weave contains intersticially looping threads. Fabrics of this class are GIRCFF fabrics number 5, 7, and 11.

From the above generalized fabric descriptions several fabric models are considered. First, the fabrics which are dense yet thin may be approximated as flat non-porous slabs. For thicker fabrics which are not well approximated by a flat plate, the fabric edge may be approximated by a curved body, with burner gases impinging normally to it. For a porous fabric, this curved edge is approximated by a cylinder of diameter equal to the fabric thickness. Fabrics with very random weaves and exposed single threads suggest the possible ignition of the individual threads. These can also be approximated by a cylindrical body.

Appropriate heat transfer models for the above fabric models will be discussed in the next sections. Determination of the appropriate film coefficient depends upon the degree to which the model chosen simulates the fabric geometry.

Thin Inert Fabric Model

Thin closely woven fabrics may be approximated by a flat plate. For forced convection of hot gases flowing parallel to a flat surface, the heat transfer rate may be obtained from Pohlhausen's equation [22] as

$$\overline{Nu}_x = 0.664 \ (Pr)^{1/3} \ (Re_x)^{1/2} \tag{35}$$

where the Nusselt number denotes heat transfer to both surfaces of the plate, and where Reynolds number is defined by

$$Re_x = \frac{V\ x}{\nu} \tag{36}$$

Thermal properties are evaluated at the mean gas temperature, and may be approximated by those of air [23]. The characteristic length for a fabric approximated by a flat plate is the fabric thickness. At distances from the leading edge less than the fabric thickness the fabric is no longer simulated by a flat plate.

Heat Transfer to a Blunt Leading Edge

For thick fabrics at distances from the leading edge of order of the fabric thickness, the geometry of the fabric model is approximated by that of a curved leading surface. The fabric is porous and allows hot combustion gases through and around its substructure. The leading edge may be thought of as a cylindrical lump of fabric mass, of diameter equal to the fabric thickness. Convective heat transfer for forced flow of combustion gases normal to a cylinder has been determined for a wide range of parameters, and is expressed empirically by

$$Nu_x = B \cdot (Re_x)^j \tag{37}$$

where $x = \delta$, and the coefficients B and j are given for Reynolds number, as

$1 < Re < 4$: $B = 0.891$ $n = .330$

$4 < Re < 40$: $B = 0.821$ $n = .385$

Nusselt numbers from equation (37) for the above range of parameters are between 0.9 and 3.5 [24].

Ignition of Individual Threads

Ignition of fabric edges exposed normally to a flame introduces the problem of heat transfer to the fabric substructure. If the fabric is tightly woven, the fabric mass with which the flame gases interact is a fabric lump which was approximated by a cylindrical fabric mass in the previous section. Depending upon the fabric weave, however, the individual threads of the substructure of the fabric may be directly exposed to the flame gases, in which case the ignition of single threads may trigger ignition of the fabric.

Heat transfer to a thread may be calculated for flow about a cylinder, using equation (37) with $x = d$ to obtain the film coefficient. Equating the heat transferred by convection to the sensible heat storage of the fabric gives

$$2\bar{h}_c \cdot \pi \cdot d \cdot (T_g - T) = m \cdot c \frac{dT}{dt} \tag{38}$$

where m is the mass per unit length of the fabric thread. Integration of equation (38) gives the destruction time

$$t_{i,m} = \frac{m}{d} \cdot \frac{c(T_{i,m} - T)}{2\bar{h}_c (T_g - T)} \tag{39}$$

where it is assumed that specific heat is independent of fabric geometry. The three fabric models described will be used to predict convective film coefficients for the reduction of ignition time data.

This completes the modeling analysis. Apparatus and equipment required for the measurement of ignition times will be discussed in the next section.

Experimental Measurements

The purpose of the ignition time tests is to relate the exposure time to a flaming heat source to the probability of fabric ignition. Measurements were required to specify fabric thread properties and to characterize the heat source. An apparatus was required to expose fabric samples to a known convective heating intensity with instrumentation capable of detecting ignition and measuring the ignition time.

Apparatus and Instrumentation

The Convective Ignition Time Apparatus was used to

expose fabric samples to a convective heat source with transient response in exposure on the order of 0.02 seconds. The CITA has been used in previous ignition studies to obtain convective destruction time measurements on fabrics exposed to the flaming heat flux source with normal impingement at the center of the fabric [5,6,16].

The operating principles of the CITA are as follows. A fabric sample, or fabric simulant, is suddenly and completely exposed to a stabilized flame by the separation of two pneumatically controlled copper shutters. Compressed air is supplied to the two air cylinders which are activated by solenoid valves. Exposure of the fabric is permitted through a six inch hole in the base plate of the apparatus. To prevent preheating of the sample the shutters are water cooled, and overlap to permit their acceleration before initial separation. The shutter system with air cylinders and solenoid valves is mounted below the base plate, and is shown in Figure 18. Associated instrumentation is shown in Figure 19. A supporting superstructure with a fabric holder support and positioning rod is used for positioning the fabric sample, or simulant, above the burner. The superstructure and support for the fabric are pictured in Figure 20.

Convective heating is provided by a blast type burner, Fisher Scientific Company, No. 3-910-5. The burner was modified by totally blocking the air ports and providing the

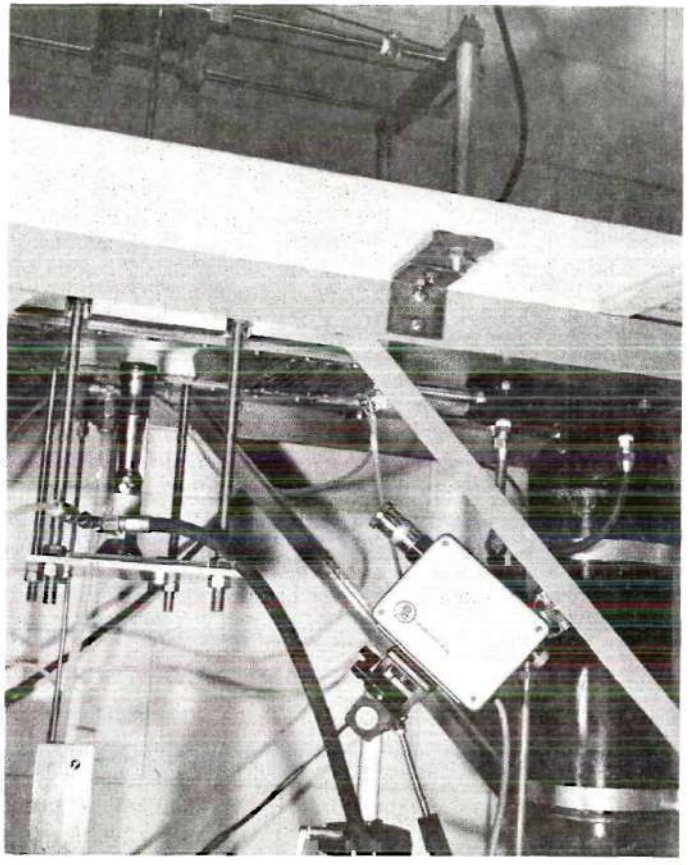

Figure 18. Lower Structure of CITA with Burner in Position.

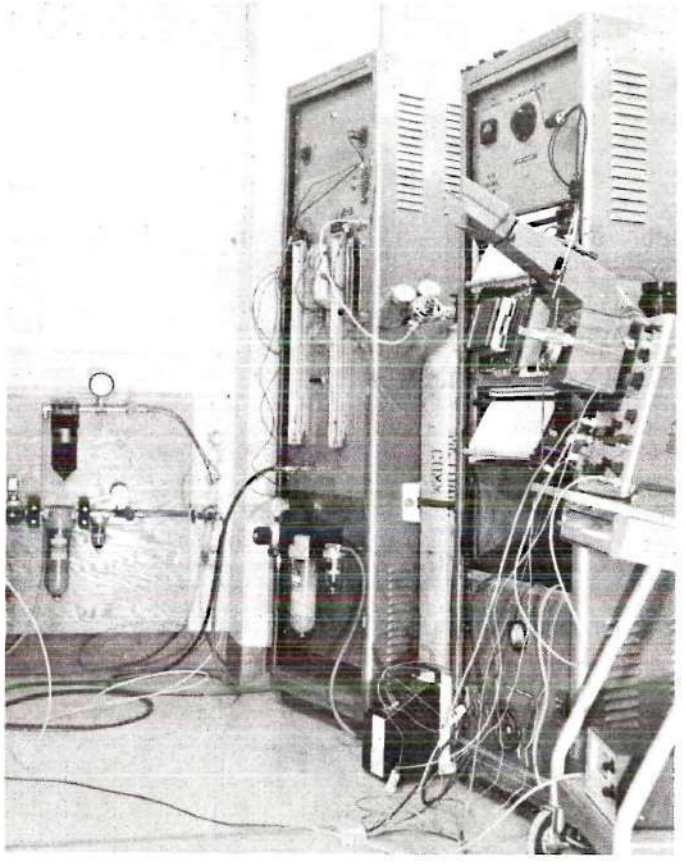

Figure 19. Recording Instrumentation, Flow Control and Flow Measuring Devices.

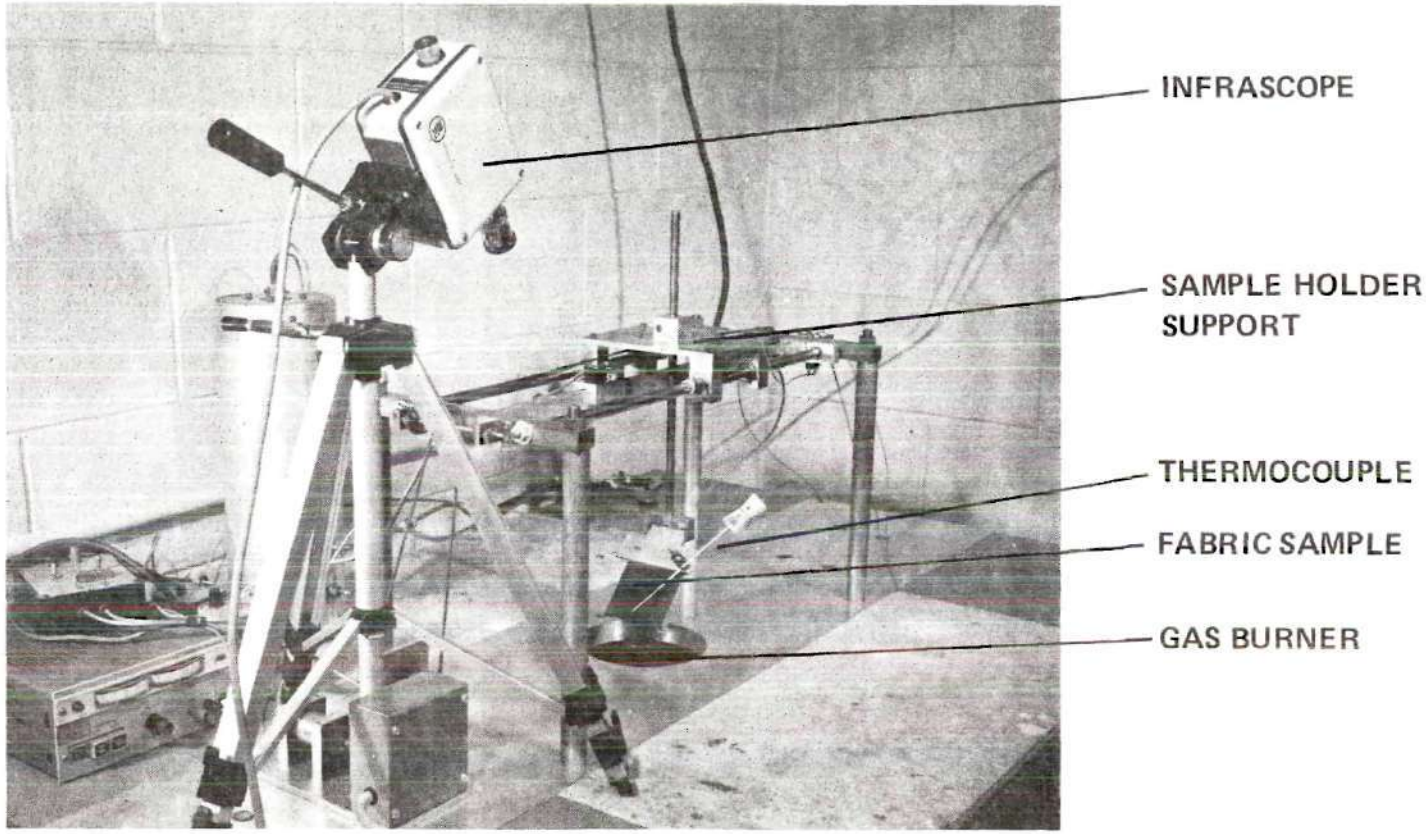

Figure 20. Experimental Arrangement of Test Section for Ignition Time Measurement on Single Fabrics at Different Orientations.

air to the burner from the compressed air supply in the laboratory (see Figure 19). The burner exit nozzle was fitted with a course screen to promote mixing, and has an exit diameter of 37 mm. This burner provides a premixed air-methane flame with a usable mixture flow rate range of 200-2900 g/h. Calibration of the flow meters for the air and methane flows were obtained from Reference [5].

A fabric holder was designed to accommodate fabric rotation about the horizontal axis, from 0° to 90° from the horizontal, and to expose the fabric edge to the flame. The holders were machined out of aluminum bar stock, and one is shown in Figure 21 with the clevis and support rod of the CITA. A 7.5 x 7.5 cm fabric sample is mounted between two 3.2 mm niconel rods with the lower edge exposed to the center of the flame. The rods are adjustable to provide uniform tension on the fabric sample without causing distortion to the fabric structure.

A fabric simulant of stainless steel was used to measure the convective heating rate of the burner. This was accomplished by measuring the thermal response of the simulant, as indicated from a thermocouple bead attached to the simulant, upon sudden exposure to the gas flame.

The fabric simulant consisted of a 200 mesh stainless steel screen fitted between asbestos insulation rings in a circular stainless steel holder. The holder afforded a 43 mm exposed straight edge of the screen. A stainless steel

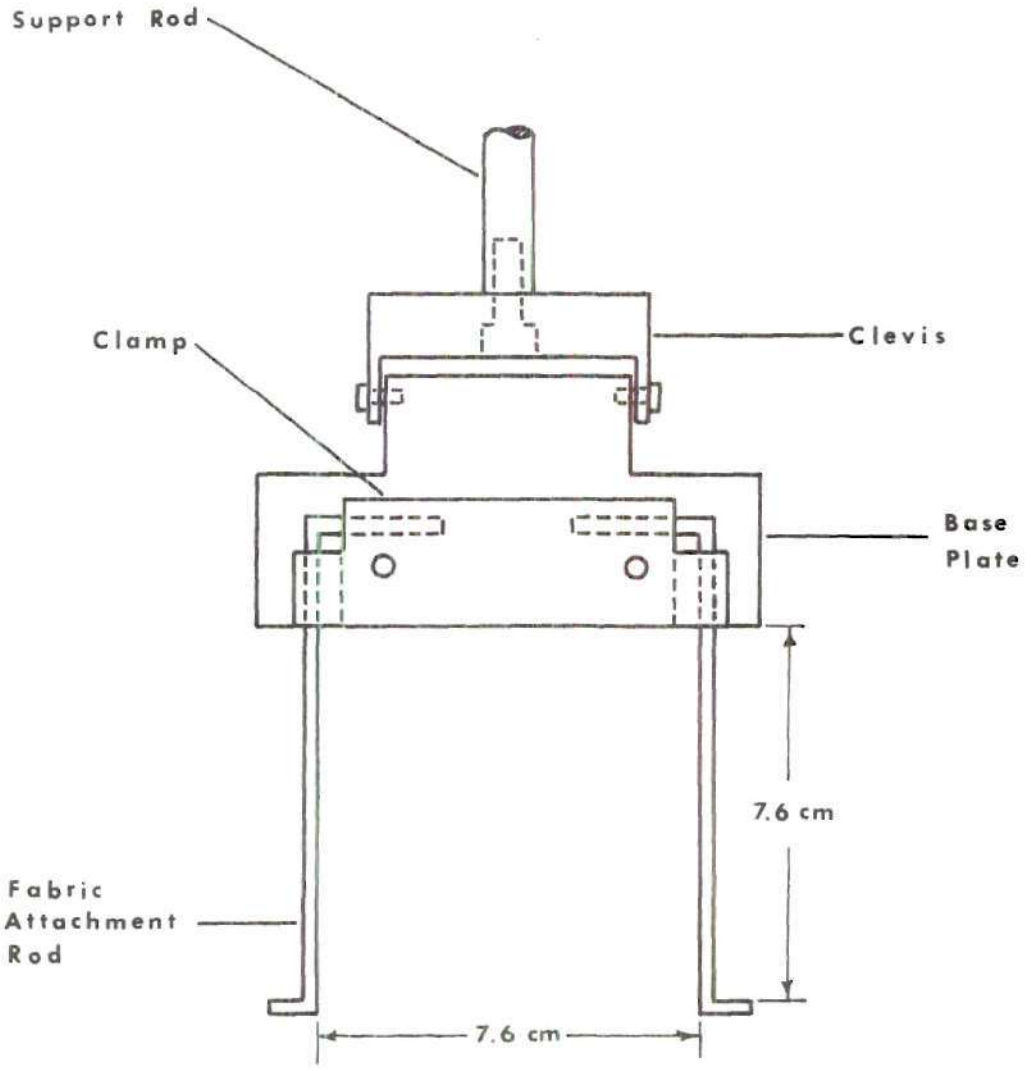

Figure 21. Sample Holder for Edge Ignition Tests

screen was cut to a three inch diameter circle (±0.015 inch) and weighed on a Christian Beckers Analytical Balance (±0.0006 gram). From these measurements the specific mass of the screen was determined. A 0.006 inch diameter 316 stainless steel wire, identical to the wire of the screen, and a 0.005 inch diameter constatan wire were welded to the screen so that the screen-constatan wire weld formed the thermocouple junction. The thermocouple weld was located at a specified distance from the exposed screen edge. The screen was mounted between asbestos rings in the stainless steel holder. The asbestos and the stainless steel screen were trimmed to yield a straight 43 mm exposed edge. Calibration of the thermocouple junction was obtained from Reference [5].

Fabric ignition was detected by the electrical output of an infrared detector, Model Mark 1 by Barnes Engineering, focused on the leading edge of the fabric sample. The infrascope measured the temperature response of the sample. A chromel-alumel thermocouple was placed behind the fabric on the 0 and 30 tests to give a secondary indication of the ignition.

Thermal response of both fabric and stainless steel screen were recorded on a dual beam Textronic oscilloscope (Model 502A). The electrical output of the infrascope amplifier (for ignition tests), or the output of the SS-constatan thermocouple junction (for film coefficient

tests) was displayed on the oscilloscope. Triggering was provided by a microswitch which was actuated by the initial separation of the shutters. The heating history was recorded on film using a Polaroid camera attachment to the oscilloscope.

Supporting instrumentation included metering for the burner flow, and temperature measurement of the gases. Methane flow was measured by a Brooks flowmeter, tube type R-2-15-B, with a glass float, and delivery pressure was measured with a U-tube mercury manometer. Air flow was measured on a Metco flowmeter, using a glass float, and the pressure measured on a U-tube manometer. The flow meter calibrations were obtained from Reference [5]. Two-pen Mosely Hewlett-Packard chart recorders (Type 7100B) recorded the premixed gas temperatures. A Leeds-Northrup potentiometer was used to measure the reference temperature of the stainless-steel screen prior to film coefficient tests.

Procedures followed in the experimental determination of film coefficients and the measurement of ignition times are presented in the next section.

Experimental Procedures

The procedures required in the determination of fabric ignition time under convective heating were the characterization of the burner, the measurement of film coefficients, the preparation of the fabric samples, and the measurement of fabric ignition time under specified heating. Film coefficent data was required for the specification of the

convective heating of the burner.

Measurement of Fabric Thread Properties. For analysis of the ignition of single threads the measurement of thread specific mass and diameter was required. Threads of six inch lengths were weighed on the analytical balance and the length recorded. Thread diameter was measured with a micrometer.

Characterization of the Heat Source. The convective heat source was characterized in terms of the burner velocity and temperature profiles, the mass flow rate, the stoichiometric equivalence ratio of the combustion, and the arrival time of the flame to reach the fabric after complete separation of the shutters. Temperature profiles were measured with a chromel-alumel thermocouple suspended in the flame from the CITA superstructure with the burner in place below the base plate. The thermocouple output was recorded on the Hewlett-Packard chart recorder.

Arrival time of the flame to reach the fabric after shutter separation was required to determine correct exposure time. This time was calculated from the response delay in the film coefficient tests, and times were determined as a function of inclination angle and burner flow rate. Geometric similarity between screen and fabric assures correct delay times.

Measurement of Convective Film Coefficients. Convective film coefficients which describe the fabric flame

interaction are determined from the thermal response of an inert wire cloth which simulates the fabric geometry. The screen was exposed to the same convective heat flux source (the Blast Type Burner) as used in the fabric ignition tests. Conservation of energy for the convective heating of the screen gives the following expression for the convective heat transfer coefficient, $2\bar{h}_c$

$$2\bar{h}_c = \frac{(\rho\delta)_s \, c_{p,s} \, (dT_s/dt)}{(T_g - T_s)} \tag{40}$$

where $(\rho\delta)_s$ is the specific mass of the screen, $c_{p,s}$ is the specific heat of the screen, T_s is the screen temperature, and T_g is the gas flame temperature. Radiation does not appear in this expression since the film coefficient, assumed to be temperature invarient, is evaluated at the initial screen temperatures at which the net radiative losses are negligible. Using the screen as one of the two dissimilar metal components of a thermocouple junction allows the direct measurement of the thermal response of the screen to the heat source. The determination of the film coefficient as defined by equation (40) requires the measurement of T_g, T_s, and (dT_s/dt).

Convective film coefficient tests were conducted using CITA with the stainless steel screen described in the previous section. The stainless steel screen was first

positioned at a height of three inches above the burner with the leading edge centered with the vertical axis of the burner. The height was measured with the burner in place with the shutters open, and the angle was set by means of a level. The shutter system was pressurized. The functioning of the infrascope and oscilloscope (which were turned on earlier to allow warm up) were set and checked. The burner was then ignited outside of CITA and the flow and pressure regulated to calibrated flow conditions of 1260 g/h or 2175 g/h and an oxygen rich mixture (stoichiometric equivalence ratio of $\phi = .86 \pm .01$) as given by Reference [5]. The reference voltage of the screen thermocouple junction was recorded using a Leeds-Northrup potentiometer. The burner was then placed under the water cooled shutters, the camera shutter was opened, and the CITA shutter solenoids activated. As the shutters separate, a microswitch detects separation and triggers the oscilloscope.

Following the initial heating period, the burner was removed from beneath the screen to prevent excessive heating of the screen. The Polaroid picture was developed and saved, and the CITA made ready for the next run.

Fabric Ignition Time Measurements. Edge ignition time measurements on fabrics utilized CITA in a similar manner as the film coefficient tests, with the exception that the oscilloscope recorded the output of a Barnes Infrascope which monitored temperature of the fabric edge.

Fabric samples were prepared from material provided by the GIRCFF. Samples were cut to a 3 x 3-1/4 inch rectangle, and the ends attached to the support rods by means of a thin cotton thread running the length of the rod. The leading edge of the fabric sample was trimmed with scissors to a straight line, free from exposed single threads. The fabric was then placed between the base and bracket and secured in place at a uniform but unstretched tension. The fabric in the holder was placed in a dessicator for a period of no less than 20 hours prior to testing to insure moisture content of less than 5%.

For alignment purposes, prior to testing, an unused fabric sample was placed in the desired testing position. This was necessary to minimize the amount of time between the removal of the sample from the dessicator and the test to minimize moisture regain. The height and the centered position was determined as in film coefficient tests. The infrascope was positioned such that it viewed the fabric normally to the fabric surface, and was focused on the exposed edge. For 0° and 30° angle tests this required positioning the infrascope below the table (as shown in Figure 18) at a focal length of 18 inches. For 60° and 90° angle tests the infrascope was positioned above the base plate (see Figure 20) at a focal length of 24 inches.

After pressurizing the shutters, checking the instrumentation, and stabilizing the burner as for the film

coefficient tests, the fabric sample was removed from the dessicator and placed in the support clevis at the preset height and position. The angle was quickly set by means of adjustable screws through the clevis, and by the level. The burner was placed beneath the shutters, and the test proceeded as for the film coefficient tests with the burner left in position until the occurrence of ignition.

Data Reduction and Results

The flame measurements and air-methane flow measurements were reduced to a resulting mixture mass flow rate and equivalent stoichiometric ratio using the calibrations obtained from Reference [5]. Temperature profile measurements were converted from emf output of the chromel-alumel thermocouple to equivalent temperatures, and then corrected for radiation losses [25]. Velocity profiles were reduced from the pressure profile measurements of Wedel [23], using the equation for conservation of momentum,

$$V = (2\ \Delta p/\rho)^{1/2} \tag{41}$$

where V is the free stream velocity, Δp is the gage pressure, and ρ is the fluid density. Temperature and velocity profiles for the two flow rates used in the film coefficient and ignition time tests are presented in Figures E3 and E4 of the Appendix.

The film coefficients were evaluated directly from

equation (40), in which $c_{p,s}$ was evaluated from the calibrations of Reference [23], at the mean screen temperature of the initial heating period. The gas flame temperature T_g used in this study was the result of averages taken over many fabric ignition time tests, as this was a more representative value than the single measurements obtained during the temperature profile tests. The specific mass of the screen $(\rho\delta)_s$ was determined as outlined in the procedures, and was found to be .02793 g/cm^2. The thermal response of the screen to the gas flame was characterized by its time-temperature profile as recorded on the oscilloscope. From each emf-time oscillogram 35 to 43 data points were obtained and their emf values were converted to equivalent temperatures using calibrations of Reference [23]. The temperature-time history was plotted, and was found to be very nearly linear after the transients associated with the arrival of the flame subsided. The screen response was then characterized by passing a first degree, least-square-fit polynomial through the linear region. The slope of the equation obtained for the linear heating region was used to obtain (dT/dt) used in equation (40).

The film coefficient tests were conducted at a height of 7.62 cm above the burner exit. Burner flow rates used were 1260 and 2175 g/h. Impingement angles (measured from the horizontal) were 0°, 30°, 60°, and 90°. To assess the effects of distance downstream from the exposed edge

upon the heat transfer, this distance was varied at 1.0 and 4.3 mm. Results from these tests are listed in Table 5. A sample film coefficient test data sheet is presented in Figure E2 of the Appendix. Calculated film coefficients, determined from the three models discussed in the modeling analysis, are presented in Table 6.

Fabric ignition times were obtained by the intercept of the tangents of the inert heating region and the exponential rise due to the onset of combustion. Due to the shortness of the ignition times had to be corrected for exposure delays, which are tabulated in Table E6 of the Appendix. Ignition tests were performed at a height of 7.62 cm above the exit of the burner. Flow rates used were 1260 and 2175 g/h. Angle of impingement was varied at 0°, 30°, 60°, and 90°. Fabrics tested were GIRCFF fabrics number 5, 9, 10, and 4 (all 100% cotton, and of light and heavy weights), and fabrics number 6 and 17 (both 65/35% polyester-cotton and of heavy and light weights). Fabric number 6 was tested at two flow rates. The ignition time tests are summarized in Table 7. A sample ignition test data sheet is presented in Figure E1 of the Appendix.

Ignition times were normalized by the Fourier number, defined by

$$Fo_{i,m} = \frac{(k/\delta)t_{i,m}}{c\ (\rho\delta)} \qquad (18)$$

Table 5. Stainless Steel Screen Convective Film Coefficients.

ϕ = 0.86 43 mm exposed edge L = 7.62 cm

angle degrees	$\dot{m}_{mix}$ g/h	T_g °C	$2\overline{h}_c$ W/cm^2-°K	
			a = 4.3 mm	a = 1.0 mm
0°	1264	1205	0.00972	0.01161
30°	1263	1205	0.00963	0.01343
60°	1261	1205	0.00647	0.01810
90°	1256	1205	0.01496	0.03058
0°	2205	1319	0.00842	0.01269
30°	2204	1319	0.01139	0.01684
60°	2203	1319	0.01053	0.01966
90°	2201	1319	0.02408	0.02930

Table 6. Calculated Convective Film Coefficients.

ϕ = 0.86 $\quad \dot{m}_{mix}$ = 1260 g/h $\quad$ L = 7.62 cm

GIRCFF Fabric Number	δ mm	d mm	$2\bar{h}_c$ W/cm^2-°K		
			eqn. (37) x = δ	eqn. (35) x = δ	eqn. (37) x = d
4	0.483	0.157	0.03217	0.05744	0.06700
5	0.516	0.071	0.03043	0.05557	0.11415
6	0.330	0.132	0.04067	0.06945	0.07539
9	0.660	0.152	0.02657	0.04911	0.06849
10	0.178	0.058	0.06475	0.09464	0.13021
17	0.193	0.056	0.05847	0.09083	0.13428

Table 7. Summary of Edge Ignition Tests.

GIRCFF Fabric No.	$\dot{m}_{mix}$	inclination angle	$t_{i,m}$
	g/h	degrees	s
4	1261	0	2.635
	1260	60	0.240
	1261	90	0.124
5	1260	90	0.369
6	1268	0	1.945
	1271	30	1.485
	1273	60	0.160
	1267	90	0.124
	2205	0	1.355
	2205	30	1.110
	2200	60	0.154
	2199	90	0.074
9	1260	90	0.317
10	1260	0	0.645
	1265	30	0.535
	1272	60	0.400
	1264	90	0.224
17	1260	90	0.299

Non-dimensionalized heating intensity for the fabric layer heating model is defined by

$$q_c^* = \frac{2\bar{h}_c}{(k/\delta)\,\ell n\left(\frac{\theta_g}{\theta_g - 1}\right)} \tag{42}$$

where the normalized flame temperature θ_g is defined by

$$\theta_g = \frac{T_g - T}{T_{i,m} - T} \tag{43}$$

The normalization of data for the ignition of individual threads requires the inclusion of the parameter (δ/d) in the definitions of normalized thread ignition time and heating intensity. These are not obtained from the governing differential equation for the heating of the fabric, but are useful parameters for plotting fabric ignition time data. The Fourier number for the ignition time of a single thread is given by

$$Fo_{i,m} = \frac{\delta}{d}\,\frac{(k/\delta)\,t_{i,m}}{c\ (m/d)} \tag{44}$$

The normalized heating intensity for an individual thread is given by

$$q_c^* = \frac{d}{\delta} \frac{2\bar{h}_c}{(k/\delta)} (\theta_g - \bar{\theta}) \tag{45}$$

where the average, normalized fabric temperature is defined by

$$\bar{\theta} = \frac{1}{t_{i,m}} \int_0^{t_{i,m}} \theta \, dt \tag{46}$$

Normalized edge ignition time results for fabric number 4 are listed in Table 8. Normalized test results for the other fabrics tested are presented in Tables E1 through E5 of the Appendix.

Edge ignition time results, using the film coefficient for the appropriate heating model, are shown in Figure 22, correlated with previous results and the inert heating model (solid line). Normalized ignition time data for 90° impingement tests are shown in Figure 23, reduced by both measured and calculated film coefficients.

Discussion of the film coefficient and ignition time tests is presented in the next section.

Discussion of Results

The results obtained were the measurement of thread specific mass and diameter, the temperature and velocity profiles of the burner, flame exposure delays, measurement of the convective film coefficient, and the determination

Table 8. Summary of Edge Ignition Tests on Fabric Number 4.

GIRCFF Fabric Number 4 (100% Cotton)

k/δ = 0.01500 $W/cm^2-°K$ Fuel: Methane

c = 1.424 $Ws/g-°K$ ϕ = 0.86

$\rho\delta$ = 29.63 mg/cm^2 Fabric edge = 76.0 mm

T_i = 297.0 °C

$\bar{\alpha}$	Exp. No.	L cm	$\dot{m}_{mix}$ g/h	T_o °C	T_g °C	θ_g	$t_{i,m}$ s	$\bar{\theta}$	$2\bar{h}_c$ $W/cm^2-°K$	Fo	q_c^*
0°	30	7.62	1260	24.0	1223	4.392	2.635	0.521	0.01161	0.937	3.061
60°	26	7.62	1259	23.8	1270	4.562	0.240	0.520	0.01810	0.085	4.771
90°	31[a]	7.62	1260	25.1	1242	4.475	0.124	0.521	0.03058	0.044	8.062
90°	31[b]	7.62	1260	25.1	1242	4.475	0.124	0.521	0.03217	0.044	8.479
90°	31[c]	7.62	1260	25.1	1242	4.475	0.124	0.521	0.05744	0.044	15.140
90°	31[d]	7.62	1260	25.1	1242	4.475	0.124	0.521	0.06700	0.145	5.778

[a] - Measured film coefficient.

[b] - Film coefficient from equation (37) with $x = \delta$.

[c] - Film coefficient from equation (35) with $x = \delta$.

[d] - Film coefficient from equation (37) with x = d.

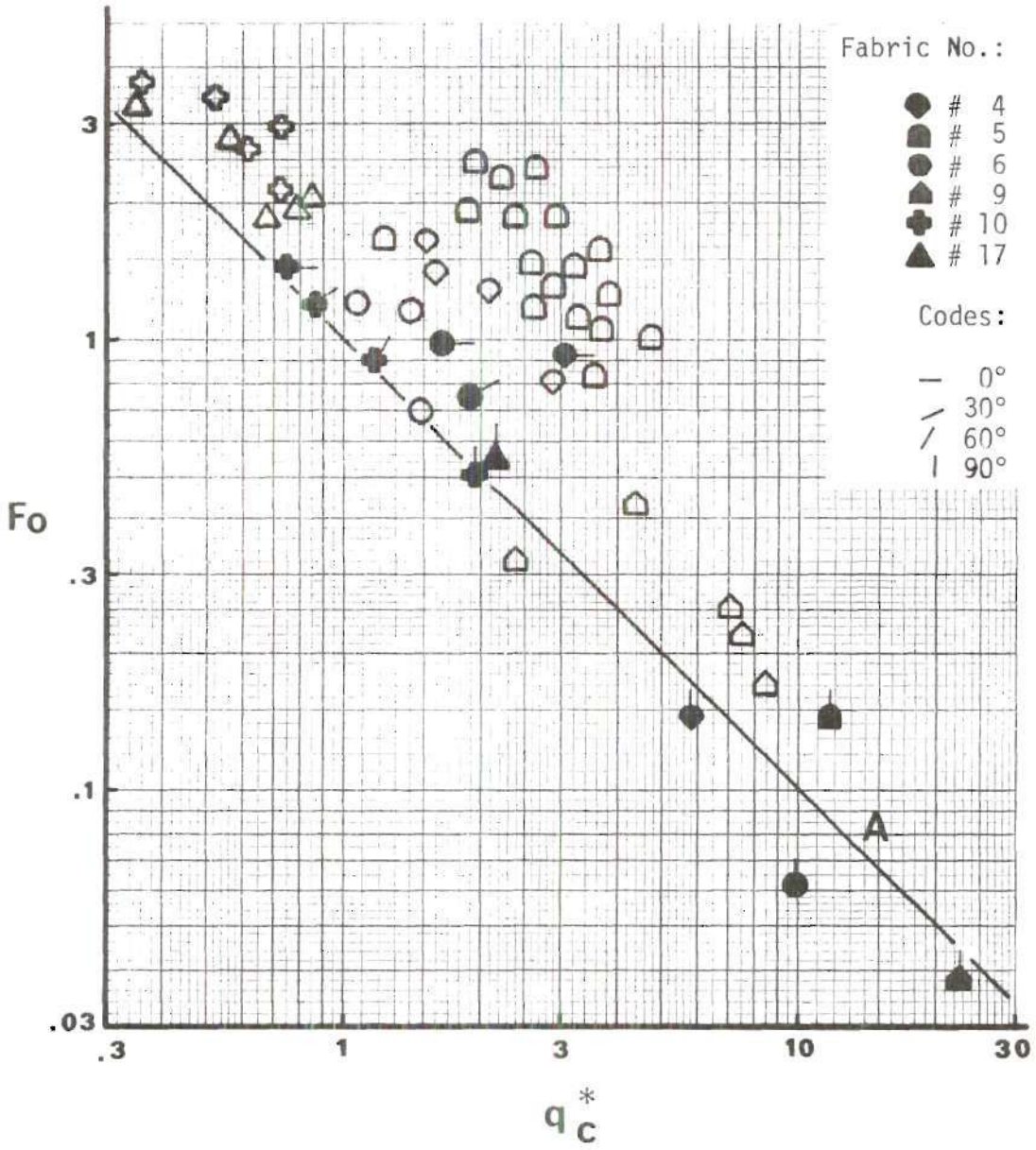

Figure 22. Normalized Fabric Edge Ignition Time Results Compared with Normal Impingement Ignition Times (Curve A is the Inert Heating Model, open points are previous normal impingement ignition times [4,5])

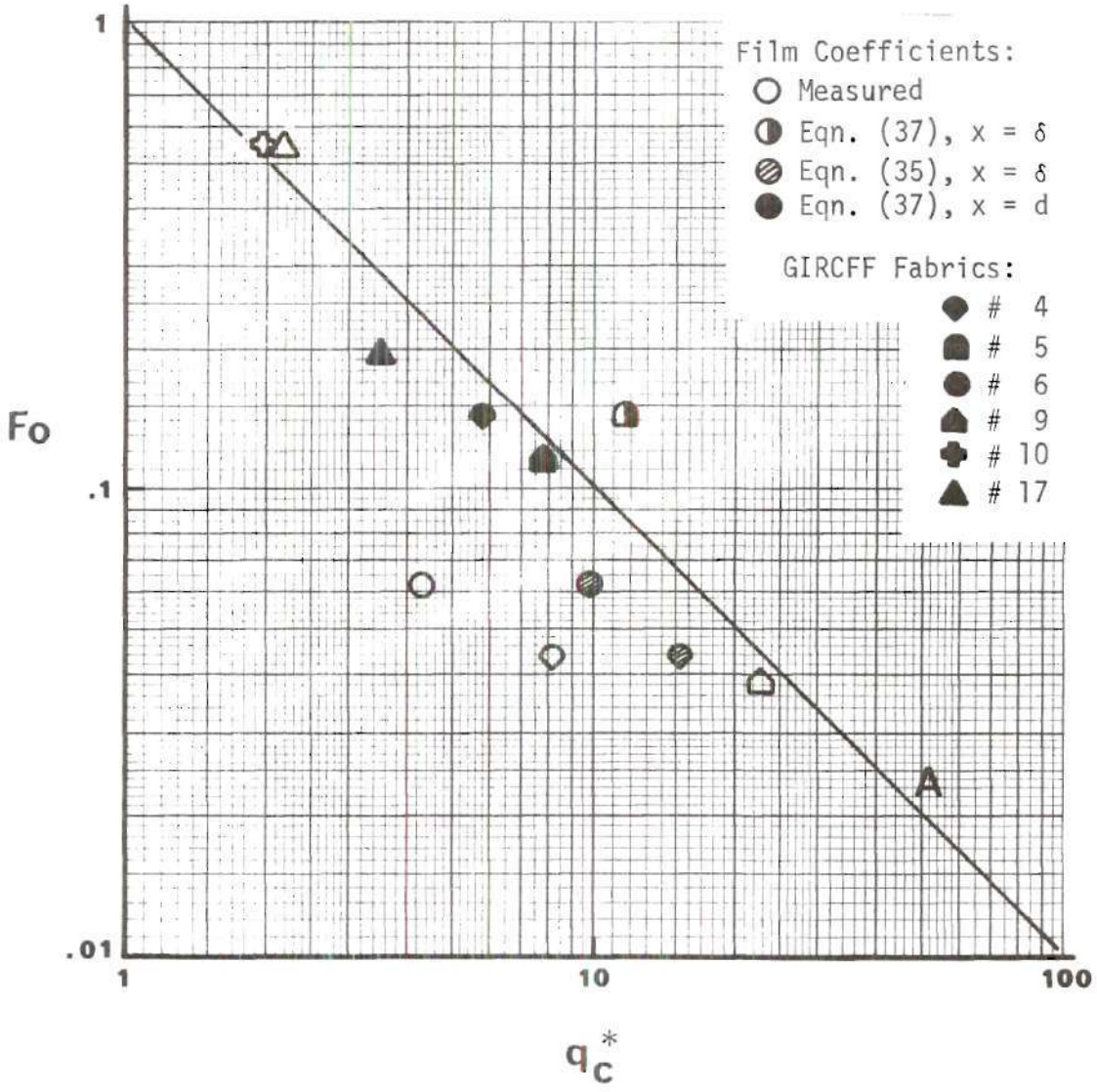

Figure 23. Normalized Fabric Edge Ignition Time Results, 90° Angle Flame Impingement; Curve A is the Inert Heating Model

of fabric ignition time.

Thread mass per unit length and thread diameter measurements were required for ignition time data reduction. The specific mass for single threads of fabrics number 9 and 4 were found to vary only slightly from specific mass of the fabrics themselves. This was due to the dense weaves of these two fabrics. Fabrics number 10 and 17 are loosely woven and thus specific mass measurements differed significantly from those of the fabrics.

The burner was characterized in terms of the temperature and velocity profiles. Temperature decreases slightly with downstream distance from the burner exit as would be anticipated due to entrainment of air into the flow. Velocity profiles show that the velocity increases with height above the burner, indicating an acceleration of the burner gases. Velocity in the potential core of a turbulent jet is expected to remain constant for 5 to 8 burner diameters downstream of the burner exit [26]. The acceleration of the combustion gases in this case is attributed to buoyancy since the exit Reynolds number indicates that the flow is not fully turbulent.

Measured film coefficients are listed in Table 5. Results for the porous stainless steel screen are lower by approximately 30% than heat transfer coefficients predicted by Pohlhausen's equation. At low inclination angle the location of thermocouple bead has little effect

on the measured film coefficient. For 90° impingement however, the film coefficient increases 100% as the bead is varied from 4.3 to 1.0 mm from the leading edge.

Ignition test data indicates that there are two distinct types of edge ignition. For tests at 60° or greater the characteristic lengths of the heat transfer mechanisms are the fabric thickness and the thread diameter. For the denser and thicker fabrics these tests yield ignition times which are ten times faster than tests at 0° and 30°.

Edge ignition time tests at low impingement angle of 30° or less are much longer than ignition times for high impingement angle. The samples in all of the edge ignition tests were centered with respect to the centerline of the burner exit. These ignition time results are similar to results obtained previously [4,5] for circular fabric samples exposed normally to the burner.

Edge ignition tests correlate well with the inert heating model. This is attributed, for the case of 60° and 90° tests, to the simpler fluid flow and the high heating rates. In tests on a circular sample exposed normally to an impinging jet, pyrolysate products evolve from the fabric and form a boundary layer between the flame gases and the fabric. This does not occur for high impingement angles.

Previous flame orientation tests of Heskestad [8] indicated an independence of fabric ignition time with

respect to flame orientation and angle of impingement. Results from Heskestad's tests were for a diffusion flame for which the combusting jet was quite laminar. The effects of burner Reynolds number and inclination angle, with predictions for heat transfer, have been investigated by Perry [27]. For burner flows producing laminar flames, Perry's data shows an independence of impingement angle upon heat transfer. However, for turbulent jets impinged on a flat surface, an increase of three to four times in heat transfer may be obtained and impingement angle decreases from 90° (normal impingement) to 15°. As ignition times are directly related to the convective heating rate, the angle of impingement is a significant parameter in ignition of fabrics exposed to a flaming heat source.

CHAPTER IV

CONCLUSIONS AND RECOMMENDATIONS

The objective of this research was to further the understanding of the hazard posed by fabric ignition. The two tasks studied were first, the interaction of parallel fabric layers under radiative heating, and secondly, the fabric behavior under edge exposure to a flame. Conclusions drawn from these studies are presented in this chapter.

Conclusions on Fabric Interaction

Radiative ignition tests were conducted to determine the effect of interaction between parallel fabric layers on the system ignition time. Incident radiant heat fluxes of 16.2 to 6.5 W/cm^2 were used. Fabric spacing was varied from .318 to 0 cm. The conclusions on the radiant heating of parallel fabric layers are discussed next.

First, the presence of the second fabric introduces two new parameters into the heating problem of a single fabric. These are the effects of the increased absorbed radiant heat due to rereflectivity between the fabric layers, and the change in convection between the layers. Both analytical and experimental results show the effect of rereflectivity in producing a decrease in ignition time, proportional to the increase in absorbed heat flux due to the

rereflectivity. The net increase in incident radiant flux due to rereflectivity makes ignition possible at lower heating intensities than is possible for a single fabric layer. Convective losses are lowest at large gaps, and thus ignition times are shorter as gap increases. At small gaps of a few millimeters, the rear fabric serves to increase the net convective losses of the front fabric, and results in an overall increase in exposure time required for ignition. This is most significant at low intensities.

A second general conclusion is that with the surface ignition model, pyrolysis is significant. Visual observations indicate ignition in the gas phase, and thus give further evidence of the significance of mass transfer.

Finally, from tests on polyester and cotton fabrics, no evidence of chemical interaction between fabric layers can be drawn.

Conclusions on Flame Orientation

Ignition time measurements were conducted on edges of fabrics exposed to a flaming heat source to determine the effect of flame orientation on fabric ignition. Incident heating rates of 60 to 10 W/cm^2 were used in the tests.

Edge heating offers higher heating rates and lower ignition times by a factor of four for low impingement angles. Transition was noted for tests at 30° and 60°. This is due to the flow characteristics of the geometry and

indicates the edge is not significant, but the effective heating rate is.

Conclusions are drawn that at high convective heating intensities ignition time results correlate well with inert heating predictions.

Experimental observations indicate that ignition starts at very small scale for high impingement angle. This and analytical results suggest that the fabric substructure and weave are important parameters. Appropriate scaling lengths are thread diameter and fabric thickness.

Recommendations for Further Work

Test data on the interaction of parallel fabric layers under radiant heating was obtained on two fabric combinations. It is recommended that to specify the nature of fabric interaction more conclusively that a broader survey of fabric combinations be tested. A single heating intensity and air gap could be used as reference testing conditions for a survey of possible fabric combinations.

It is also recommended for further work that specific fabric pairs be selected and tested to examine the effects upon ignition time of the rereflectivity between fabric layers and relative difference in heat capacities of front and rear fabrics.

Edge ignition tests have shown the significance of fabric substructure upon fabric ignition time. It is

recommended that an additional criterion for characterizing the flammability of a specific fabric is the flammability of individual threads of the fabric. It is recommended that tests on ignition of fabric threads be conducted to supplement tests on fabrics.

APPENDICES

APPENDIX A

THERMOPHYSICAL PROPERTIES OF GIRCFF FABRICS

This appendix contains the thermal and physical properties of the GIRCFF fabrics tested in this study. Property data is obtained from References [4,5] except for thread thickness and specific mass which were measured in the laboratory. The reported ignition temperatures of Reference [5] were obtained by the heating of fabric samples in a Setchkin furnace.

Moisture desorption data is for 30% relative humidity; thermal conductance data is for a constant pressure of 528 N/m^2.

Table A1. Property Summary, GIRCFF Fabric No. 2 [4,5].

1. Description — Fiber Composition: 100% Polyester; Color: Yellow

2. Specific Mass — Fabric, $\rho\delta$: 7.51 mg/cm^2; Thread, m:* -- mg/cm

3. Fabric Thickness, δ: 0.201 mm; Thread Diameter, d:* --- mm

4. Specific Heat

Temperature, T:	50	125	200	°C
Specific heat, c:	1.42	1.42	1.42	Ws/g-°K

5. Thermal Conductance

Temperature, T:	73.0	93.1	124.6	°C
Conductance, k/δ:	20.3	21.0	22.8	mW/cm^2-°K

6. Melting Temperature, T_m 259 °C

7. Infrared Optical Properties

Source	Original 3160 °K	Original .6-2.5 μm	Charred at 134 °C 3160 °K
absorbtivity, α:	.164	.153	.175
reflectivity, $\tilde{\rho}$:	.560	.501	.582
transmissivity, τ:	.276	.346	.243

8. Reaction Kinetics

	E,kWs/g mole	K,1/s	n	Δi,Ws/g
moisture desorp.	---	---	---	---
pyrolysis	363.8	1.04×10^{24}	1.7	389.0
exothermic react.	---	---	---	---

* measured in this study

Table A2. Property Summary, GIRCFF Fabric No. 4 [4,5].

1. Description — Fiber Composition: 100% Cotton; Color: Navy Blue

2. Specific Mass — Fabric, $\rho\delta$: 29.63 mg/cm^2; Thread, m:* .4359 mg/cm

3. Fabric Thickness, δ:* 0.483 mm; Thread Diameter, d:* 0.157 mm

4. Specific Heat

Temperature, T:	50	125	200	°C
Specific heat, c:	1.17	1.35	1.50	Ws/g-°K

5. Thermal Conductance

Temperature, T:	65.2	107.7	159.1	°C
Conductance, k/δ:	9.02	10.88	14.62	mW/cm^2-°K

6. Ignition Temperature, T_i — self: 288 °C pilot: 285 °C

7. Infrared Optical Properties

Source	Original 3160 °K	Original .6-2.5μm	Charred at 162 °C 3160 °K
absorbtivity, α:	.445	.372	.511
reflectivity, β:	.450	.491	.401
transmissivity, τ:	.105	.137	.088

8. Reaction Kinetics

	E,kWs/g mole	K,1/s	n	Δi,Ws/g
moisture desorp.	97.4	4.88×10^{13}	2.6	101.6
pyrolysis**	--	--	---	---
exothermic react.	--	--	---	---

* measured in this study
** see GIRCFF fabric no. 5

Table A3. Property Summary, GIRCFF Fabric No. 5 [4,5].

1. Description — Fiber Composition: 100% Cotton; Color: White

2. Specific Mass — Fabric, $\rho\delta$: 13.71 mg/cm^2; Thread, m:* .1872 mg/cm

3. Fabric Thickness, δ: 0.529 mm; Thread Diameter, d:* 0.071 mm

4. Specific Heat

Temperature, T:	50	125	200	°C
Specific heat, c:	1.05	1.47	1.91	Ws/g-°K

5. Thermal Conductance

Temperature, T:	70.9	130.5	206.0	°C
Conductance, k/δ:	7.32	8.81	10.82	mW/cm^2-°K

6. Ignition Temperature, T_i — self: 314 °C; pilot: 306 °C

7. Infrared Optical Properties

	Original		Charred at 162 °C
Source	3160 °K	.6-2.5 μm	3160 °K
absorbtivity, α:	.179	.183	.225
reflectivity, ρ:	.533	.521	.491
transmissivity, τ:	.288	.296	.284

8. Reaction Kinetics

	E,kWs/g mole	K,1/s	n	Δi,Ws/g
moisture desorp.	97.4	4.88×10^{13}	2.6	101.6
pyrolysis	219.5	9.54×10^{12}	1.1	376.8
exothermic react.	142.6	9.20×10^{9}	1.6	14780

* measured in this study

Table A4. Property Summary, GIRCFF Fabric No. 6 [4,5].

1. Description — Fiber Composition: 65/35% Polyester-Cotton; Color: White

2. Specific Mass — Fabric, $\rho\delta$: 23.57 mg/cm^2; Thread, m:* .5840 mg/cm

3. Fabric Thickness, δ:* 0.330 mm; Thread Diameter, d:* 0.132 mm

4. Specific Heat

Temperature, T:	50	125	200	°C
Specific heat, c:	1.10	1.26	1.48	Ws/g-°K

5. Thermal Conductance

Temperature, T:	66.8	126.8	160.6	°c
Conductance, k/δ:	9.90	10.74	15.60	mW/cm^2-°K

6. Ignition Temperature, T_i — self: 412 °C; pilot: 341 °C

7. Infrared Optical Properties

Source	Original 3160 °K	Original .6-2.5 μm	Charred at 219 °C 3160 °K
absorbtivity, α:	.199	.135	.373
reflectivity, $\bar{\rho}$:	.581	.581	.339
transmissivity, τ:	.220	.284	.288

8. Reaction Kinetics

	E,kWs/g mole	K,1/s	n	Δi,Ws/g
moisture desorp.	----	---	---	---
pyrolysis	365.5	1.28×10^{27}	2.1	---
exothermic react.**	----	---	---	---

---

* measured in this study
** see GIRCFF fabric no. 17

Table A5. Property Summary, GIRCFF Fabric No. 9 [4,5].

1. Description — Fiber Composition: 100% Cotton; Color: White

2. Specific Mass — Fabric, $\rho\delta$: 26.48 mg/cm^2; Thread, m:* .4940 mg/cm

3. Fabric Thickness, δ:* 0.661 mm; Thread Diameter, d:* 0.152 mm

4. Specific Heat

Temperature, T:	50	125	200	°C
Specific heat, c:	1.13	1.45	1.64	Ws/g-°K

5. Thermal Conductance

Temperature, T:	69.7	117.4	175.3	°C
Conductance, k/δ:	2.34	2.79	3.62	mW/cm^2-°K

6. Ignition Temperature, T_i — self: 302 °C; pilot: 294 °C

7. Infrared Optical Properties

Source	Original 3160 °K	Original .6-2.5 μm	Charred at 162 °C 3160 °K
absorbtivity, α:	.113	.146	.242
reflectivity, $\tilde{\rho}$:	.681	.623	.627
transmissivity, τ:	.206	.231	.131

8. Reaction Kinetics

	E,kWs/g mole	K,1/s	n	Δi,Ws/g
moisture desorp.	97.4	4.88×10^{13}	2.6	101.6
pyrolysis**	206.9	3.07×10^{21}	1.4	---
exothermic react.	---	---	---	---

* measured in this study
** see GIRCFF fabric no. 5

Table A6. Property Summary, GIRCFF Fabric No. 10 [4,5].

1. Description — Fiber Composition: 100% Cotton; Color: Yellow

2. Specific Mass — Fabric, $\rho\delta$: 6.65 mg/cm^2; Thread, m:* .074 mg/cm

3. Fabric Thickness, δ: 0.177 mm; Thread Diameter, d:* 0.058 mm

4. Specific Heat

Temperature, T:	50	125	200	°C
Specific heat, c:	1.37	1.77	---	Ws/g-°K

5. Thermal Conductance

Temperature, T:	67.8	128.4	195.8	°C
Conductance, k/δ:	17.48	20.19	29.67	mW/cm^2-°K

6. Ignition Temperature, T_i — self: 437 °C; pilot: 345 °C

7. Infrared Optical Properties

Source	Original 3160 °K	Original .6-2.5 μm	Charred at 230 °C 3160 °K
absorbtivity, α:	.221	.200	.387
reflectivity, $\tilde{\rho}$:	.418	.406	.219
transmissivity, τ:	.361	.394	.394

8. Reaction Kinetics

	E,kWs/g mole	K,1/s	n	Δi,Ws/g
moisture desorp.	89.5	1.77×10^{12}	2.9	101.6
pyrolysis**	228.3	2.85×10^{13}	1.1	367.8
exothermic react.**	119.6	2.52×10^{8}	3.2	14780

* measured in this study
** see GIRCFF fabric no. 5

Table A7. Property Summary, GIRCFF Fabric No. 17 [4,5].

1. Description — Fiber Composition: 65/35% Polyester-Cotton; Color: White

2. Specific Mass

Fabric, $\rho\delta$:	8.55	mg/cm^2
Thread, m:*	--	mg/cm

3. Fabric Thickness, δ: 0.152 mm
   Thread Diameter, d:* 0.056 mm

4. Specific Heat

Temperature, T:	50	125	200	°C
Specific heat, c:	1.27	1.47	1.66	Ws/g-°K

5. Thermal Conductance

Temperature, T:	72.6	128.0	199.3	°C
Conductance, k/δ:	17.34	22.48	26.75	mW/cm^2-°K

6. Ignition Temperature, T_i — self: 471 °C; pilot: 376 °C

7. Infrared Optical Properties

Source	Original 3160 °K	Original .6-2.5 μm	Charred at 252 °C 3160 °K
absorbtivity, α:	.151	.164	.425
reflectivity, $\tilde{\rho}$:	.485	.464	.255
transmissivity, τ:	.364	.372	.320

8. Reaction Kinetics

	E,kWs/g mole	K,1/s	n	Δi,Ws/g
moisture desorp.	--	---	---	35.6
pyrolysis	310.3	1.80×10^{19}	1.6	118.9
exothermic react.	105.4	2.67×10^{6}	3.0	---

* measured in this study

APPENDIX B

INERT HEATING WITH CONVECTIVE LOSSES

The heating of two parallel fabric layers may be approximated by the radiant heating and convective cooling of two inert semi-transparent slabs. For the fabric model shown in Figure 1, the governing differential equations may be expressed as

$$(\rho\delta)_f \, c_f \frac{dT_f}{dt} = \alpha_f^* W_o - h_2(T_f - T_b) - h_1(T_f - T_\infty) \qquad \text{(B1)}$$

$$(\rho\delta)_b \, c_b \frac{dT_b}{dt} = \alpha_b^* W_o - h_3(T_b - T_f) - h_4(T_b - T_\infty) \qquad \text{(B2)}$$

and further simplified, assuming $h_2 = h_3$ and $h_1 = h_4$, to

$$T_f' + \frac{(h_2+h_1)}{(\rho\delta)_f \, c_f} T_f - \frac{h_2}{(\rho\delta)_f \, c_f} T_b = \frac{\alpha_f^* W_o + h_1 T_\infty}{(\rho\delta)_f \, c_f} \qquad \text{(B3)}$$

$$T_b' + \frac{(h_2+h_1)}{(\rho\delta)_b \, c_b} T_b - \frac{h_2}{(\rho\delta)_b \, c_b} T_f = \frac{\alpha_b^* W_o + h_1 T_\infty}{(\rho\delta)_b \, c_b} \qquad \text{(B4)}$$

Non-dimensionalized temperatures are defined by

$$T_f^* = \frac{T_f}{T_\infty} - A_6 \tag{B5}$$

$$T_b^* = \frac{T_b}{T_\infty} - A_7 \tag{B6}$$

where the following parameters are defined for algebraic convenience

$$\left.\begin{aligned}
A_1 &= \frac{h_2}{h_2 + h_1} \\
A_2 &= \frac{[(\rho\delta)_f c_f + (\rho\delta)_b c_b]^2}{(\rho\delta)_f c_f (\rho\delta)_b c_b} \\
A_3 &= \frac{h_2 + h_1}{(\rho\delta)_f c_f + (\rho\delta)_b c_b} \\
A_4 &= \frac{\alpha_f^* W_o + h_1 T_\infty}{T_\infty (h_2 + h_1)} \\
A_5 &= \frac{\alpha_b^* W_o + h_1 T_\infty}{T_\infty (h_2 + h_1)} \\
A_6 &= \frac{A_4 + A_1 A_5}{1 - A_1^2} \\
A_7 &= \frac{A_5 + A_1 A_4}{1 - A_1^2}
\end{aligned}\right\} \tag{B7}$$

Introducing the differential operator, D = d/dt, the

equations (B3) and (B4) may be uncoupled to yield

$$D^2 T_f^* + A_2A_3 D T_f^* + A_2A_3^2(1-A_1) T_f^* = 0 \qquad (B8)$$

$$D^2 T_b^* + A_2A_3 D T_b^* + A_2A_3^2(1-A_1) T_b^* = 0 \qquad (B9)$$

The solutions to equations (B8) and (B9) are given by

$$T_f^* = C_1 \exp(\lambda_1 t) + C_2 \exp(\lambda_2 t) \qquad (B10)$$

$$T_b^* = C_3 \exp(\lambda_1 t) + C_4 \exp(\lambda_2 t) \qquad (B11)$$

where the eigenvalues are given by

$$\lambda_{1,2} = \frac{1}{2} A_2A_3 [-1 \pm (1-4(1-A_1)/A_2)^{1/2}] \qquad (B12)$$

Application of the initial conditions $T_f(0) = T_\infty$ and $T_b(0) = T_\infty$ reduces the number of unknown constants by two, yielding

$$C_2 = 1-A_6-C_1 \qquad (B13)$$

$$C_4 = 1-A_7-C_3 \qquad (B14)$$

Substitution of these expressions into equations (B10) and (B11) yields expressions for T_f^* and T_b^* in terms of two unknowns, C_1 and C_4. Substitution of these expressions for temperature into (B3), in which T_f^* and T_b^* are coupled, will yield the following relation from which C_1 and C_4 are determined

$$[C_1(\lambda_1 + \frac{h_2+h_1}{(\rho\delta)_f c_f}) - \frac{h_2}{(\rho\delta)_f c_f} C_3] \exp(\lambda_1 t) +$$

$$[(C_1 + A_6 - 1)(\lambda_2 + \frac{h_2+h_1}{(\rho\delta)_f c_f}) - (C_3 + A_7 - 1)(\frac{h_2}{(\rho\delta)_f c_f})]\exp(\lambda_2 t)$$

$$= 0 \qquad \text{(B15)}$$

Since the parameters in the brackets are not time dependent, either the trivial case of zero eigenvalues must hold (in which case equation (B15) is time invariant), or the values within the brackets must be zero. Thus using the two relations from equation (B15), the constants are determined, and are given by

$$C_1 = \frac{1}{\lambda_2 - \lambda_1} [\lambda_2 + \frac{h_1}{(\rho\delta)_f c_f} - A_6(\lambda_2 + \frac{h_2+h_1}{(\rho\delta)_f c_f}) + A_7 \frac{h_2}{(\rho\delta)_f c_f}] \qquad \text{(B16)}$$

$$C_2 = [\lambda_1 + \frac{h_2+h_1}{(\rho\delta)_f c_f}] [\frac{h_2}{(\rho\delta)_f c_f}]^{-1} \cdot C_1 \qquad \text{(B17)}$$

The final solutions for the temperature response of the front and back fabrics are given by

$$T_f = T_\infty[A_6 + C_1\exp(\lambda_1 t) + C_2\exp(\lambda_2 t)] \qquad \text{(B18)}$$

$$T_b = T_\infty[A_7 + C_3\exp(\lambda_1 t) + C_4\exp(\lambda_2 t)] \qquad \text{(B19)}$$

A plot of equations (B18) and (B19) for the case of two fabrics number 5 at 9.25 W/cm^2 and 0.318 cm gap is shown in Figure B1.

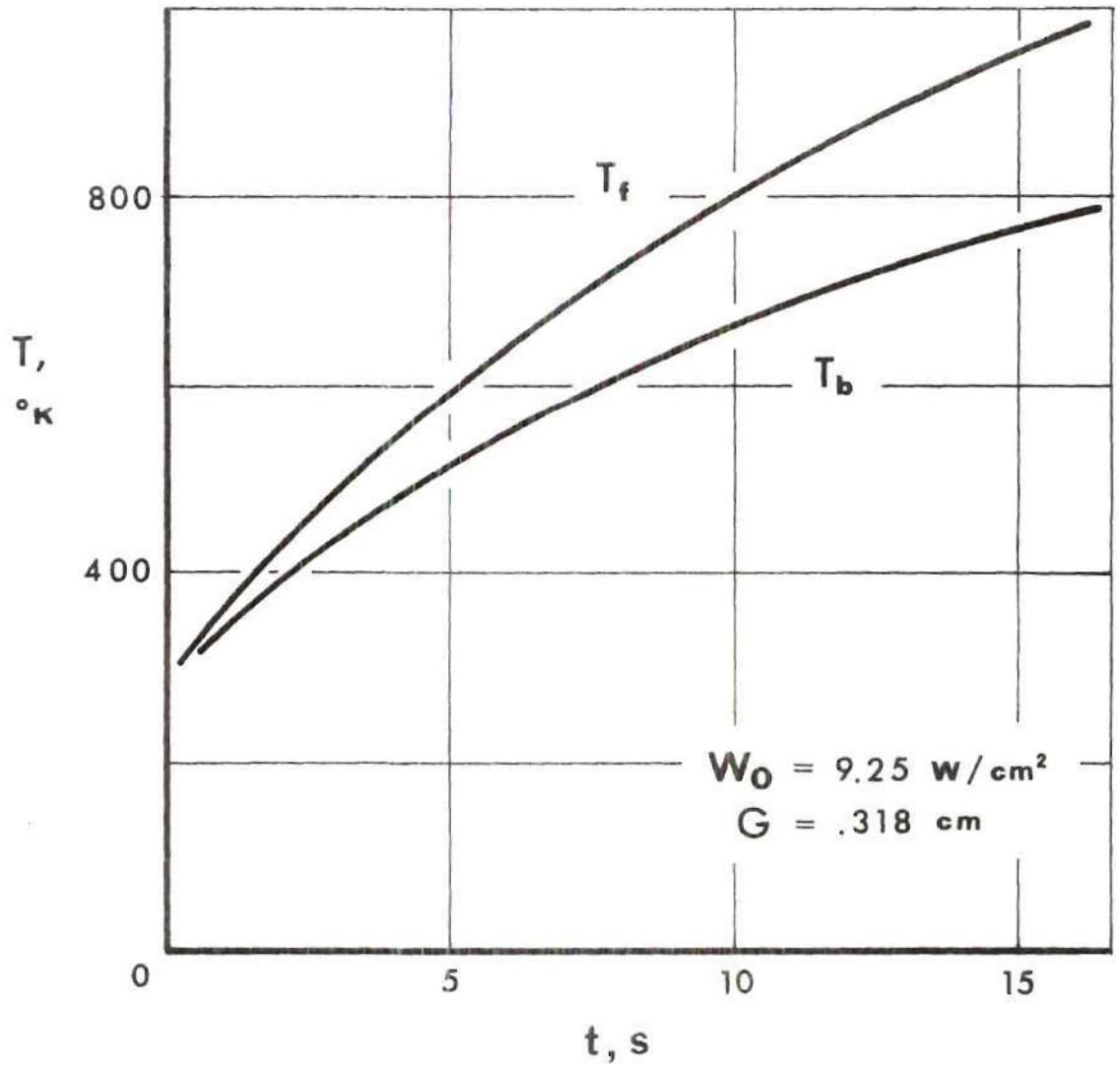

Figure B1. Temperature Response for Inert Heating with Convective Losses (GIRCFF Fabric No. 5 front and back)

APPENDIX C

NUMERICAL SOLUTION FOR RADIATIVE HEATING

This appendix contains results of the numerical solution of the system of equations which describe the radiative heating of two parallel fabric layers. The eight equations presented in Chapter II are integrated simultaneously using Runge-Kutta integration. Figures C1 through C5 are for the radiative heating of two fabrics number 5 (100% cotton) using thermophysical properties from Reference [4], with the exception that pyrolysis reaction enthalpy and activation energy are varied as specified in the figures.

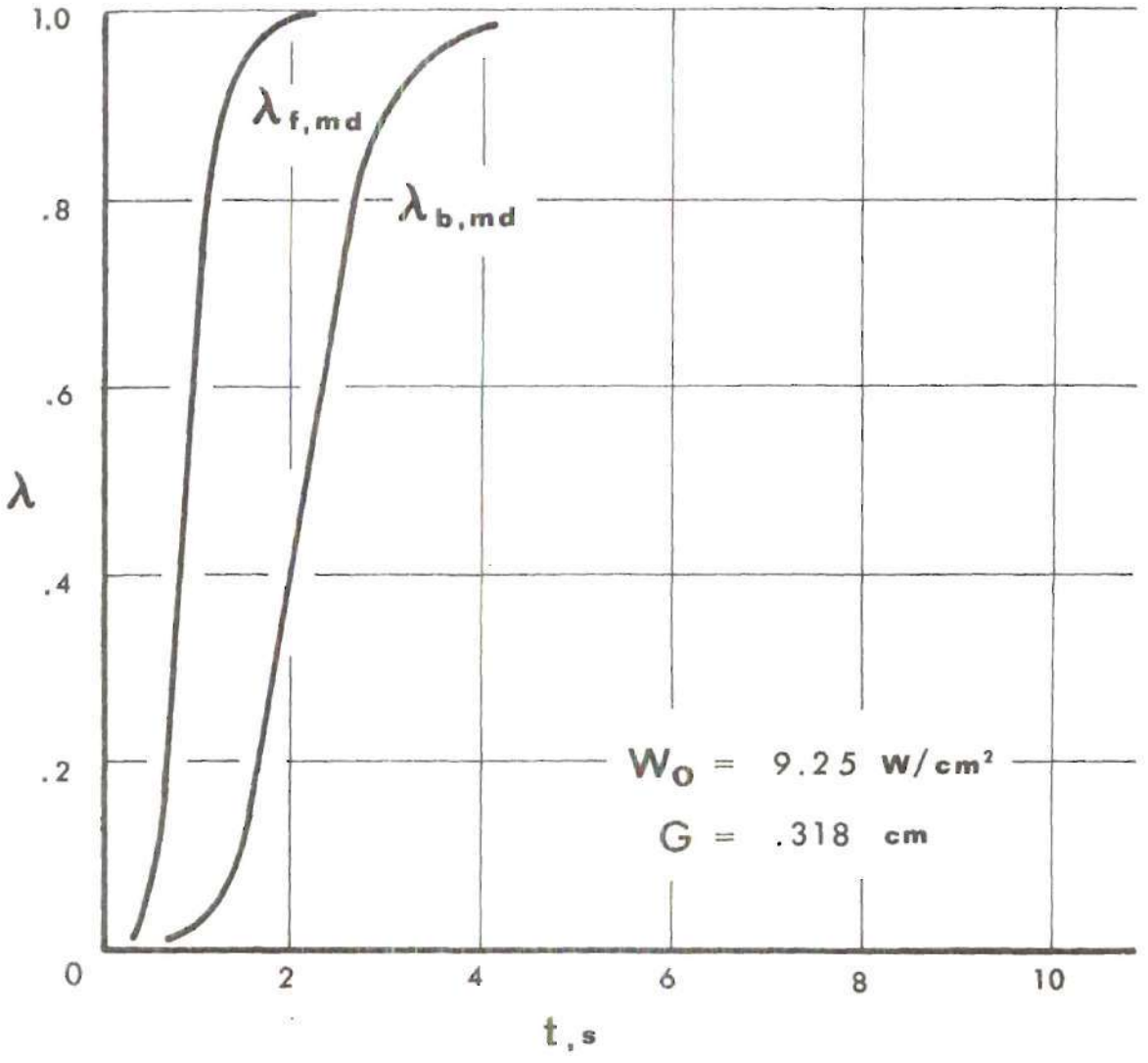

Figure C1. Moisture Desorption Rates (Fabric assembly of GIRCFF fabric no. 5 front with no. 5 back)

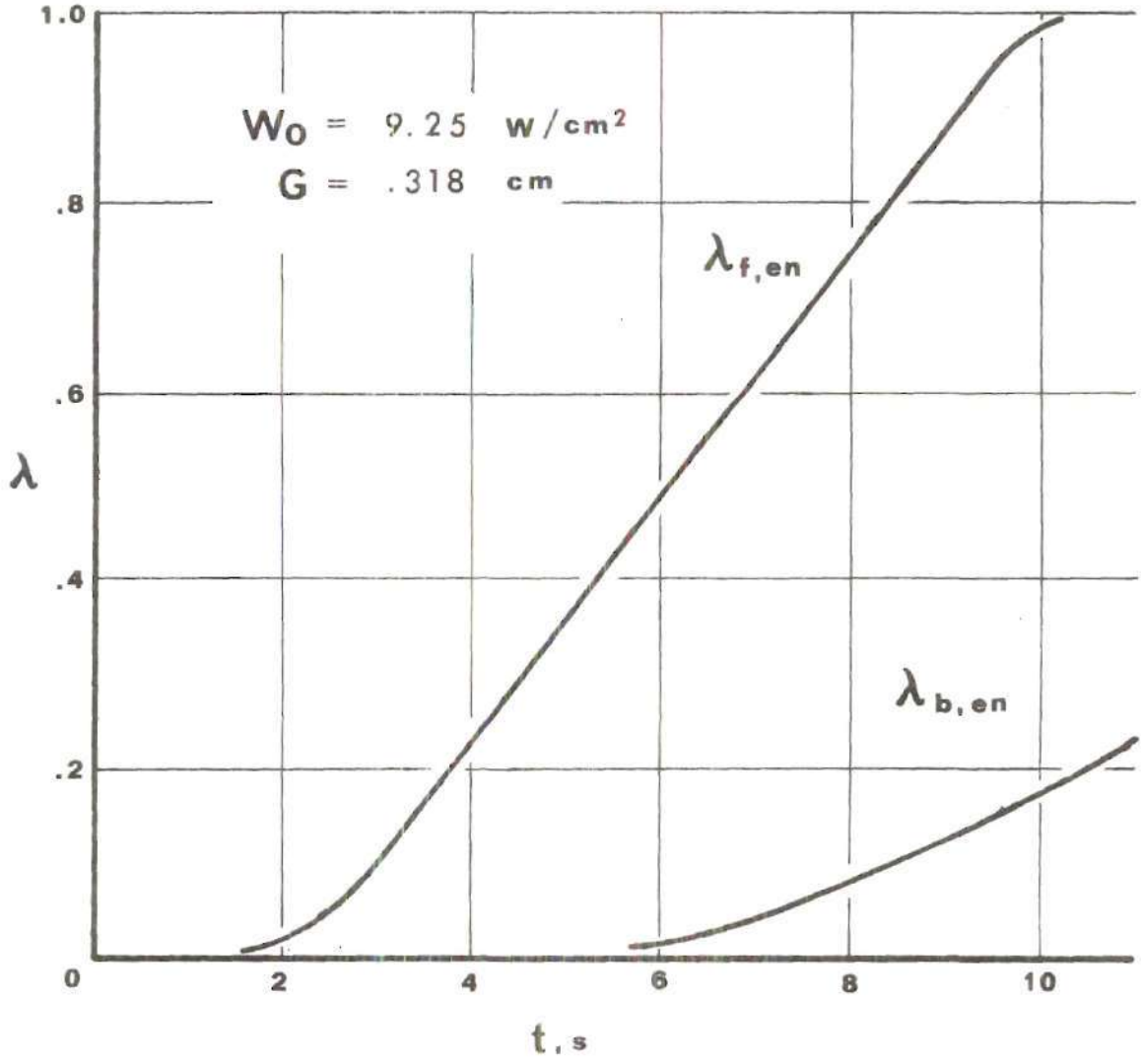

Figure C2. Endothermic Decomposition Rates (GIRCFF fabric no. 5 front with no. 5 back)

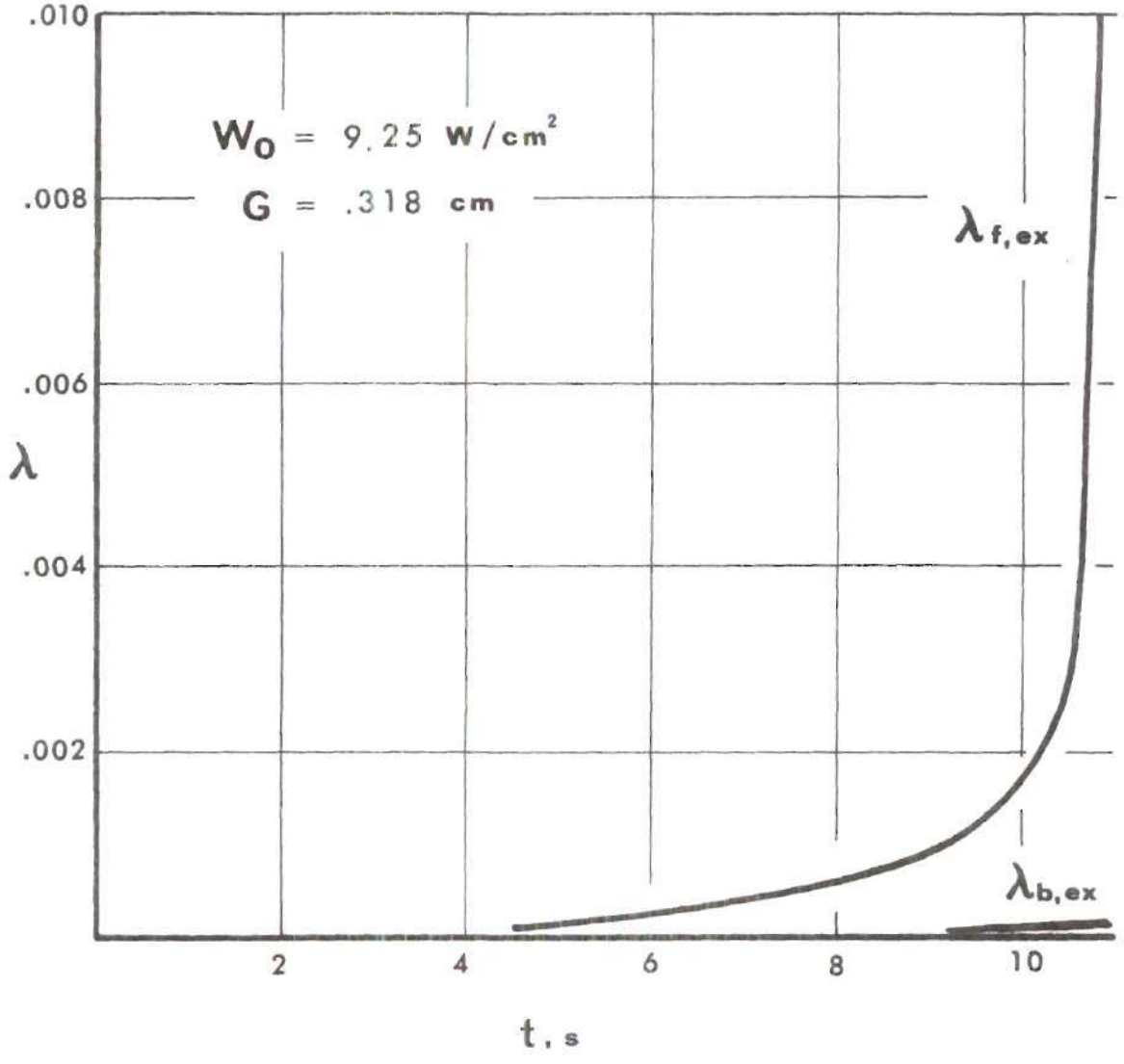

Figure C3. Exothermic Decomposition Rates (GIRCFF fabric no. 5 front with fabric no. 5 back)

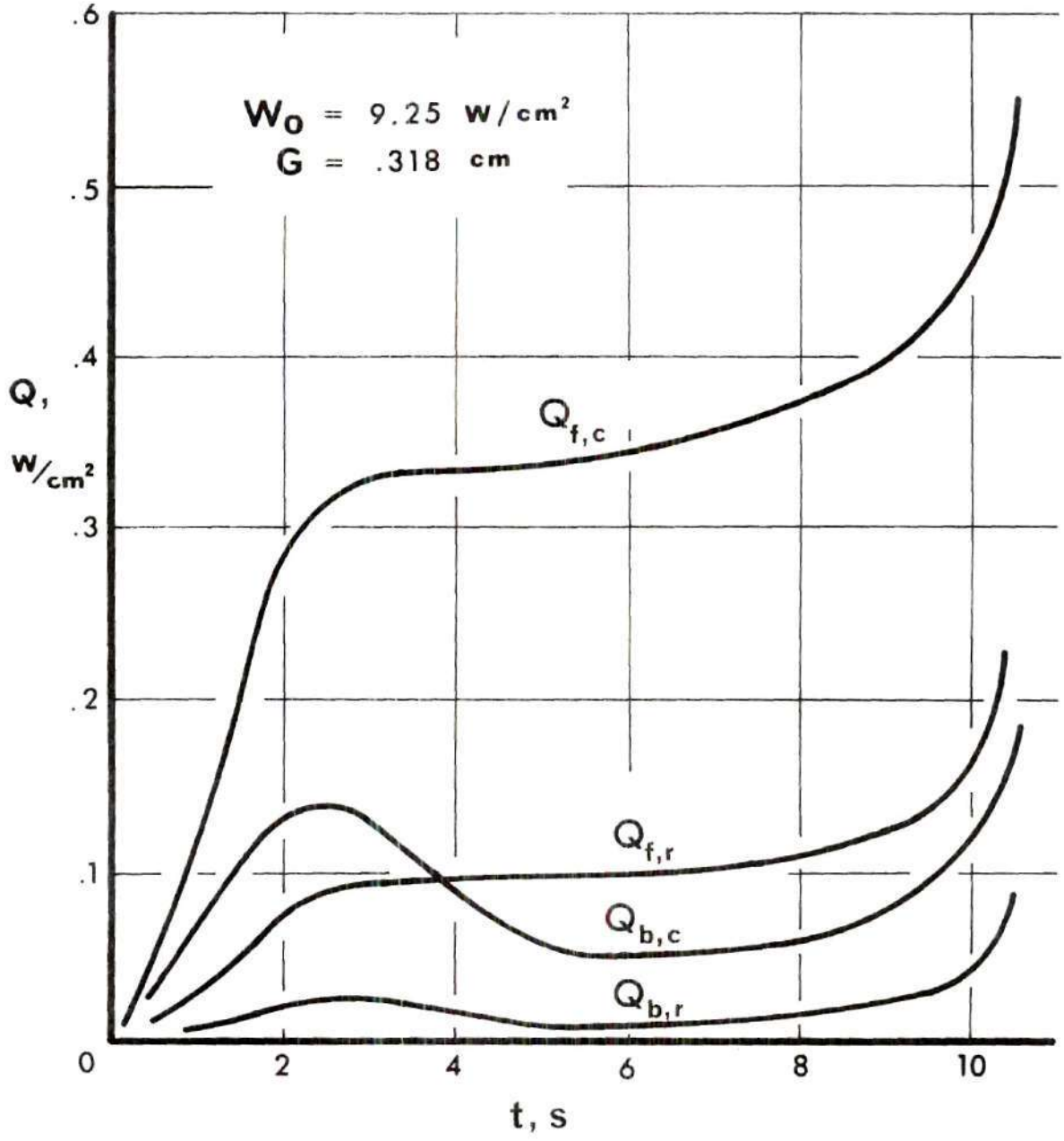

Figure C4. Convective and Radiative Heating Components (GIRCFF fabric no. 5 front with fabric no. 5 back)

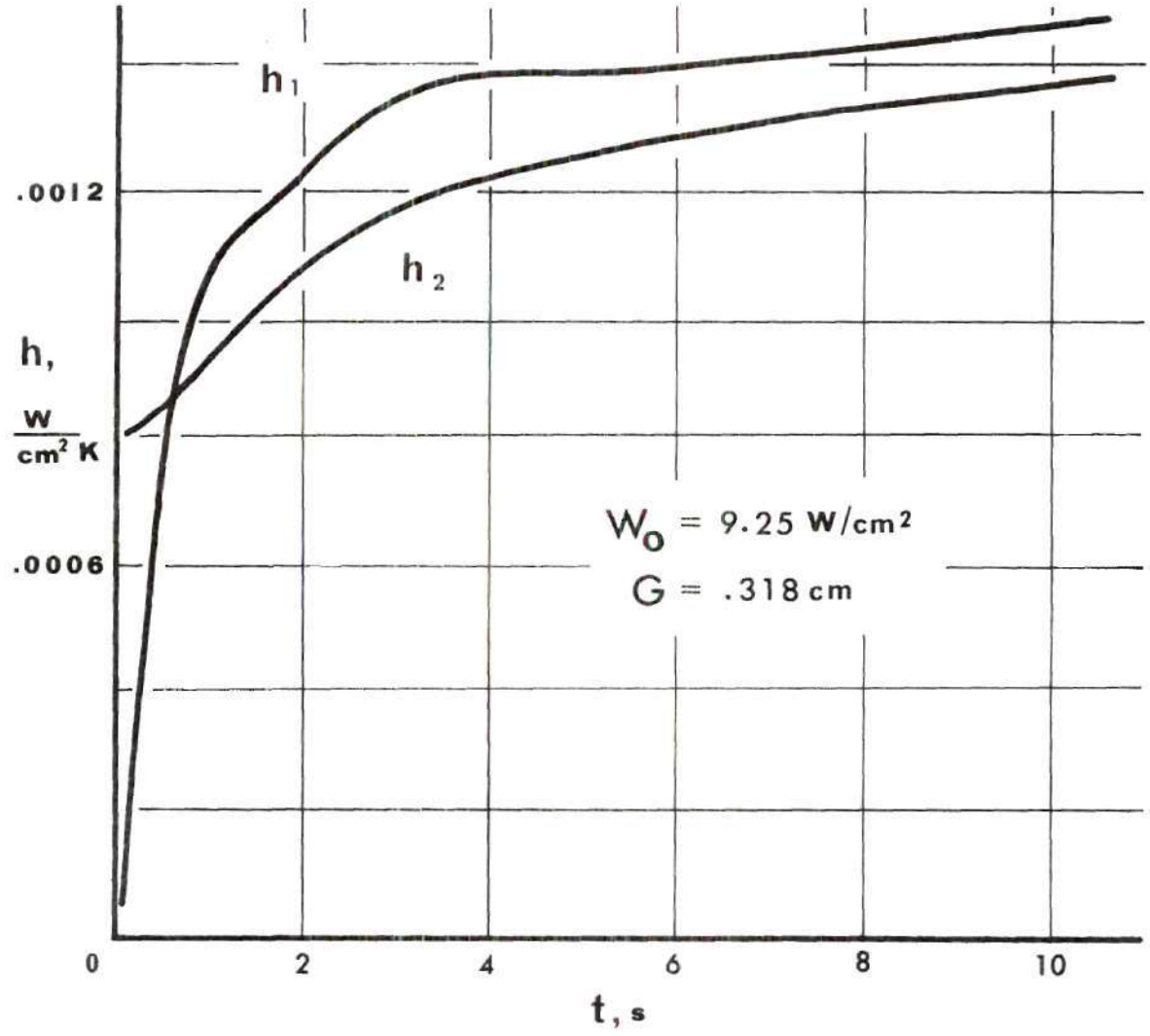

Figure C5. Variation of Convective Film Coefficients with Time (GIRCFF fabric no. 5 front with fabric no. 5 back)

APPENDIX D

RADIATIVE IGNITION TESTS

This appendix contains sample data sheets obtained for destruction time tests on fabric pairs consisting of fabric no. 5 front with fabric no. 5 back and fabric no. 2 front with fabric no. 5 back. A schematic of the Radiative Ignition Time Apparatus electrical circuitry and instrumentation is presented in Figure D3.

FABRIC ASSEMBLY IGNITION TIME TESTS

Test No. 77 Date 1-3-74 Experimentors RA & CL

GIRCFF Fabric No.: Front #5 Back #5

Gap .318 cm Idle Heater Voltage 75 V

Incident Heat Flux 6.5 W/cm^2 Relative Humidity 31 %

Infrascope Trace:

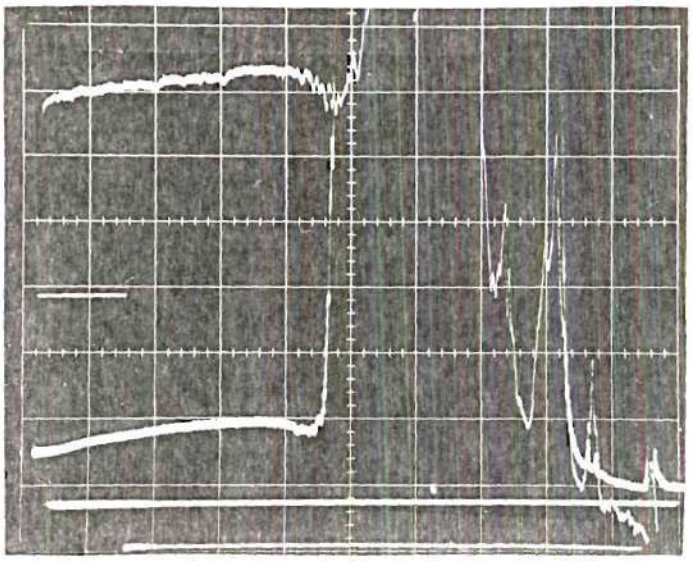

Front infrascope,
Upper beam 10 mV/cm

Back infrascope,
Lower beam 50 mV/cm

Sweep rate 5 s/cm

Front infrascope:

scale A
emissivity 1.0

Back infrascope:

scale T
emissivity 1.0

Ignition time: 4.7 cm, 23.5 s

Remarks: _____

Visual Observations: flame at 23.2 seconds

Figure D1. Sample Fabric Assembly Ignition Time Test

FABRIC ASSEMBLY IGNITION TIME TESTS

Test No. 142 Date 15-10-74 Experimentors RA

GIRCFF Fabric No.: Front #2 Back #5

Gap .159 cm Idle Heater Voltage 90 V

Relative Humidity 29 % Incident Heat Flux 9.25 W/cm^2

Infrascope Trace:

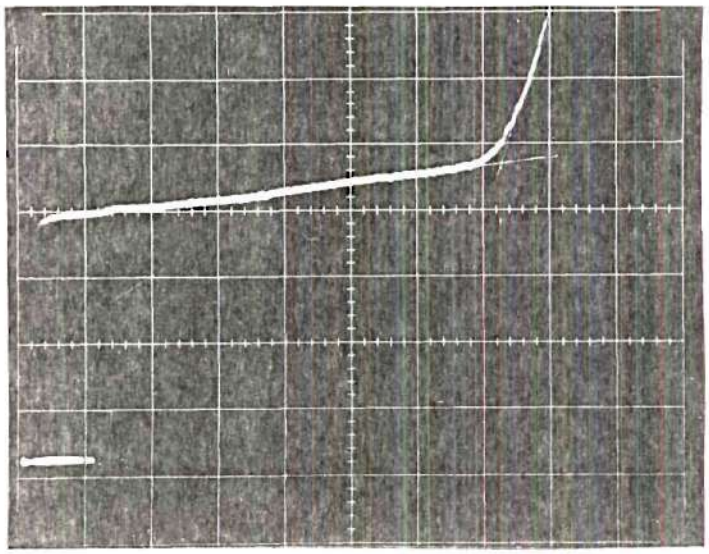

Front infrascope,
Upper beam — mV/cm

Back infrascope,
Lower beam 10 mV/cm

Sweep rate 1.0 s/cm

Front infrascope:

scale —
emissivity —

Back infrascope:

scale 8
emissivity 1.0

Ignition Time: 7.3 cm, 7.3 s

Remarks:

Visual Observations: ignition of back fabric at 23.1 seconds

Figure D2. Sample Fabric Assembly Melting Time Test

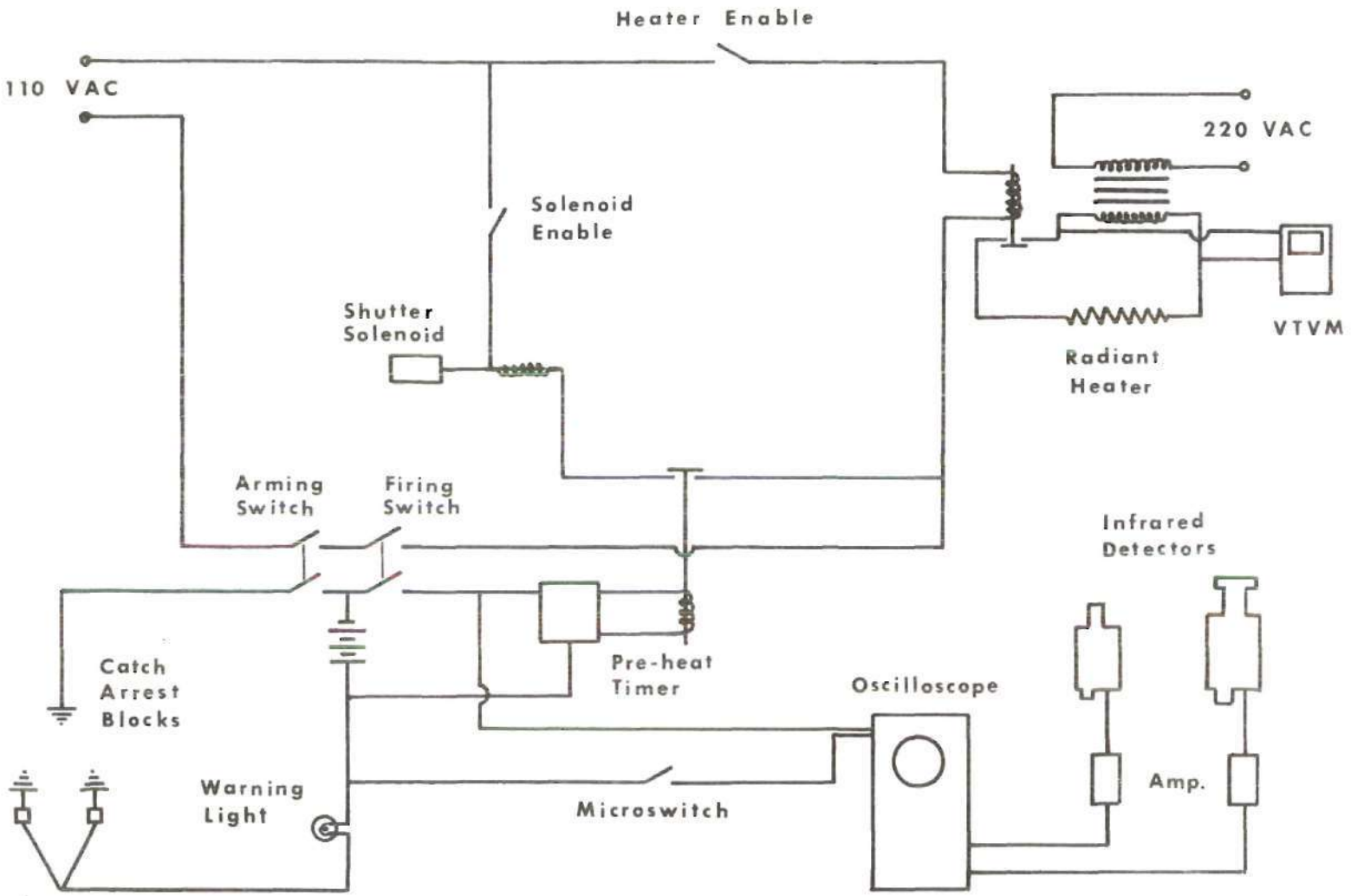

Figure D3. Schematic of Radiative Ignition Time Apparatus and Supporting Instrumentation

APPENDIX E

CONVECTIVE IGNITION TESTS

This appendix contains sample edge ignition time data, and sample film coefficient data. Reduced ignition time data is presented in Tables E1 through E5. Exposure time delays, velocity profiles, and temperature profiles are also shown. A schematic of instrumentation circuitry is shown in Figure E5.

CITA - EDGE IGNITION TESTS

Test No. 32 Date 26-6-74 Experimentors RA

GIRCFF Fabric No. 6 Sample size 3"x 3"

Inclination Angle 30 ° Height above burner 3"

Room Temp. 76 °F Barometric pressure 28.94 " Hg R.H. 55 %

Thermocouples: Air Ic CH_4 Ic Flame cA , .020 in. bead

Flame Temperature 50.96 mV, 1259.2 °C

Flow Rates:

	T(mV)	T(°F)	P("Hg)	R(div)	R(cfh)	Delivery pressure
CH_4	1.2632	76.5	13.0	94.5	3.516	6 psi
Air	1.2240	75.1	13.6	68.5	52.096	27 psi

Infrascope Trace:

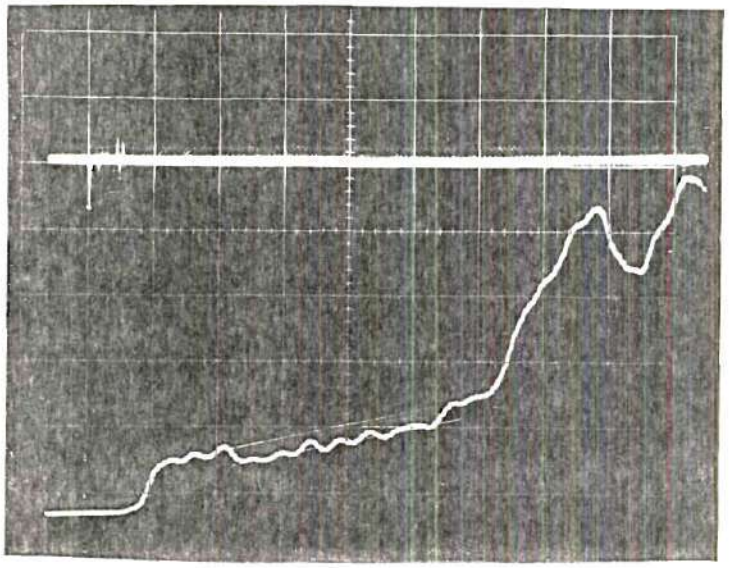

Upper beam 5 V/cm

Lower beam 20 mV/cm

Sweep rate .20 s/cm

Infrascope scale B

Emissivity 1.0

Ignition Time:

Infrascope

6.25 cm 1.25 s

Figure E1. Sample Edge Ignition Time Test

CONVECTIVE HEAT TRANSFER COEFFICIENT TESTS

Test No. 13 Date 10-8-74 Experimentors RA

Height above burner 7.62 cm Inclination angle 90 °

TC bead location 1.0 mm Screen temp 1.269 mV, 29.1 °C

Room temp. 76 °F Barometric pressure 29.06 "Hg Rel. Hum. 63 %

Thermocouples: Air IC CH_4 IC

Flow Rates:

	T(mV)	T(°F)	P("Hg)	R(div)	R(cfh)	Delivery pressure
CH_4	1.2368	75.6	13.7	94.5	3.516	6 psi
Air	1.2096	74.6	13.6	68.5	52.10	20 psi

Oscilloscope Trace:

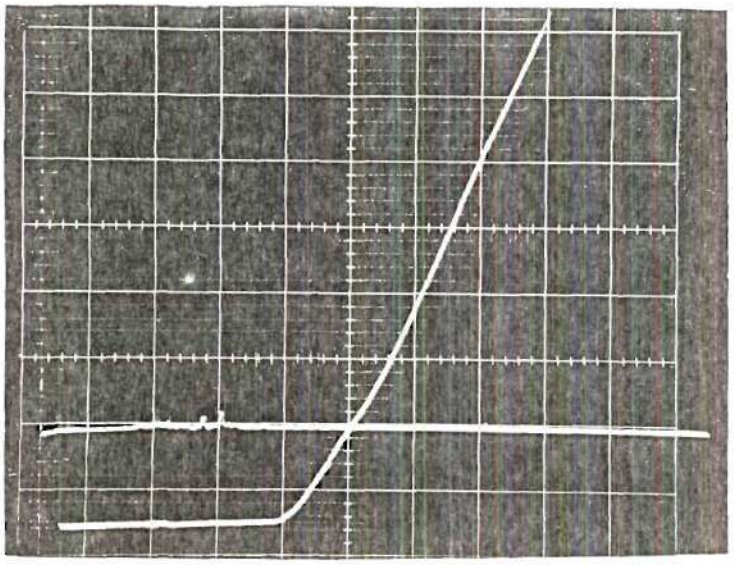

Upper beam 2 V/cm

Lower beam 1 mV/cm

Sweep rate 20 ms/cm

Figure E2. Sample Film Coefficient Test

Table E1. Summary of Edge Ignition Tests on Fabric Number 5.

GIRCFF Fabric Number 5 (100% Cotton)

k/δ = 0.00950 W/cm^2-°K

c = 1.761 Ws/g-°K

$\rho\delta$ = 13.71 mg/cm^2

T_i = 311.0 °C

Fuel: Methane

ϕ = 0.86

Fabric edge = 76.0 mm

α	Exp. No.	L cm	$\dot{m}_{mix}$ g/h	T_o °C	T_g °C	θ_g	$t_{i,m}$ s	$\bar{\theta}$	$2\bar{h}_c$ W/cm^2-°K	Fo	q_c^*
90°	38[a]	7.62	1272	22.0	1229	4.176	0.369	0.522	0.03058	0.145	11.760
90°	38[b]	7.62	1272	22.0	1229	4.176	0.369	0.522	0.03043	0.145	11.700
90°	38[c]	7.62	1272	22.0	1229	4.176	0.369	0.522	0.05557	0.145	22.090
90°	38[d]	7.62	1272	22.0	1229	4.176	0.369	0.522	0.11415	0.351	9.446

---

[a] - Measured film coefficient.

[b] - Film coefficient from equation (37) with x = δ.

[c] - Film coefficient from equation (35) with x = δ.

[d] - Film coefficient from equation (37) with x = d.

Table E2. Summary of Edge Ignition Tests on Fabric Number 6.

GIRCFF Fabric Number 6 (65/35% Polyester-Cotton)

k/δ = 0.01830 W/cm^2-°K

c = 1.545 Ws/g-°K

$\rho\delta$ = 23.57 mg/cm^2

T_i = 416.0 °C

Fuel: Methane

ϕ = 0.86

Fabric edge = 76.0 mm

$\bar{\alpha}$	Exp. No.	L cm	$\dot{m}_{mix}$ g/h	T_o °C	$\bar{T}_g$ °C	θ_g	$t_{i,m}$ s	$\bar{\theta}$	$2\bar{h}_c$ W/cm^2-°K	Fo	q_c^*
0°	18	7.62	1267	22.2	1231	3.069	1.945	0.532	0.01161	0.977	1.631
30°	13	7.62	1270	21.9	1257	3.134	1.485	0.531	0.01343	0.746	1.887
60°	17	7.62	1272	22.2	1234	3.077	0.160	0.532	0.01810	0.080	2.542
90°	23[a]	7.62	1267	23.8	1318	3.300	0.124	0.530	0.03058	0.062	4.295
90°	23[b]	7.62	1267	23.8	1318	3.300	0.124	0.530	0.04067	0.062	5.711
90°	23[c]	7.62	1267	23.8	1318	3.300	0.124	0.530	0.06945	0.062	9.753
90°	23[d]	7.62	1267	23.8	1318	3.300	0.124	0.530	0.07539	0.083	4.235

---

a - Measured film coefficient.

b - Film coefficient from equation (37) with x = δ.

c - Film coefficient from equation (35) with x = δ.

d - Film coefficient from equation (37) with x = d.

Table E2. Summary of Edge Ignition Tests on Fabric Number 6 (Continued).

α	Exp. No.	L cm	$\dot{m}_{mix}$ g/h	T_o °C	T_g °C	θ_g	$t_{i,m}$ s	$\bar{\theta}$	$2\bar{h}_c$ W/cm^2-°K	Fo	q^*_c
0°	29	7.62	2205	23.8	1260	3.152	1.355	0.531	0.01269	0.681	1.920
30°	32	7.62	2205	24.4	1292	3.237	1.110	0.530	0.01684	0.558	2.550
60°	25	7.62	2200	24.4	1262	3.160	0.154	0.531	0.01966	0.077	2.976
90°	28[a]	7.62	2198	24.4	1280	3.206	0.074	0.531	0.02930	0.037	4.434
90°	28[b]	7.62	2198	24.4	1280	3.206	0.074	0.531	0.05151	0.037	7.798
90°	28[c]	7.62	2198	24.4	1280	3.206	0.074	0.531	0.07816	0.037	11.829
90°	28[d]	7.62	2198	24.4	1280	3.206	0.074	0.531	0.09549	0.049	6.902

---

[a] - Measured film coefficient.

[b] - Film coefficient from equation (37) with $x = \delta$.

[c] - Film coefficient from equation (35) with $x = \delta$.

[d] - Film coefficient from equation (37) with $x = d$.

Table E3. Summary of Edge Ignition Tests on Fabric Number 9.

GIRCFF Fabric Number 9 (100% Cotton)

k/δ = 0.00500 W/cm^2-°K

c = 1.558 Ws/g-°K

$\rho\delta$ = 26.48 mg/cm^2

T_i = 308.0 °C

Fuel: Methane

ϕ = 0.86

Fabric Edge = 76.0 mm

α	Exp. No.	L cm	$\dot{m}_{mix}$ g/h	T_o °C	T_g °C	θ_g	$t_{i,m}$ s	$\bar{\theta}$	$2\bar{h}_c$ W/cm^2-°K	Fo	q_c^*
90°	36[a]	7.62	1272	22.0	1229	4.220	0.317	0.522	0.03058	0.038	22.620
90°	36[b]	7.62	1272	22.0	1229	4.220	0.317	0.522	0.02657	0.038	19.650
90°	36[c]	7.62	1272	22.0	1229	4.220	0.317	0.522	0.04911	0.038	36.320
90°	36[d]	7.62	1272	22.0	1229	4.220	0.317	0.522	0.06849	0.115	7.817

---

a - Measured film coefficient.

b - Film coefficient from equation (37) with $x = \delta$.

c - Film coefficient from equation (35) with $x = \delta$.

d - Film coefficient from equation (37) with x = d.

Table E4. Summary of Edge Ignition Tests on Fabric Number 10.

GIRCFF Fabric Number 10 (100% Cotton)

k/δ = 0.03600 $W/cm^2-°K$ Fuel: Methane

c = 2.398 $Ws/g-°K$ ϕ = 0.86

$\rho\delta$ = 6.65 mg/cm^2 Fabric edge = 76.0 mm

T_i = 443.0 °C

$\bar{\alpha}$	Exp. No.	L cm	$\dot{m}_{mix}$ g/h	T_o °C	T_g °C	θ_g	$t_{i,m}$ s	$\bar{\theta}$	$2\bar{h}_c$ $W/cm^2-°K$	Fo	q_c^*
0°	20	7.62	1259	23.6	1211	2.831	0.645	0.536	0.01161	1.456	0.741
30°	21	7.62	1265	22.7	1279	2.989	0.535	0.533	0.01343	1.208	0.857
60°	15	7.62	1272	22.2	1185	2.763	0.400	0.537	0.01810	0.903	1.154
90°	22[a]	7.62	1264	24.0	1175	2.747	0.224	0.537	0.03058	0.506	1.951
90°	22[b]	7.62	1264	24.0	1175	2.747	0.224	0.537	0.06475	0.506	4.130
90°	22[c]	7.62	1264	24.0	1175	2.747	0.224	0.537	0.09464	0.506	6.036
90°	22[d]	7.62	1264	24.0	1175	2.747	0.224	0.537	0.k3021	0.069	3.182

[a] - Measured film coefficient.

[b] - Film coefficient from equation (37) with x = δ.

[c] - Film coefficient from equation (35) with x = δ.

[d] - Film coefficient from equation (37) with x = d.

Table E5. Summary of Edge Ignition Tests on Fabric Number 17.

GIRCFF Fabric Number 17 (65/35% Polyester-Cotton)

k/δ = 0.02900 W/cm^2-°K

c = 1.840 Ws/g-°K

$\rho\delta$ = 8.55 mg/cm^2

T_i = 480.0 °C

Fuel: Methane

ϕ = 0.86

Fabric edge = 76.0 mm

$\bar{\alpha}$	Exp. No.	L cm	$\dot{m}_{mix}$ g/h	T_o °C	T_f °C	θ_g	$t_{i,m}$ s	$\bar{\theta}$	$2\bar{h}_c$ W/cm^2-°K	Fo	α^*_c
90°	37[a]	7.62	1261	24.2	1221	2.626	0.299	0.538	0.03058	0.551	2.162
90°	37[b]	7.62	1261	24.2	1221	2.626	0.299	0.538	0.05847	0.551	4.133
90°	37[c]	7.62	1261	24.2	1221	2.626	0.299	0.538	0.09083	0.551	6.420
90°	37[d]	7.62	1261	24.2	1221	2.626	0.299	0.538	0.13428	0.197	3.479

---

[a] - Measured film coefficient.

[b] - Film coefficient from equation (37) with x = δ.

[c] - Film coefficient from equation (35) with x = δ.

[d] - Film coefficient from equation (37) with x = d.

Table E6. Exposure Delay Times.

L = 7.62 cm

inclination angle	t, seconds	
degrees	Burner Mass Flow Rate, g/h	
	1260	2175
0	0.105	0.145
30	0.105	0.140
60	0.100	0.126
90	0.096	0.076

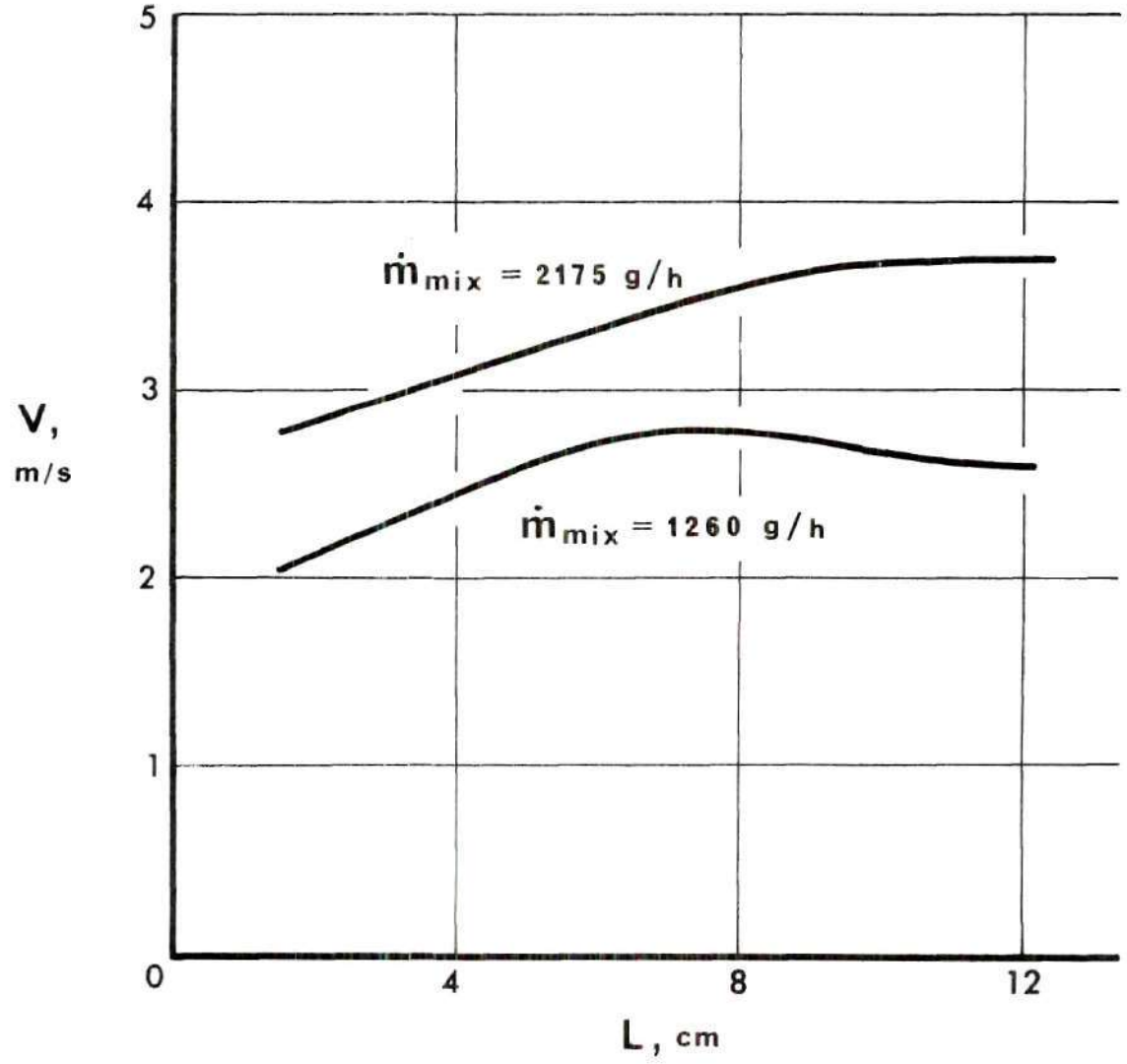

Figure E3. Velocity Profiles for Air-Methane Combusting Jet (Burner Diameter D_e = 3.7 cm)

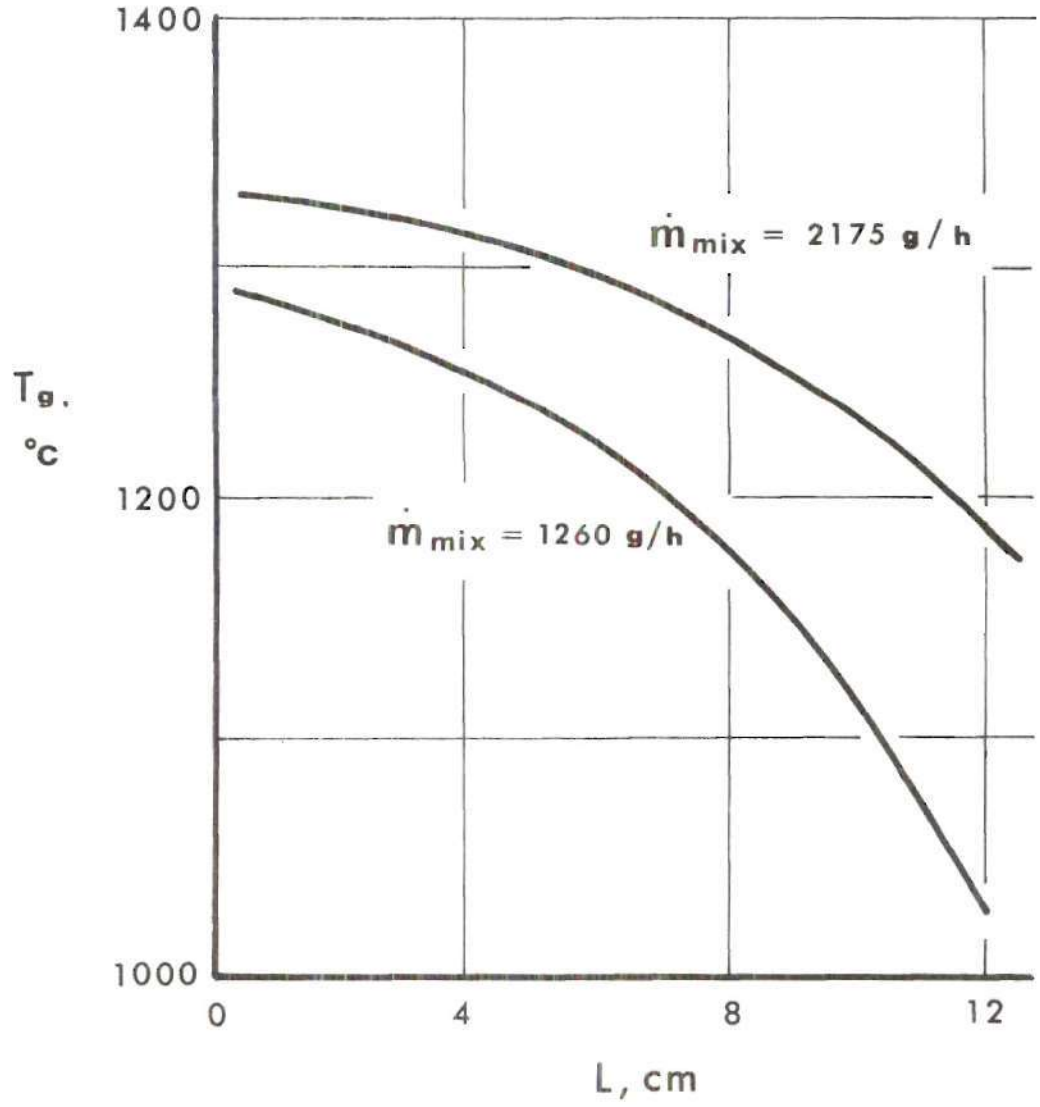

Figure E4. Flame Temperature Profiles (Air-Methane flame with ϕ = 0.86)

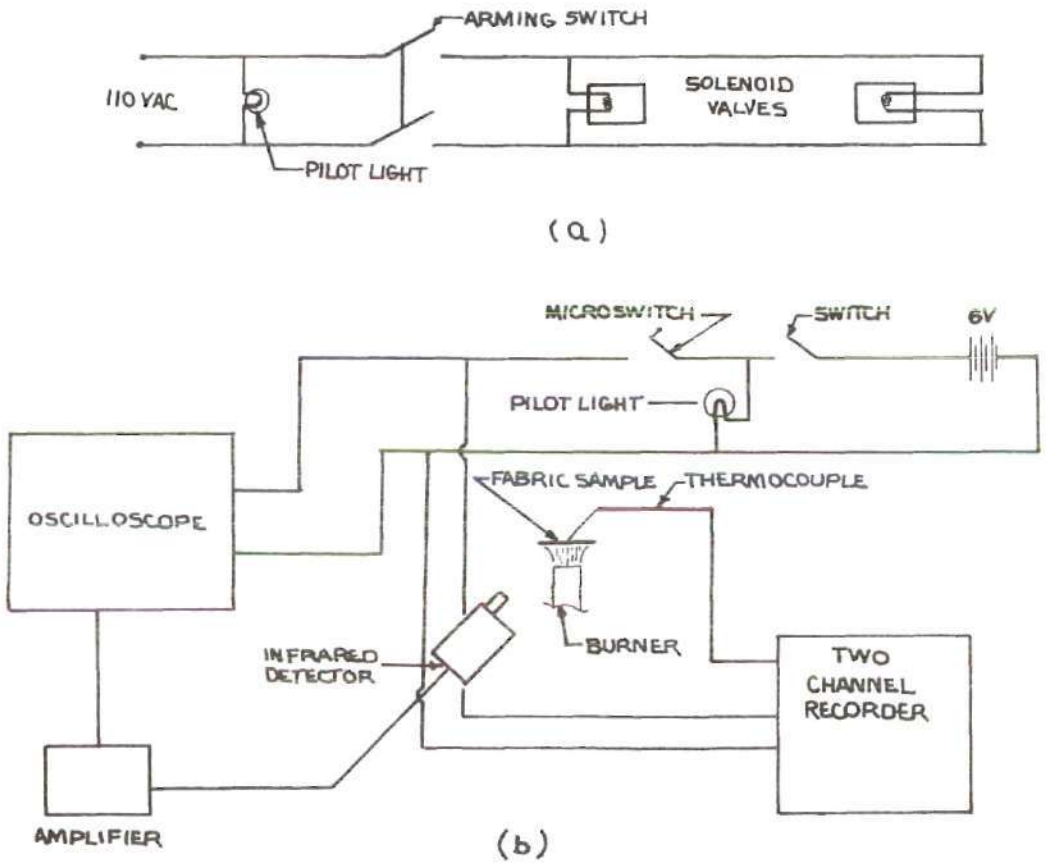

Figure E5. (a) Schematic of Shutter Activation Electrical Circuit
(b) Schematic of Fabric Destruction Detection and Destruction Time Measuring Instrumentation, Static Tests

BIBLIOGRAPHY

1. "America Burning," The National Commission on Fire Prevention and Control, U. S. Government Printing Office, Washington, D. C., Stock Number 5200-00004, May, 1973.

2. "Studies of Death, Injuries, and Economic Losses Resulting from Accidental Burning of Products, Fabrics or Related Materials," U. S. Department of Health, Education and Welfare, Fourth Annual Report, U. S. Government Printing Office, Washington, D. C., 1972.

3. Evans, R.B., Wulff, W., and Zuber, N., "The Study of Hazards from Burning Apparel and The Relation of Hazards to Test Methods," Research Proposal Submitted by the School of Mechanical Engineering, Georgia Institute of Technology, to the Government-Industry Research Committee on Fabric Flammability, July, 1970.

4. Alkidas, A., Hess, R.W., Wulff, W., and Zuber, N., "Study of Hazards from Burning Apparel and the Relation of Hazards to Test Methods," Final Report, NSF Grant No. GK-27189, Georgia Institute of Technology, Atlanta, Georgia, December, 1971, National Technical Information Access No. COM-73-10954.

5. Alkidas, A., Champion, E.R., Durbetaki, P., Giddens, W., Hess, R.W., Kumar, B., Naveda, O.A.A., Williams, P.T., and Wulff, W., "Study of Hazards from Burning Apparel and the Relation of Hazards to Test Methods," Second Annual Report, NSF Grant No. GI-31882, Georgia Institute of Technology, Atlanta, Georgia, December, 1972, National Technical Information Access No. COM-73-10956.

6. Acree, R.L., Champion, E.R., Durbetaki, P., Lee, C.K., Naveda, O.A.A., Wedel, G.L., Williams, P.T., and Wulff, W., "Fabric Ignition," Third Annual Report, NSF Grant No. GI-31882A#1, Georgia Institute of Technology, Atlanta, Georgia, March, 1974.

7. Mehta, A.K., and Wong, F., "Measurements of Flammability and Burn Potential of Fabrics," Summary Report, NSF Grant No. GI-31881, Massachusetts Institute of Technology, Cambridge, Massachusetts, February, 1973.

8. Heskestad, G., "Ease of Ignition of Fabrics Exposed to Flaming Heat Sources," Final Report, Factory Mutual Research Corporation, Norwood, Massachusetts, FMRC Serial Number 19967 RC73-T-4, January, 1973.

9. Heskestad, G., Kalelkar, A.S., and Kung, H.C., "A Study of Pre-Ignition Heat Transfer Through a Fabric-Skin System Subjected to a Heat Source," Factory Mutual Research Corporation, Norwood, Massachusetts, FMRC Serial Number 19967, December, 1971.

10. Arnold, G., Fisher, A., and Frohnsdorff, G., "Hazards from Burning Garments," Final Report for the GIRCFF, The Gilette Company Research Institute, March, 1973.

11. The Government-Industry Research Committee on Fabric Flammability, "Study of Hazards from Burning Apparel and the Relation of Hazards to Test Methods," A Work Statement Prepared by the Research Committee, Dr. E. Passaglia, Chairman, National Bureau of Standards, June, 1970.

12. Morse, H.L., Thompson, J.G., Clark, K.J., Green, K.A., and Moyer, C.B., "Analysis of the Thermal Response of Protective Fabrics," Air Force Materials Laboratory, Wright-Patterson AFB, Ohio, Technical Report AFML-TR-73-17, January, 1973.

13. Morris, M.A., "Thermal Insulation of Single and Multiple Layers of Fabrics," Textile Research Journal, Vol. 25, pp.766-773, 1955.

14. Miller, B., "The Thermal and Flammability Behavior of Multicomponent Fibrous Polymer Systems," NSF Grant No. GI-37805, A Progress Report Presented at the NSF/RANN Conference on Fire Research, Georgia Institute of Technology, Atlanta, Georgia, May, 1974.

15. Miller, B., "Transfer of Flame Retardant Effects," Textile Research Journal, Vol. 42, pp.629-633, 1972.

16. Champion, E.R., "Determination of Fabric Ignition Times Through Use of a Convective Heat Source Apparatus," M.S. Thesis, Georgia Institute of Technology, Atlanta, Georgia, June, 1973.

17. Eckert, E.R.G., and Drake, R.M., Heat and Mass Transfer, Second Edition, McGraw-Hill Book Company, New York, 1959, pp.403-407.

18. Holman, J.P., Heat Transfer, Second Edition, McGraw-Hill Book Company, New York, 1968, pp.195-197.

19. Eckert, E.R.G., and Carlson, W.O., "Natural Convection in an Air Layer Enclosed Between Two Vertical Plates with Different Temperatures," International Journal of Heat and Mass Transfer, Vol. 2, pp.106-120, 1961.

20. Tesner, P.A., "The Activation Energy of Gas Reactions with Solid Carbon," Eighth Symposium (International) on Combustion, The Williams and Wilkins Company, Baltimore, Maryland, pp.807-814, 1962.

21. Davies, J.M., McQue, B., and Hoover, T.B., "Heat Transferred by Decomposition Products from Cotton Fabrics Exposed to Intense Thermal Radiation," Textile Research Journal, Vol. 35, pp.757-769, 1965.

22. Jacob, M., Heat Transfer, Volume 1, John Wiley and Sons, New York, pp.554-564, 1949.

23. Wedel, G.L., "Determination of Film Coefficients With Simulated Pyrolysate Evolution," M.S. Thesis, Georgia Institute of Technology, Atlanta, Georgia, August, 1974.

24. McAdams, W.H., Heat Transmission, Third Edition, McGraw-Hill Book Company, New York, 1954, pp.258-261.

25. Fishenden, M., and Saunders, O.A., "The Errors in Gas Temperature Measurements and Their Calculation," Journal of the Institute of Fuel, Vol. 12, pp.S5-S12, 1939.

26. Gardon, R., and Akfirat, J.C., "The Role of Turbulence in Determining the Heat Transfer Characteristics of Impinging Jets," The International Journal of Heat and Mass Transfer, Vol. 8, pp.1261-1272, 1955.

27. Perry, K.P., "Heat Transfer By Convection From a Hot Gas Jet to a Plane Surface," The Institute of Mechanical Engineers, Proceedings, Vol. 168, London, pp.775-780, 1954.